

5-2018

Identifying Subunit Organization and Function of the Nuclear RNA Exosome Machinery

Jillian Losh

Follow this and additional works at: https://digitalcommons.library.tmc.edu/utgsbs_dissertations

 Part of the [Medicine and Health Sciences Commons](#)

Recommended Citation

Losh, Jillian, "Identifying Subunit Organization and Function of the Nuclear RNA Exosome Machinery" (2018). *UT GSBS Dissertations and Theses (Open Access)*. 835.

https://digitalcommons.library.tmc.edu/utgsbs_dissertations/835

This Dissertation (PhD) is brought to you for free and open access by the Graduate School of Biomedical Sciences at DigitalCommons@TMC. It has been accepted for inclusion in UT GSBS Dissertations and Theses (Open Access) by an authorized administrator of DigitalCommons@TMC. For more information, please contact laurel.sanders@library.tmc.edu.

IDENTIFYING SUBUNIT ORGANIZATION AND FUNCTION OF THE NUCLEAR RNA EXOSOME MACHINERY

by

Jillian Strother Losh, A.S., B.S.

APPROVED:

Ambro van Hoof, Ph.D.
Advisory Professor

Danielle A. Garsin, Ph.D.

Michael C. Lorenz, Ph.D.

Kevin A. Morano, Ph.D.

Eric J. Wagner, Ph.D.

APPROVED:

Dean, The University of Texas
MD Anderson Cancer Center UTHealth Graduate School of Biomedical Sciences

**IDENTIFYING SUBUNIT ORGANIZATION AND FUNCTION
OF THE NUCLEAR RNA EXOSOME MACHINERY**

A
DISSERTATION

Presented to the Faculty of
The University of Texas
MD Anderson Cancer Center UTHealth
Graduate School of Biomedical Sciences
in Partial Fulfillment
of the Requirements
for the Degree of

DOCTOR OF PHILOSOPHY

by
Jillian Strother Losh, A.S., B.S.

Houston, TX

May 2018

DEDICATION

This work is dedicated to my father, Daniel Strother Losh.

Dad, thank you for consistently supporting me in all of my endeavors, big and small. As I enter the professional world, I hope to model what you have done: achieve an extremely successful career, while constantly maintaining the balance between work, family, and self-acceptance. I love you and I am proud to share my accomplishments with you.

ACKNOWLEDGEMENTS

First and foremost, thank you to Ambro van Hoof, my mentor. I am so grateful that you have always respected my career goals and cheered my pursuit of them. You have encouraged me to have fun and given me emotional support during the moments where there was no fun at all. You have constantly pushed me to improve my skills and allowed me to fully take ownership of my work, while being a patient advisor and my friend.

I would like to thank Anita Corbett, Milo Fasken, and their laboratory at Emory University for a wonderful partnership on our PCH1b work. This was my first foray into formal science collaboration and it was a fantastic experience. I am glad that we have developed this project, as well as friendships. Thank you to Sean Johnson and his laboratory at Utah State University for assistance with fluorescence anisotropy analysis of TRAMP complex subunits.

Thank you to the members of my Advisory Committee: Danielle Garsin, Eric Wagner, Kevin Morano, and Michael Lorenz for your continued guidance and encouragement. Thank you to the two additional members of my Qualifying Exam Committee: Nayun Kim and Heidi Kaplan. I am extremely appreciative to have had faculty members on both of these committees, as well as in my classes, who are such a motivating force. Also, thank you to those of you who have provided me with the use of equipment, reagents, and other materials. I would also especially like to thank Eric Solberg and Stephen Linder for providing me with opportunities to learn more about science policy and for pushing me to exercise that knowledge.

Special thanks to Danielle Garsin for welcoming me into her lab as an undergraduate student in 2011. Danielle, as well as Garsin Lab members Katie McCallum, Liz Gendel, Ransom van der Hoeven, and Sruti DebRoy, introduced me to graduate school and encouraged me to pursue a Ph.D., even when I was not

yet sure of myself. Thank you to my undergraduate faculty at University of Houston-Downtown, especially Akif Uzman, Poonam Gulati, and Lisa Morano. I would also like to give very special acknowledgment to the Morano family. In addition to Kevin's guidance throughout graduate school, Lisa was the first person to ever tell me that I should consider pursuing a Ph.D. degree. You are both my role-models as researchers, advisors, and all-around wonderful humans.

I would like to thank the GSBS Deans and staff for their support of my academic and extracurricular pursuits on campus. Thank you to GSBS, the R.W. Butcher family, GSEC, and Dean Barbara Stoll of McGovern Medical School for granting me awards during graduate school that have been so beneficial to my growth as a scientist. Additional thanks to the MMG/MID staff, especially Lyz Culpepper and Chris McKenzie, for all of your help with student-related and science-related matters. I am so very fortunate to have joined MMG/MID, a wonderfully close-knit group of faculty, students, technicians, and staff with a strong passion for learning, collaboration, and Halloween costumes.

Thank you to all of my wonderful GSBS friends, especially: Kara Schoenemann for being my personal stand-up comedian and a pretty swell gal, Sara Peffer for the Netflix/PBS binging and to-do-list mastering, Doug Litwin for the gossiping, Jennifer Abrams for the dancing, Aundrietta Duncan and Kimiya Mermarzadeh for starting and continuing our wonderful GSA Officer family, and Alex Perakis for the continuous partnership in global domination.

Thank you to all of the past and present members of the van Hoof Lab, especially to Ale King for her initial guidance into both my thesis project and working with yeast. Also, shout-out to my three undergraduate mentees, Alex Morano, Jillian Vaught, and Keta Patel. I am so happy to have been your "Science Big Sister" and am immensely proud of all three of you! I will be forever thankful to

my long-term labmates, Jaeil Han and Minseon Kim for their endless supply of friendship, positivity, and support (and cat babysitting) over the years. Also, I want to extend a warm welcome to the newest van Hoovian, Jennifer Hurtig. I am happy and excited to leave the future of my project in your hands!

To Alex Marshall, my best friend and true soul sister: I am glad to have earned this degree, but I am equally glad to have gotten to sit back-to-back with you for 1 million years while we figured out how to get through grad school. I would do it with you for 100 million more years if the lab wasn't so cold.

Thank you to my father, Dan Losh, for just honestly being the best dad in the universe. Thank you to Uncle Richard, Aunt Carol, and my stepmom Becky for your sincere love and joy whenever I succeed at something. Thank you to my pets, Hooligan and Bubba, for keeping me humble and covered in fur. Gracias a toda mi familia Peruana, especialmente a Nora y William Ojeda, quienes me han apoyado, amado, y considerado una hija desde el comienzo.

To my husband, Matthew: Thank you for the constant encouragement, the fun, the food, and the unconditional love. I love you.

IDENTIFYING SUBUNIT ORGANIZATION AND FUNCTION OF THE NUCLEAR RNA EXOSOME MACHINERY

Jillian Strother Losh, A.S., B.S.

Advisory Professor: Ambro van Hoof, Ph.D.

The eukaryotic RNA exosome processes and degrades many classes of RNA. It is present in the nucleus and the cytoplasm, highly evolutionarily conserved, and essential for viability. Since the RNA exosome is such a significant component of the RNA degradation machinery, it is unsurprising that even single point mutations in a few of its subunits have been linked to human disease. For example, at least eight point mutations in a single subunit of the RNA exosome have been linked to pontocerebellar hypoplasia subtype 1b (PCH1b). My work has included the development of a laboratory model system to assess the specific effects of these mutations on the structure and function of the RNA exosome. My collaborators and I have employed the common model organism *Saccharomyces cerevisiae* for this work since both the RNA exosome and other components of RNA degradation machinery are conserved throughout eukaryotes. Our research has shown that at least one PCH1b-associated mutation negatively affects the stability of the RNA exosome, although it remains functional. The effect of this mutation is conserved between yeast and mouse cells.

The RNA exosome requires various cofactors in both the nucleus and the cytoplasm for substrate delivery. The other half of my work focuses on a nuclear cofactor of the RNA exosome, the TRAMP complex. This complex is comprised of an RNA helicase and a poly(A) polymerase, as well as an RNA-binding subunit. However, it is currently unclear how the TRAMP complex is specifically assembled and moreover, if it is essential for life. The poly(A) polymerase subunit consists of a catalytic domain, as well as disordered regions that

are required for protein interactions. My work has shown that the catalytic core of the TRAMP complex is necessary and sufficient for its essential functions, although a specific interaction between the two enzymatic subunits is required for snoRNA biogenesis and possibly other cellular functions. These and future studies will help define the role of the TRAMP complex in the RNA degradation process and determine its importance for cellular viability.

TABLE OF CONTENTS

	Page No.
Approval Sheet	i
Title Page	ii
Dedication	iii
Acknowledgements	iv
Abstract	vii
Table of Contents	ix
List of Figures	xii
List of Tables	xv
Chapter 1: Background and Significance	1
Background	
Eukaryotic RNA Degradation.....	2
<i>The Two Pathways of RNA Degradation</i>	3
Functions of the RNA Exosome.....	3
<i>Nuclear Functions</i>	4
<i>Cytoplasmic Functions</i>	6
Composition of the RNA Exosome.....	6
<i>RNA Exosome Structure</i>	6
<i>RNA Exosome Subunits</i>	9
Diseases Linked to RNA Exosome Dysfunction.....	11
Cofactors of the RNA Exosome.....	15
<i>Nuclear Cofactors</i>	17
<i>Cytoplasmic Cofactors</i>	19

Function of the TRAMP Complex.....	20
Composition of the TRAMP Complex.....	20
<i>Trf4 and Trf5 are Poly(A) Polymerases</i>	22
<i>Air1 and Air2 are RNA-Binding Proteins</i>	24
<i>Mtr4 is an RNA Helicase</i>	26
Conservation of the TRAMP Complex and Its Subunits.....	28
Diseases Linked to Dysfunctional Cofactors of the RNA Exosome.....	30
Significance	
Investigating the Impact of RNA Processing and Degradation on Cellular Physiology.....	31
Elucidating Interactions Within and Between the RNA Exosome and TRAMP Complex.....	31
 Chapter 2: Materials and Methods	 33
Materials	
Plasmids.....	34
Yeast Strains.....	36
Oligonucleotides.....	39
Methods	
Plasmid Cloning.....	42
Bacterial Transformation.....	42
Yeast Transformation.....	42
Yeast DNA Isolation.....	43
Yeast Homologous Recombination.....	43
Yeast Plasmid Shuffle Assay.....	45
Yeast Mating.....	45
Yeast Growth Assays.....	47
Yeast <i>his3-nonstop</i> Reporter Assay.....	48

Yeast Protein Isolation.....	48
Western Blotting.....	49
Yeast RNA Isolation.....	50
Northern Blotting.....	51
qRT-PCR.....	51
Transcriptome Sequencing.....	51
Multiple Sequence Alignment.....	52
Chapter 3: Assessing Human PCH1b-Associated Mutations with Yeast Models.....	54
Introduction.....	55
Results.....	61
Conclusions and Future Directions.....	86
Chapter 4: Identifying the Importance of Maintaining TRAMP Complex Assembly.....	96
Introduction.....	97
Results.....	105
Conclusions and Future Directions.....	144
Chapter 5: Final Conclusions and Perspectives.....	151
RNA Exosome Dysfunction Leads to Widespread Negative Cellular Effects.....	152
TRAMP Complex Subunit Interactions are Important for Maintaining Its Function.....	155
Concluding Remarks.....	159
Bibliography.....	160
Vita.....	190

LIST OF FIGURES

	Page No.
Chapter 1: Background and Significance	
1.1	Composition of the RNA exosome.....8
1.2	RNA exosome activity depends on many nuclear and cytoplasmic cofactors.....16
1.3	Composition of the TRAMP complex.....21
Chapter 3: Assessing Human PCH1b-Associated Mutations with Yeast Models	
3.1	Human and yeast nomenclature of RNA exosome subunits.....57
3.2	Protein sequence alignment of EXOSC3 orthologs.....62
3.3	PCH1b-associated substitutions occur at EXOSC3 residues located near RNA exosome subunit interfaces.....65
3.4	Yeast expressing <i>rrp40</i> -W195R or <i>rrp40</i> -W195A as the sole copy of Rrp40 exhibit impaired growth at 37°C.....67
3.5	Yeast expressing <i>rrp40</i> -W195R or <i>rrp40</i> -W195A as the sole copy of Rrp40 exhibit impaired growth in the presence of 5-fluorouracil (5-FU).....69
3.6	Yeast expressing <i>rrp40</i> -D152A as the sole copy of Rrp40 exhibit impaired growth at 37°C.....71
3.7	PCH1b-associated <i>rrp40</i> mutations do not impact cytoplasmic function of the RNA exosome.....74
3.8	PCH1b-associated <i>rrp40</i> mutations do not impact mitochondrial respiration.....76
3.9	Model for cooperation between the tRNA splicing endonuclease complex and the RNA exosome.....81
3.10	PCH1b-associated mutations do not interfere with the degradation of cleaved <i>CBP1</i> mRNA.....82

3.11	Expression of rrp4-G58V as the sole copy of Rrp4 in yeast is lethal but rrp4-G226D is not.....	85
3.12	Model for RNA exosome assembly and function.....	91

Chapter 4: Identifying the Importance of Maintaining TRAMP Complex Assembly

4.1	Model for TRAMP complex conformation and function.....	99
4.2	Protein sequence alignment of fungal Trf4/5 orthologs.....	103
4.3	Disrupting stable TRAMP complex formation does not affect the degradation of a cryptic unstable transcript.....	107
4.4	Disrupting stable TRAMP complex formation results in increased levels of 3' extended snoRNA species.....	110
4.5	Disrupting stable TRAMP complex formation results in a variety of snoRNA processing defects.....	117
4.6	Disrupting stable TRAMP complex formation does not significantly impair yeast cell growth.....	121
4.7	Trf4/5 protein variants that have lost the ability to interact with Mtr4 are expressed at wild-type levels.....	123
4.8	Disrupting stable TRAMP complex formation results in the overexpression of many snoRNA genes.....	125
4.9	Maintaining the Mtr4-Trf4/5 interaction is not increasingly important during heat stress.....	127
4.10	Maintaining the Mtr4-Trf4/5 interaction is not increasingly important during exposure to 5-fluorouracil.....	129
4.11	The N- and C-termini of Trf4/5 are not required for viability.....	131
4.12	Trf4/5 protein variants that lack the N- and C-termini are expressed at wild-type levels.....	133

4.13	Loss of both Trf4/5 N- and C-termini results in the overexpression of many snoRNA genes.....	135
4.14	The catalytic activity of Trf4/5 is required for viability.....	138
4.15	Model of TRAMP complex assembly in the presence or absence of the Mtr4-Trf4/5 interaction.....	140
4.16	An additional deletion of <i>AIR2</i> in Trf4/5 mutant strains results in growth impairment but not loss of viability.....	143

Chapter 5: Final Conclusions and Perspectives

5.1	Model of TRAMP complex activity when specific subunit interactions are lost.....	158
------------	--	-----

LIST OF TABLES

	Page No.
Chapter 1: Background and Significance	
1.1 RNA exosome subunits and cofactors implicated in human disease.....	14
Chapter 2: Materials and Methods	
2.1 Plasmids used in this study.....	35
2.2 Yeast strains used in this study.....	37
2.3 Oligonucleotides used in this study.....	40
Chapter 3: Assessing Human PCH1b-Associated Mutations with Yeast Models	
3.1 Subtypes of pontocerebellar hypoplasia (PCH).....	56
3.2 Major <i>EXOSC3</i> mutations in PCH1b patients.....	60
Chapter 4: Identifying the Importance of Maintaining TRAMP Complex Assembly	
4.1 Genes identified by RNA-Seq as overexpressed in cells lacking the Mtr4-Trf5 interaction.....	113

CHAPTER 1
Background and Significance

BACKGROUND

Eukaryotic RNA Degradation

Despite the variety of RNA within cells, nearly every type of transcript requires processing before becoming fully functional. RNA surveillance mechanisms are required to safeguard against deleterious events because both transcription and post-transcriptional modifications are error-prone, despite tight regulation. Eukaryotic RNA metabolism is an intricate system of RNA synthesis, processing, quality control, and degradation pathways. While mature transcripts are broken down into nucleotide monophosphates when they are no longer needed, quality control mechanisms ensure that aberrant RNA species are degraded as well.

In eukaryotes, there is a distinct difference between transcript and protein half-life, or the amount of time it takes for half of the original sample size to be degraded. For example, in *Saccharomyces cerevisiae* the average mRNA half-life is twenty minutes, in contrast with an average protein half-life of forty minutes (Wang *et al.*, 2002; Belle *et al.*, 2006). Moreover, the average mRNA half-life in human cells is ten hours, while the average protein half-life is thirty-six hours (Cambridge *et al.*, 2011; Schwanhäusser *et al.*, 2013). Cells must possess effective pathways of RNA degradation, as excess transcripts must be degraded in order to ensure continued cellular viability. In addition to out-competing necessary RNA for processing and interactions with transcription factors, surplus RNA in the nucleus can stimulate double-stranded breaks by binding to homologous regions on DNA (Wahba *et al.*, 2013). Therefore, cells must maintain mechanisms to rapidly clear even the most optimally transcribed and processed RNA species.

Aberrant transcripts arise due to many types of faulty gene expression and typically have defective structure or incorrect associations with proteins. Genetic mutations can lead to the transcription of RNA species with premature stop codons or no stop codons at all. Defective processing events, such as improper splicing, can also result in aberrant

transcripts. Since mistakes at many steps in the process of RNA biogenesis can lead to the formation of faulty RNA species, it is not surprising that they are targeted by the same degradation machinery that is involved in normal RNA turnover.

The Two Pathways of RNA Degradation

RNA can be degraded in either a 5'-3' or a 3'-5' direction. Both of these essential pathways are present in both the nucleus and cytoplasm. Moreover, each pathway contains ribonucleases (RNases), which can be further classified as 5' exoribonucleases, 3' exoribonucleases, or endoribonucleases. These RNase enzymes are capable of cleaving transcripts from RNA polymerase I, II, and III. While RNA polymerase I and III transcripts can be rapidly degraded from either end, the degradation of RNA polymerase II transcripts includes additional steps. Once an RNA polymerase II transcript has been deadenylated, which is a signal for degradation, 5'-3' RNA decay begins with the removal of the transcript's 5' cap. This allows for 5'-3' exoribonucleases to start degrading at the now-exposed 5' end. In contrast, exoribonucleases of the 3'-5' RNA decay pathway begin degrading at the deadenylated 3' end of transcripts. The RNA exosome contains the essential ribonuclease of the 3'-5' RNA degradation and processing pathway.

Functions of the RNA Exosome

The highly ubiquitous RNA exosome is a ten-subunit complex that is present in both the nucleus and the cytoplasm of cells (Allmang *et al.*, 1999a). Within multicellular eukaryotes, the RNA exosome is found within the cells of most types of tissues (Uhlén *et al.*, 2015). This complex contributes several essential functions to the intricate pathway of RNA metabolism. The RNA exosome processes precursor transcripts by trimming them at specific sites, leading to mature RNA products. It also contributes to the regulation of gene expression by degrading mature transcripts that are no longer needed. The RNA exosome is important for RNA quality control since it degrades aberrant transcripts as well.

Substrates of the RNA exosome for processing and/or degradation include nearly every type of RNA, including products of all three RNA polymerases (Allmang *et al.*, 1999b; Mitchell *et al.*, 1997; Wlotzka *et al.*, 2011). Moreover, this 3'-5' machinery targets transcripts produced by the additional two RNA polymerases found in plants (Shin *et al.*, 2013). The broad targeting characteristic of the RNA exosome is conserved throughout eukaryotes, highlighting the importance of this complex.

Nuclear Functions

The RNA exosome machinery targets many known types of non-protein-coding RNA (ncRNA). This large class of RNA includes two important components of protein translation machinery, ribosomal RNA (rRNA) and transfer RNA (tRNA). After its transcription, rRNA requires multiple rounds of processing in order to become part of a functional ribosome. Specifically, sequences for several mature rRNA species are included within precursor 35S rRNA. This precursor is additionally flanked by an external transcribed spacer (ETS) at each end. The RNA exosome is required for the degradation of the 5' ETS after it has been cleaved from the precursor RNA (de la Cruz *et al.*, 1998). The 35S rRNA is then cleaved into shorter precursors, such as 7S rRNA. The RNA exosome machinery is additionally required for further processing 7S rRNA into 3' extended precursor 5.8S rRNA (Briggs *et al.*, 1998; Allmang *et al.*, 1999b). The precursor 5.8S rRNA can then be exported to the cytoplasm, where it is further processed into its mature form (Thomson and Tollervey, 2010). The RNA exosome can also degrade the byproducts that arise when it processes rRNA. For example, it degrades 5' extended 21S and 23S rRNA intermediates that result during the processing of mature 18S rRNA (Allmang *et al.*, 2000). Additionally, precursor tRNA is one of the most highly targeted substrates of the nuclear RNA exosome (Schneider *et al.*, 2012). It is processed at its 3' end by the RNA exosome machinery, although the 5' ends of these transcripts can also be threaded through the central channel of the RNA exosome for degradation (Delan-Forino *et al.*, 2017). In addition to processing precursors or degrading

byproducts, the RNA exosome can degrade aberrant or unnecessary mature rRNA and tRNA in the nucleus (Zanchin and Goldfarb, 1999; Allmang *et al.*, 2000; Kadaba *et al.*, 2004; Wichtowska *et al.*, 2013; Delan-Forino *et al.*, 2017).

Like rRNA and tRNA, other examples of functionally characterized ncRNA include small nuclear and small nucleolar RNA (snRNA and snoRNA). snRNA is important for mRNA maturation, while snoRNA induces chemical modifications that are important for the maturation of rRNA, tRNA, and snRNA. The snoRNA class can be divided into two main subsets, C/D box and H/ACA box, which guide methylation or pseudouridylation modifications, respectively. After precursor snRNA transcripts are cleaved by the nuclease Rnt1, their 3' ends are exposed. This allows for specific bases to be removed by the RNA exosome machinery, leading to the formation of mature snRNA (Allmang *et al.*, 1999b; van Hoof *et al.*, 2000a). The RNA exosome machinery also trims the 3' end of many precursor snoRNA transcripts, regardless of whether they are independently transcribed or derived from introns (Allmang *et al.*, 1999b; van Hoof *et al.*, 2000a). As with other classes of transcripts, the RNA exosome can degrade snRNA and snoRNA that is aberrant or no longer needed.

The RNA exosome degrades several types of short, largely uncharacterized ncRNA, such as cryptic unstable transcripts (CUTs), promoter upstream transcripts (PROMPTs), and stable unannotated transcripts (SUTs) (Wyers *et al.*, 2005; Preker *et al.*, 2008; Marquardt *et al.*, 2011). These short transcripts, derived from intragenic and intergenic regions, may be involved in eukaryotic gene regulation or silencing. Intergenic transcripts that are over 200 nucleotides, known as long ncRNA (lncRNA), are also targeted by the nuclear RNA exosome (Wlotzka *et al.*, 2011). Additionally, the human RNA exosome can degrade transcription start site-associated RNA (xTSS-RNA) and upstream antisense RNA (uaRNA) in the nucleus (Flynn *et al.*, 2011; Pefanis *et al.*, 2014).

Finally, protein-coding messenger RNA (mRNA) can also be processed and degraded by the nuclear RNA exosome. The RNA exosome machinery is important for 3' end formation of some, but not all, precursor mRNA transcripts (Ciais *et al.*, 2008; Roth *et al.*, 2009). This 3' end modification is required for the maturation of these transcripts. As with ncRNA species, the RNA exosome can also degrade precursor and mature mRNA that is aberrant or unnecessary (Bousquet-Antonelli *et al.*, 2000).

Cytoplasmic Functions

In the cytoplasm, the RNA processing activity of the RNA exosome is not necessary. However, its role in cytoplasmic RNA degradation is important. The cytoplasmic RNA exosome will degrade mRNA that is no longer required, which helps regulate gene expression. Furthermore, it plays a role in cellular surveillance by degrading aberrant RNA species. These targets for cytoplasmic RNA exosome-mediated degradation include transcripts that cause long ribosomal pausing (no-go transcripts), possess premature stop codons (nonsense transcripts), lack in-frame stop codons (nonstop transcripts), or lack a poly(A) tail (van Hoof *et al.*, 2002; Lejeune *et al.*, 2003; Gatfield and Izaurralde, 2004; Orban and Izaurralde, 2005; Doma and Parker, 2006; Meaux and van Hoof, 2006). As in the nucleus, the cytoplasmic RNA exosome also targets CUTs and SUTs for degradation (Marquardt *et al.*, 2011).

Composition of the RNA Exosome

All ten subunits of the RNA exosome are essential for cellular viability. Moreover, the structure of the RNA exosome is conserved throughout eukaryotes. Its composition remains the same, regardless if the complex is in the nucleus or the cytoplasm.

RNA Exosome Structure

In *S. cerevisiae*, six protein subunits (Mtr3, Rrp41, Rrp42, Rrp43, Rrp45, and Rrp46) comprise the non-catalytic core ring of the RNA exosome (**Figure 1.1 A, B**). An RNA substrate is threaded through the central channel of this ring with its 3' end leading. Three

putative RNA-binding proteins (Csl4, Rrp4, and Rrp40) contact the core ring on the substrate's side of entry (**Figure 1.1 A, B**). Rrp44, the catalytic subunit of the RNA exosome, resides on the opposite side of the core ring (**Figure 1.1 A**). This subunit provides the complex with both endo- and exoribonuclease activities (Dziembowski *et al.*, 2007; Lebreton *et al.*, 2008; Schaeffer *et al.*, 2009; Schneider *et al.*, 2009).

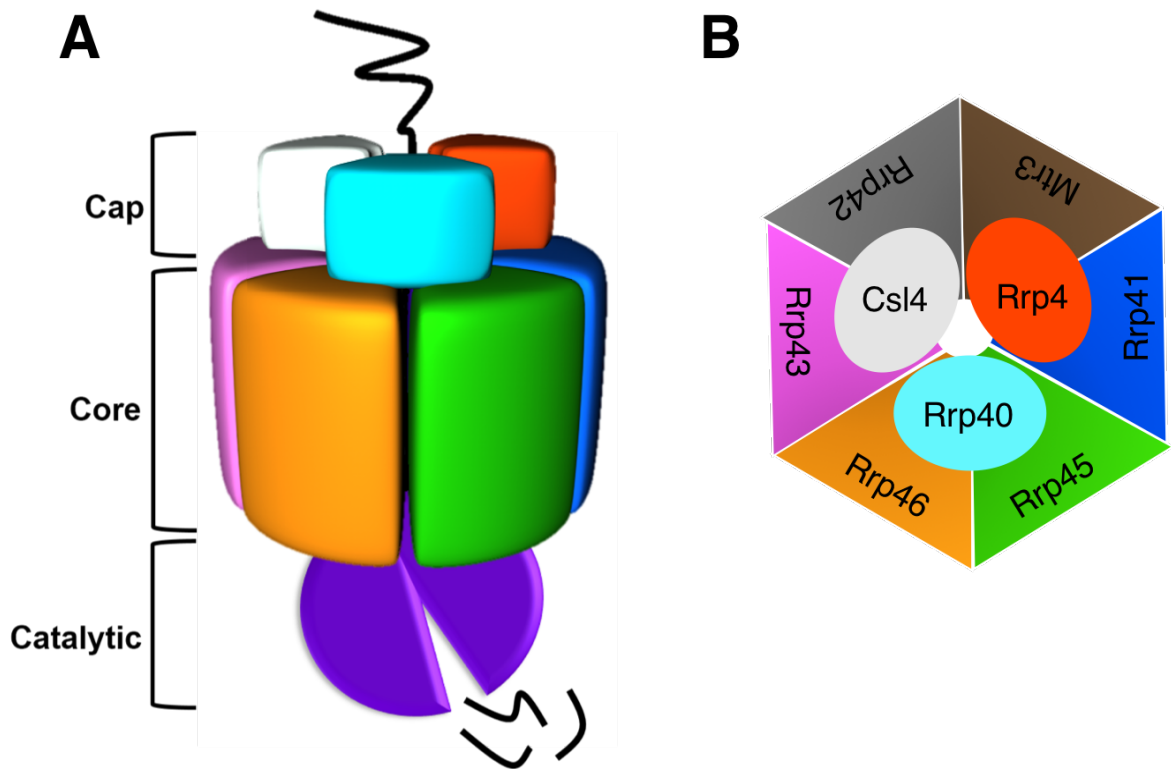


Figure 1.1 Composition of the RNA exosome. **(A)** The nine non-catalytic subunits of the RNA exosome are organized into the “cap” and “core” domains, through which an RNA is threaded through. The RNA substrate encounters the sole catalytic subunit, Rrp44, on the opposite side. The endo- or exoribonuclease activity of Rrp44 will ensure that the substrate is degraded or processed, as needed. **(B)** A view of the RNA exosome from a substrate’s site of entry. The three subunits of the RNA exosome cap (Csl4, Rrp4, Rrp40) possess RNA-binding capability and are believed to be important for feeding the substrate into the central channel of the core ring (Mtr3, Rrp41, Rrp42, Rrp43, Rrp45, Rrp46).

RNA Exosome Subunits

Several subunits of the RNA exosome, as well as RNA cofactors, were independently identified by multiple studies several years before the identification of the complex itself. Eight of the ten subunits of the RNA exosome now have an Rrp (ribosomal RNA processing) designation, although many of them were initially identified in a genetic screen for yeast mutants that were defective in nuclear mRNA transport (Kadowaki *et al.*, 1994). One subunit has retained its initial Mtr3 (mRNA transport) designation and was further identified in a screen for yeast mutants that accumulated polyadenylated RNA in the nucleolus (Kadowaki *et al.*, 1995). Another one of these subunits was later identified in a screen for yeast mutants that were not able to carry out the final step of rRNA maturation. This study designated this protein as Rrp44 and also characterized it as a 3'-5' ribonuclease (Mitchell *et al.*, 1996). Additionally, two RNA exosome subunits, Rrp41 and Csl4, were initially identified in a screen for yeast mutants that expressed viral toxins (Ridley *et al.*, 1984). In hindsight, these two mutant strains were likely expressing these toxins because their altered RNA exosomes were not able to degrade viral RNA.

The first study describing the RNA exosome as a multi-subunit complex comprised of these previously identified proteins was published twenty years ago (Mitchell *et al.*, 1997). Further studies indicated that it is the yeast homolog of the human PM-Scl complex, identified over a decade earlier (Reimer *et al.*, 1986; Allmang *et al.*, 1999a). However, the function of this human complex had not been well-characterized so the identification and detailed study of the yeast RNA exosome was a breakthrough in the field of RNA metabolism.

The six subunits of the core ring all have significant sequence homology to *Escherichia coli* RNase PH, a 3'-5' exoribonuclease that processes precursor tRNA into its mature form (Allmang *et al.*, 1999a; Wen *et al.*, 2005). Moreover, the barrel structure of the eukaryotic RNA exosome core is similar to the hexameric ring structure of RNase PH (Liu *et*

al., 2006). The archaeal RNA exosome also shares similar structure and 3'-5' catalytic activity with RNase PH (Evguenieva-Hackenberg *et al.*, 2003; Lorentzen *et al.*, 2005). However, unlike in archaea, the core subunits in yeast and animals do not maintain the catalytic function of this bacterial enzyme. Although they were also initially thought to be active ribonucleases, conserved mutations in their RNase PH-like catalytic sites have rendered the core subunits inactive in many eukaryotic genomes (Dziembowski *et al.*, 2007). Interestingly, a recent study using the common laboratory plant model, *Arabidopsis thaliana*, has shown that the RNA exosome core remains catalytic in this organism and perhaps in other plants as well. This study also included sequence analysis, which indicated that core RNA exosome subunits may have retained catalytic activity in several amoeboid protists (Sikorska *et al.*, 2017). Therefore, it is possible that loss of this catalytic activity in the RNA exosome core is unique to the animal and fungal branches of Eukaryota, although significant sequence and functional analyses would be required to elucidate this.

Rrp4, Rrp40, and Csl4 comprise the “cap” of the RNA exosome. Each of these attach to two specific subunits of the core ring (**Figure 1.1 B**) (Liu *et al.*, 2006). These three proteins have putative individual RNA-binding activity, which is enhanced by their cooperative binding. Rrp4 and Rrp40 both contain similar terminal and central domains. Specifically, their central S1 domain and C-terminal KH domains are the most likely sites for RNA-binding (Oddone *et al.*, 2007). Yet despite their general structural similarity, both full-length proteins are required for viability (Schaeffer *et al.*, 2009). Csl4 has the same N-terminal and central domains as Rrp4 and Rrp40, but its C-terminus contains a zinc-ribbon domain. Interestingly, the zinc-ribbon domain is the only essential region of Csl4. Moreover, this domain is only required for cytoplasmic mRNA decay, but not for RNA exosome structure or its nuclear functions (Schaeffer *et al.*, 2009). By interacting with an RNA and/or the cofactor protein that is delivering it to the RNA exosome for processing or degradation,

these three cap subunits independently provide the RNA exosome with the ability to accept different substrates.

Rrp44, the catalytic subunit of the RNA exosome, has been identified as a homolog of *E. coli* RNase R, a 3'-5' exoribonuclease that selectively targets mRNA (Mitchell *et al.*, 1997; Cheng and Deutscher *et al.*, 2005). As previously stated, Rrp44 functions as both an endo- and exoribonuclease. These domains are at least partially redundant, since only one functional ribonucleolytic domain is required to maintain cellular viability (Lebreton *et al.*, 2008; Schaeffer *et al.*, 2009). The endoribonuclease domain is located within the N-terminus of Rrp44. However, this region also has an essential structural function since it is required for attaching Rrp44 to the core ring of the RNA exosome (Schaeffer *et al.*, 2009; Schneider *et al.*, 2009). The C-terminus of Rrp44, which contains the exoribonuclease domain, resides at the exit site of the complex's central channel.

In addition to the well-characterized model of a substrate's entry and exit through the central channel of the RNA exosome, recent models have shown that RNA can come into direct interaction with Rrp44 without passing through the rest of the complex (Liu *et al.*, 2014; Han and van Hoof, 2016). This requires a conformational change of the RNA exosome. While direct interaction with the catalytic Rrp44 subunit seems like a more straightforward process than entering the central channel, this alternative RNA exosome conformation has limited activity. Specifically, it is only reported to be important for the degradation of 5S rRNA and tRNA within the nucleus (Han and van Hoof, 2016). However, this highlights the multifaceted specificity of the RNA exosome, in terms of its cellular location, substrates, and ability to process or degrade.

Diseases Linked to RNA Exosome Dysfunction

Since the RNA exosome is such a significant component of the RNA processing and degradation machinery, it is not surprising that even single point mutations in a few of its subunits have been linked to deleterious phenotypes in humans (**Table 1.1**). Humans have

three Rrp44 variant orthologs, known as DIS3, DIS3L (Dis3-like), and DIS3L2. Although yeast Rrp44 is associated with both the nuclear and cytoplasmic RNA exosome, DIS3 is specifically nuclear. DIS3L and DIS3L2 are cytoplasmic, although only DIS3L is believed to interact with the human RNA exosome core (Lubas *et al.*, 2013; Malecki *et al.*, 2013). While DIS3L2 does not bind to the RNA exosome core, inactivation of the *DIS3L2* gene results in Perlman syndrome, a serious disorder characterized by enlarged organs and increased risk for kidney tumors (Astuti *et al.*, 2012).

Mutations in *DIS3* are associated with multiple myeloma (Tomecki *et al.*, 2014). Recurrent mutations in this gene have also been implicated in acute myeloid leukemia relapse (Ding *et al.*, 2012). Decreased *DIS3* gene expression was recently linked to an increased risk of pancreatic cancer (Hoskins *et al.*, 2016). As this is the only catalytic subunit of the RNA exosome, it is not unexpected that it is linked to such serious phenotypes. However, several subunits of the RNA exosome cap and barrel have been connected to very different symptoms, mainly neurological.

Mutations in at least two RNA exosome subunits lead to pontocerebellar hypoplasia (PCH), a rare group of neurodegenerative conditions that are all primarily characterized by an atrophied cerebellum and pons. Autosomal recessive mutations in the RNA exosome cap subunit EXOSC3 and core subunit EXOSC8 cause PCH type 1b and 1c, respectively (Wan *et al.*, 2012; Boczonadi *et al.*, 2014). These proteins are the human orthologs of yeast Rrp40 and Rrp43. A recessive mutation in another core subunit, EXOSC9/Rrp45, has recently been shown to result in PCH phenotypes as well, although it has not yet been definitively linked to a PCH subtype (Donkervoort *et al.*, 2017). In addition to brain abnormalities, PCH patients typically exhibit spinal motor neuron degeneration and widespread muscular atrophy. Most patients do not live past early childhood.

Recently, a third structural subunit of the RNA exosome was associated with human phenotypes. Mutations in cap subunit EXOSC2/Rrp4 cause premature aging, retinal

deformities, hypothyroidism, and other mild physical and mental disabilities (Di Donato *et al.*, 2016). Collectively, these phenotypes are now considered to be a unique disorder, recently termed SHRF (short stature, hearing loss, retinitis pigmentosa, and distinctive facies). Interestingly, these symptoms are very different from those caused by mutations in the EXOSC3/Rrp40 subunit of the RNA exosome cap. This is somewhat unexpected, due to the functional and structural similarities between these two cap proteins. One possibility for explaining these phenotypic variations is that these disease-associated mutations may interfere with different interactions that take place between the RNA exosome and its many cofactors. Human diseases that are associated with RNA exosome cofactors will be discussed later in this chapter.

Table 1.1 RNA exosome subunits and cofactors implicated in human disease		
Human Disease	RNA Exosome-Associated Protein	Reference
Acute myeloid leukemia	DIS3	(Ding <i>et al.</i> , 2012)
Multiple myeloma	DIS3	(Tomecki <i>et al.</i> , 2014)
Pancreatic cancer	DIS3	(Hoskins <i>et al.</i> , 2016)
Perlman syndrome	DIS3L2	(Astuti <i>et al.</i> , 2012)
SHRF disorder	EXOSC2	(Di Donato <i>et al.</i> , 2016)
Pontocerebellar hypoplasia type 1b	EXOSC3	(Wan <i>et al.</i> , 2012)
Pontocerebellar hypoplasia type 1c	EXOSC8	(Boczonadi <i>et al.</i> , 2014)
Pontocerebellar hypoplasia-like phenotypes	EXOSC9	(Donkervoort <i>et al.</i> , 2017)
Spinal motor neuropathy	RBM7	(Giunta <i>et al.</i> , 2016)
Trichohepatoenteric syndrome	SKI2	(Fabre <i>et al.</i> , 2012)
Trichohepatoenteric syndrome	SKI3	(Hartley <i>et al.</i> , 2010)

Table 1.1 RNA exosome subunits and cofactors implicated in human disease. Mutations in the genes encoding components of the RNA exosome machinery have been linked with a variety of human phenotypes. Catalytic subunits (DIS3, DIS3L2) are primarily associated with cancerous symptoms, while mutations in several non-catalytic subunits (EXOSC3, EXOSC8, EXOSC9) and a nuclear cofactor (RBM7) are associated with neurological abnormalities. However, mutations in an additional RNA exosome subunit (EXOSC2) and components of a cytoplasmic cofactor complex (SKI2, SKI3) are implicated in diseases with widespread, varied phenotypes.

Cofactors of the RNA Exosome

While the structure and composition of the RNA exosome remain the same in both the nucleus and the cytoplasm, the cofactors that interact with this complex differ between these cellular locations (**Figure 1.2**). Furthermore, substrates of the RNA exosome vary greatly in length, sequence, and structure so it has long been hypothesized that interactions with cofactors help determine the fate of a targeted transcript. Several *in vitro* assays with purified RNA exosome have indicated that this complex only possesses distributive enzymatic activity, meaning that it catalyzes only one reaction upon encountering a substrate before disassociation occurs. This supports the hypothesis that the RNA exosome is dependent upon cofactors for its catalytic activation (Chlebowski *et al.*, 2010). Indeed, the RNA exosome appears to be mostly catalytically inactive in the absence of cofactors, which may be a method of preventing inappropriate reactions with RNA substrates (Mitchell *et al.*, 1997). Here I will discuss the most characterized RNA exosome cofactors although, due to its importance and functional variety, the RNA exosome likely has cofactors which have yet to be identified.

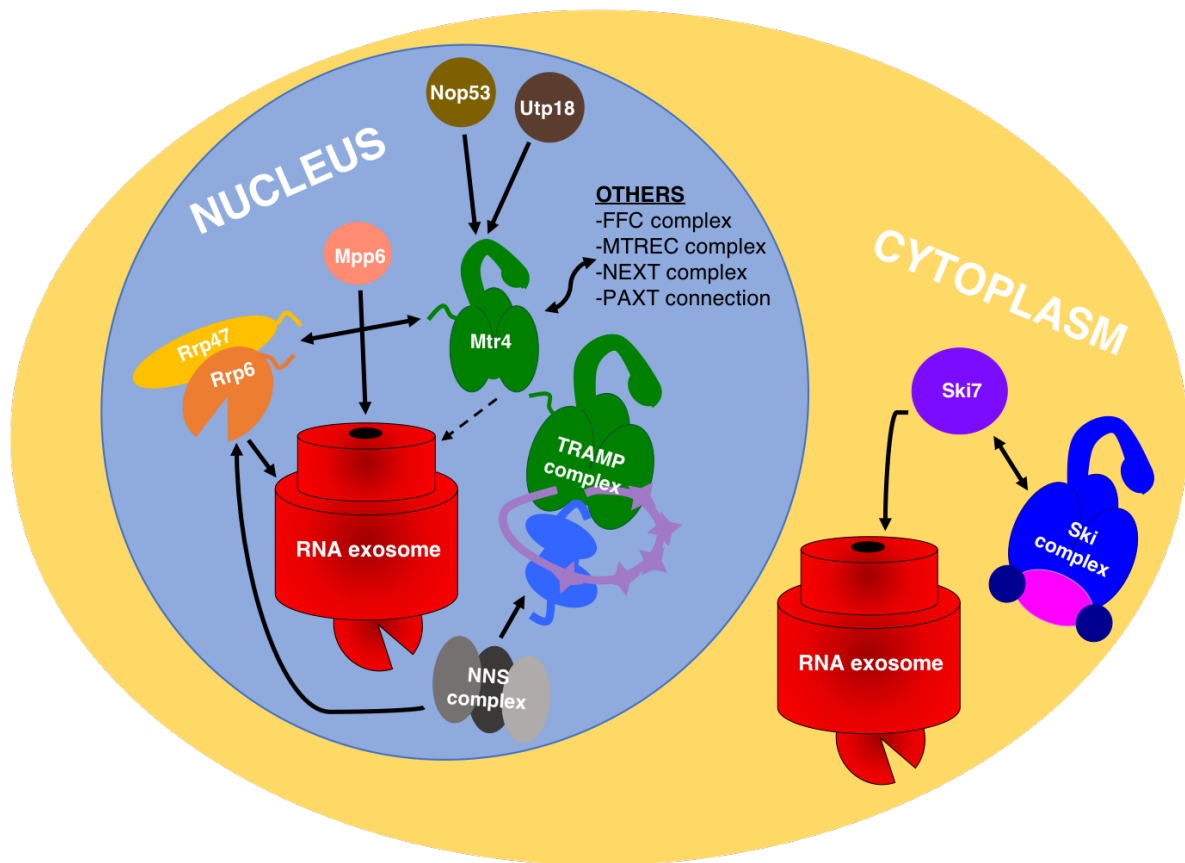


Figure 1.2 RNA exosome activity depends on many nuclear and cytoplasmic cofactors. Collectively, these cofactors carry out several functions, including identifying, binding, tagging, unwinding, and delivering substrates to the RNA exosome. Direct interaction or substrate handoff between cofactors and the RNA exosome are indicated by solid arrows. While several cofactors have been identified as assembled complexes, others directly interact with each other. For example, interactions between the N-termini of Mtr4 and the N-termini of the Rrp6-Rrp47 heterodimer, as well as with Mpp6, presumably occur when Mtr4 is and is not incorporated into the TRAMP complex. Mtr4 also contains conserved residues on its bottom face that may allow for direct interaction with the RNA exosome cap, although this interaction has not yet been definitively identified (dashed arrow). In addition to incorporation within the TRAMP complex, homologs of Mtr4 are also present within other human and fungal complexes, which will be discussed later in this chapter.

Nuclear Cofactors

Yeast Rrp6 is a prominent RNA exosome cofactor, as is its human homolog PM/Scf-100 (Briggs *et al.*, 1998; Allmang *et al.*, 1999a). To ensure continued efficiency, RNA processing and degradation pathways typically contain RNases with overlapping activities. Rrp6 is one such example as it is a 3'-5' exoribonuclease, although it is nonessential (Briggs *et al.*, 1998). As previously mentioned, many subunits of the RNA exosome maintain homology with *E. coli* RNA degradation machinery. Interestingly Rrp6 is homologous to RNase D, one of the seven 3'-5' exoribonucleases present in *E. coli* (Briggs *et al.*, 1998). Rrp6 is important for the processing of 5.8S rRNA, snRNA, and snoRNA (Allmang *et al.*, 1999b; van Hoof *et al.*, 2000a). Upon binding to an additional small protein, Rrp47, it can aid the nuclear RNA exosome in both processing and degradation activities (Mitchell *et al.*, 2003). During this interaction with Rrp6, Rrp47 is able to bind structured regions of RNA, as well as DNA, although this binding affinity is not particularly strong (Stead *et al.*, 2007). However, it has been previously shown that Rrp6 alone lacks the ability to fully degrade transcripts that contain secondary structures (Liu *et al.*, 2006). Therefore, it is possible that this catalytic function of Rrp6 is significantly improved when bound to Rrp47, despite a weak interaction between Rrp47 and a structured substrate. In addition to targeting RNA, an Rrp6-Rrp47 dimer that is already bound to an RNA exosome can also bind to the N-terminus of an essential RNA helicase, Mtr4, allowing it to interact with the RNA exosome as well (Schuch *et al.*, 2014) (**Figure 1.2**).

Another RNA exosome cofactor, Mpp6, targets aberrant precursor mRNA, rRNA, and other ncRNA species for degradation in the nucleus (Milligan *et al.*, 2008). Mpp6 is not essential, although deleting it results in transcript accumulation. Studies in both humans and yeast have revealed its unique binding preference for poly(U) and poly(C) regions (Schilders *et al.*, 2005; Milligan *et al.*, 2008). Recent structural assays confirmed that Mpp6 directly binds to Rrp40, one of the cap subunits of the RNA exosome, as well as to the Rrp6-Rrp47

heterodimer (**Figure 1.2**). Interestingly, when Mpp6 is bound to the Rrp6-Rrp47 heterodimer, the Mtr4 helicase delivered transcripts to the RNA exosome more efficiently (Wasmuth *et al.*, 2017; Falk *et al.*, 2017a). This indicates that, in addition to its own RNA-binding capabilities, Mpp6 is also able to position the Rrp6-Rrp47 heterodimer and Mtr4 in such a way that improves substrate delivery into the central channel of the RNA exosome.

Mtr4 was one of the first proteins considered to be a possible nuclear cofactor of the RNA exosome because the levels of RNA that accumulated in a temperature sensitive *mtr4* mutant yeast strain were similar to the levels detected in RNA exosome mutant strains (Kadowaki *et al.*, 1994; Liang *et al.*, 1996). This essential RNA helicase is required for 5.8S rRNA maturation because it must unwind 7S rRNA, which allows the precursor transcript to be processed by the RNA exosome and subsequently, exported from the nucleus for final maturation steps (de la Cruz *et al.*, 1998; Schuller *et al.*, 2018). Furthermore, it has an important role in snRNA and snoRNA processing (van Hoof *et al.*, 2000a).

Although Mtr4 can directly bind RNA, it is also able to directly bind other nuclear proteins, such as the previously mentioned Rrp6-Rrp47 dimer. Mtr4 also interacts with ribosomal biogenesis proteins, Nop53 and Utp18, indicating that it is involved in the delivery of pre-ribosomal substrates to the RNA exosome (Thoms *et al.*, 2015) (**Figure 1.2**). In addition to its importance in 3'-5' RNA processing, Mtr4 also has a role in 3'-5' RNA degradation. It can bind with Trf4/5 and Air1/2 to form the heterotrimeric TRAMP complex, which will be discussed in detail later in this chapter (**Figure 1.2**). This RNA exosome cofactor adds a short poly(A) tail to its bound targets, which promotes appropriate and specific 3'-5' RNA degradation (LaCava *et al.*, 2005). Within the TRAMP complex, the helicase activity of Mtr4 unwinds these targets, resulting in the delivery of a linear, polyadenylated substrate to the RNA exosome.

The TRAMP complex can additionally assist another nuclear RNA exosome cofactor, the heterotrimeric Nrd1-Nab3-Sen1(NNS) complex, by polyadenylating and unwinding

substrates of the NNS complex that are destined for degradation (Tudek *et al.*, 2014; Fasken *et al.*, 2015) (**Figure 1.2**). The NNS complex is important for the termination of various types of non-coding RNA transcribed by RNA polymerase II (Thiebaut *et al.*, 2006; Schulz *et al.*, 2013). Nab3 and Nrd1 bind transcripts at specific sequences that are four bases long (Carroll *et al.*, 2004). The helicase, Sen1, carries out ATP hydrolysis to dissociate the targeted transcript from the RNA polymerase II complex (Porrua and Libri, 2013). The transcripts targeted by the NNS complex are then delivered to Rrp6 and/or the RNA exosome to be processed or degraded (Vasiljeva and Buratowski, 2006; Fox *et al.*, 2015) (**Figure 1.2**). Yet while the NNS complex has been well characterized in *S. cerevisiae*, it is not clear if this RNA exosome cofactor is conserved in other eukaryotes. SETX has been described as the human homolog of Sen1, but no homologs of Nab3 and Nrd1 have been identified in the human genome. Interestingly, at least ten mutations in the *SETX* gene cause phenotypes similar to those associated with *EXOSC3*, *EXOSC8*, and *EXOSC9* mutations in the RNA exosome (Moreira *et al.*, 2004).

Cytoplasmic Cofactors

The SKI complex, a cytoplasmic RNA exosome cofactor, has a somewhat similar composition to the TRAMP complex and also plays a role in RNA degradation. In fact, the RNA exosome requires the SKI complex for all of its cytoplasmic activities (Jacobs Anderson and Parker, 1998; van Hoof *et al.*, 2002; Mitchell and Tollervey, 2003; Doma and Parker, 2006). Like the TRAMP complex, it is multimeric and contains an RNA helicase, Ski2, which belongs to the same protein family as Mtr4 (Jacobs Anderson and Parker, 1998; Brown *et al.*, 2000). Its other subunits are the scaffolding protein Ski3 and a dimer of Ski8 (Wang *et al.*, 2005; Synowsky and Heck, 2008). However, unlike the TRAMP complex, the SKI complex does not polyadenylate its targets nor can it make direct deliveries to the RNA exosome on its own. For the latter function, it requires Ski7 (Araki *et al.*, 2001) (**Figure 1.2**).

Ski7 is not essential, but its deletion does cause a significant defect in mRNA degradation (van Hoof *et al.*, 2000b). This protein brings the SKI complex in proximity with the cytoplasmic RNA exosome so that substrate degradation can occur. Specifically, the N-terminus of Ski7 binds to Ski3 and Ski8, as well as to the cytoplasmic RNA exosome (Araki *et al.*, 2001; Wang *et al.*, 2005).

Function of the TRAMP Complex

The Trf4/Air2/Mtr4 polyadenylation complex was first identified in 2005 and additional subunits, Trf5 and Air1, were isolated soon after (LaCava *et al.*, 2005; Houseley and Tollervey, 2006). Its unique ability to add a short poly(A) tail, which acts as a signal for degradation, and further unwind the substrate in preparation for the RNA exosome highlights its usefulness in promoting efficient RNA degradation.

The TRAMP complex targets products from RNA polymerases I, II, and III (Wyers *et al.*, 2005; Wlotzka *et al.*, 2011). Specifically, these substrates include aberrant mRNA, rRNA, snRNA, snoRNA, and tRNA transcripts (LaCava *et al.*, 2005; Rougemaille *et al.*, 2007; Grzechnik and Kufel, 2008; San Paolo *et al.*, 2009). Additionally, this complex has been implicated in the degradation of the relatively uncharacterized transcripts, CUTs and SUTs (Wyers *et al.*, 2005; San Paolo *et al.*, 2009; Xu *et al.*, 2009). Like the RNA exosome, this wide variety of substrates emphasizes the importance of the TRAMP complex in the process of RNA degradation.

Composition of the TRAMP Complex

Each TRAMP complex is comprised of one non-canonical poly(A) polymerase (Trf4 or Trf5), one RNA-binding protein (Air1 or Air2), and the RNA helicase Mtr4 (**Figure 1.3**).

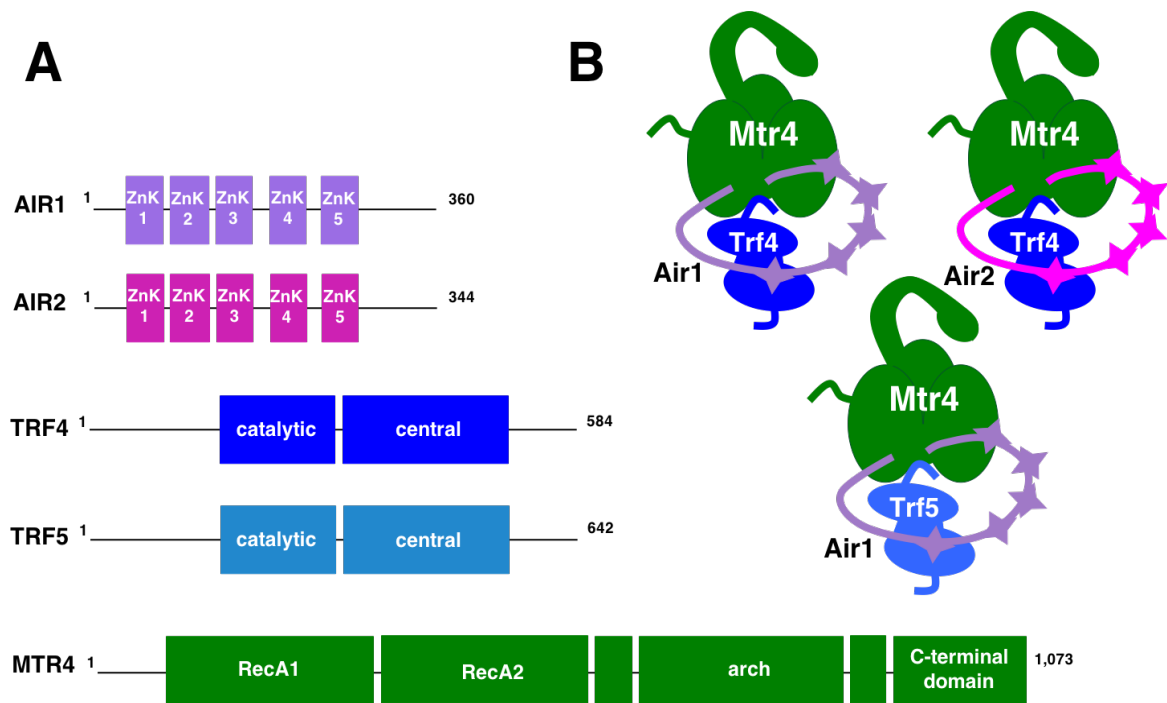


Figure 1.3 Composition of the TRAMP complex. **(A)** Each subunit of the TRAMP complex has defined domains, which provide the complex with its overall ability to bind an RNA (Air1/2), add a poly(A) tail (Trf4/5), and unwind it (Mtr4) so that it can be more easily threaded into the RNA exosome. **(B)** There are three possible conformations of the TRAMP complex. While Mtr4 is present in every conformation, only one poly(A)polymerase (Trf4 or Trf5) and one RNA-binding subunit (Air1 or Air2) are needed to complete the heterotrimer. Air1 forms a complex with both Trf4 and Trf5, but Air2 has only been shown to interact with Trf4.

Trf4 and Trf5 are Poly(A) Polymerases

Trf4 and Trf5 (DNA topoisomerase I-related function) are paralogs that arose from a whole-genome duplication event that occurred 100 million years ago in an ancestor of *S. cerevisiae* (Kellis *et al.*, 2004; Byrne and Wolfe, 2005). They share 55% identity and 72% sequence similarity. Although single deletion strains are viable, the loss of both polymerases results in lethality (Castaño *et al.*, 1996).

While we now know their role in 3'-5' RNA degradation, Trf4/5 were first associated with topoisomerase activity, as indicated by their name. Topoisomerase I and II work together as a swiveling apparatus that prevents supercoils, which can impede DNA replication. In yeast, these enzymes also employ the swiveling mechanism during transcription of mRNA and rRNA (Brill *et al.*, 1987). While the yeast topoisomerase II enzyme (Top2) is essential, the Top1 enzyme is not. This is surprising since both enzymes are involved in and important for replication and transcription. Trf4 was first identified in a 1995 study, which attempted to identify genes whose products had overlapping functions with Top1, or were dependent upon it (Sadoff *et al.*, 1995). The following year, the same group identified the *TRF5* gene and characterized the similarity of Trf4 and Trf5 (Castaño *et al.*, 1996).

The first assays performed after the identification of Trf4 revealed that *trf4* and *top1* mutant strains exhibited similar phenotypes, but the same phenotypes were not seen when comparing *trf4* and *top2* mutant strains. Furthermore, *trf4* mutants exhibited unaltered Top2 activity (Sadoff *et al.*, 1995). These data indicated that Trf4 could be important for a function of Top1 that is distinct from the characterized Top1-Top2 swivel mechanism. Trf5 was included in further studies, as its expression rescued the synthetic lethality of a *trf4* Δ , *top1* Δ strain. Double *trf4*, *top1* mutants had previously indicated a genetic interaction with mitotic checkpoint protein Mad1 and both *trf4* and *trf5* mutant strains were found to be hypersensitive to thiabendazole, an anti-microtubule drug. Therefore, it was hypothesized

that Trf4/5 and Top1's common function may be important during a late step of chromatin assembly (Sadoff *et al.*, 1995; Castaño *et al.*, 1996).

Several years later, the Trf4/5 proteins were functionally characterized as poly(A) polymerases. While results of the earliest studies indicated that these proteins had DNA polymerase activity, Trf4/5 are only able to polyadenylate RNA (Wang *et al.*, 2000; Haracska *et al.*, 2005; Vaňáčková *et al.*, 2005). Moreover, they only target RNA that is aberrantly folded (Vaňáčková *et al.*, 2005). Poly(A) polymerases catalyze reactions between ATP and RNA that culminate in an ADP byproduct and the addition of an extra adenosine to the transcript's 3' end. Sequence alignments of Trf4/5 revealed that these proteins have the same domains as other known nuclear poly(A) polymerases. Specifically, these similar features include the central domain, a strand loop motif, and a conserved N-terminal catalytic region (**Figure 1.3 A**). However, one key difference between Trf4/5 and other nuclear poly(A) polymerases is the lack of an RNA-binding domain in the Trf4/5 protein sequence (Vaňáčková *et al.*, 2005).

Trf4/5 function also differs from that of canonical poly(A) polymerases because substrates of the TRAMP complex are given a short 3' end poly(A) tail. While long poly(A) tails added to eukaryotic transcripts by canonical poly(A) polymerases act to protect against premature degradation and promote nuclear export, these short destabilizing tails are functionally homologous to those added by poly(A) polymerase I in *E. coli* (O'Hara *et al.*, 1995). The average tail length of yeast transcripts is twenty-seven nucleotides, but these short tails added by Trf4/5 within the TRAMP complex are only an average length of four nucleotides (Wlotzka *et al.*, 2011; Subtelny *et al.*, 2014). This polyadenylation-linked degradation was likely retained in the nucleus after the evolution of the nuclear membrane. It is possible that these short tails act as a site of initial attachment for a ribonuclease since it is difficult for these enzymes to begin degrading at RNA secondary structures (Cheng and Deutscher, 2005).

In addition to the well-defined poly(A) polymerase activity of Trf4/5, these proteins may have a TRAMP complex-independent role in DNA damage repair. Synthetic-lethal interactions have been reported between Trf4/5 and several proteins involved in DNA repair (Houseley and Tollervey, 2011). Moreover, *in vitro* assays have indicated that Trf4 may have DNA repair activity. Specifically, its C-terminus contains a lyase domain, which could allow for contact with damaged DNA and aid in abasic residue excision (Gellon *et al.*, 2008). The reported base excision repair activity of Trf4 and Trf5 was not identical, which could be a basis for incomplete functional redundancy between these proteins.

However, distinctive substrate targeting provides a more striking explanation for a lack of complete functional redundancy between Tr4/5. Microarray analysis revealed very little overlap between Trf4 and Trf5 substrates (San Paolo *et al.*, 2009). Specifically, this study compared gene expression in wild-type cells with that of *trf4* Δ or *trf5* Δ strains. However, the reason behind this substrate disparity is unclear, since both proteins are able to polyadenylate species belonging to every class of RNA that is known to be targeted by the TRAMP complex. A likely explanation is that the Air1/2 subunits of the TRAMP complex determine the substrate preference of Trf4/5, since Air1/2 have the ability to directly bind RNA.

Air1 and Air2 are RNA-Binding Proteins

As in the case of Trf4/5, Air1 and Air2 (arginine methyltransferase-interacting RING finger) are paralogs that resulted from the yeast whole-genome duplication (Kellis *et al.*, 2004; Byrne and Wolfe, 2005). Their sequences are 45% identical to each other (Inoue *et al.*, 2000). While the loss of both proteins does not result in lethality, an *air1* Δ , *air2* Δ double mutant exhibits a severe slow-growth phenotype. This growth defect can be rescued by complementation with either protein (Inoue *et al.*, 2000).

When initially identified, the Air1/2 proteins were not linked to RNA degradation. Instead, they were first implicated in the methylation of Npl3 by Hmt1 (Inoue *et al.*, 2000).

Npl3 is important for mRNA export from the yeast nucleus, as well as pre-mRNA splicing (Kadowaki *et al.*, 1994; Kress *et al.*, 2008). Npl3 can be methylated by the arginine methyltransferase Hmt1, which alters how it interacts with substrates (Siebel and Guthrie, 1996). Specifically, these regions of Npl3 are arginine-glycine-rich (RGG) domains. A screen for proteins that could interact with both Npl3 and Hmt1 revealed both Air1 and Air2 (Inoue *et al.*, 2000).

Air1/2 each contain five zinc knuckle domains that bind exposed guanosine residues on RNA (D'Souza and Summers, 2005; Hamill *et al.*, 2010) (**Figure 1.3 A**). NMR titration experiments have revealed that the second, third, and fourth zinc knuckles (ZnK2-4) bind to RNA (**Figure 1.3 B, pink and purple stars**). Moreover, the fourth linker region and the fifth zinc knuckle (ZnK5) interact with the central domain of Trf4, and likely Trf5 as well (Holub *et al.*, 2012). Trf4 interacts with both Air1/2 proteins, yet Trf5 has only been shown to interact with Air1, resulting in three possible compositions of the TRAMP complex (Wyers *et al.*, 2005; Houseley and Tollervey, 2006) (**Figure 1.3 B**). One explanation for this is that other than the conservation of ZnK5 and a short IWRxYxL motif within the fourth linker region, the sequence of the hypothesized Tr4/5-interaction region varies greatly between the Air1/2 proteins (Hamill *et al.*, 2010). The presence of Air1/2 stimulates the poly(A) polymerase activity of Trf4/5, which is understandable because Trf4/5 are not believed to have direct RNA-binding capabilities (Wyers *et al.*, 2005; Fasken *et al.*, 2011). Therefore, within the TRAMP complex, the presence of the Air1/2 subunit is likely required for establishing contact between a substrate and the Trf4/5 subunit.

Air1 and Air2 can each bind various classes of RNA and consequently, have an important role in determining substrate specificity of both the TRAMP complex and the RNA exosome. Yet Air1/2 have only partial functional redundancy, as they each target distinct snoRNA and mRNA transcripts. In comparison to Air1, RNA-Seq analysis indicated that Air2 preferentially targets precursor snoRNA species and mRNA transcripts that are important for

metabolic or iron-response pathways (Schmidt *et al.*, 2012). However, elucidating the substrate preferences of each Air1/2 protein is not straightforward, since Air1 is still able to target snoRNA and mRNA species.

The N- and C-termini of Air1/2 may be important for TRAMP complex formation. Upon identification of the TRAMP complex, conflicting experimental results could not clarify if a direct interaction between Mtr4 and Air1/2 exists (LaCava *et al.*, 2005). However, later analyses indicated the presence of an Mtr4-Air2 interaction. Removal of the first twenty-five residues of the Air2 N-terminus completely abolishes interaction with Mtr4 and deletion of the entire C-terminus severely weakens it (Holub *et al.*, 2012). The importance of the termini for this interaction with Mtr4 is unexpected since these regions are poorly conserved, especially in comparison to the zinc knuckle sequences. Multiple structural and binding analyses have indicated that Air1/2 can interact with Mtr4 at multiple sites (Falk *et al.*, 2014; Losh, King *et al.*, 2015; Losh and van Hoof, 2015; Falk *et al.*, 2017b).

Mtr4 is an RNA Helicase

As previously mentioned, Mtr4 (mRNA transport) is an essential, ATP-dependent RNA helicase. Therefore, in the presence of ATP, this enzyme can unwind RNA secondary structures into a linear form that is more conducive for degradation. This linearization is especially ideal for loading a substrate into the narrow channel of the RNA exosome. Mtr4 was first identified in two studies focused on characterizing yeast mutants that exhibited nuclear accumulation of polyadenylated RNA (Kadowaki *et al.*, 1994; Liang *et al.*, 1996). As mentioned earlier in this chapter, Mtr4 is involved in targeting several different classes of RNA for RNA exosome-mediated processing or degradation, either as an independent cofactor or as a member of a cofactor complex.

Mtr4 is a member of the DExH/D family of ATP-dependent helicases, also known as DEAD-box helicases (Weir *et al.*, 2010). The core of Mtr4 is comprised of two RecA domains, which are typical regions of ATP hydrolysis and nucleotide binding (**Figure 1.3 A**).

Specifically, RNA helicases separate self-annealed transcripts by using energy from ATP hydrolysis to disrupt hydrogen bonds that have formed between nucleotides. The helicase activity of Mtr4 is provided by a DExH motif located within the C-terminal catalytic domain (**Figure 1.3 A**). To be unwound, an RNA substrate passes through a channel formed by the core domains of Mtr4. There is a site on the bottom face of the Mtr4 core, opposite from its characteristic arch domain, which is the most likely region for unwound RNA to exit from. Interestingly, the sequence of this bottom face is highly conserved and is about the same diameter as the RNA exosome cap (Jackson *et al.*, 2010). Mtr4 co-purifies with the RNA exosome and has recently been shown to specifically contact the RNA exosome cap subunit, Rrp4 (Chen *et al.*, 2001; Schuller *et al.*, 2018) (**Figure 1.2**). This region of Mtr4 may be a site of direct interaction with the RNA exosome, however this interaction may be dependent upon other proteins. As previously stated, the N-terminus of Mtr4 interacts with the N-termini of heterodimerized Rrp6-Rrp47, which brings it into proximity with the RNA exosome for efficient substrate delivery (Schuch *et al.*, 2014; Schuller *et al.*, 2018). This process appears to be enhanced by Mpp6 (Falk *et al.*, 2017a; Schuller *et al.*, 2018).

Mtr4 also has a pronounced structural arch that enhances *in vivo* processing activity by the RNA exosome but is not important for RNA exosome-mediated degradation (Jackson *et al.*, 2010) (**Figure 1.3 B**). At one end of the arch there is a Kyrpides-Ouzounis-Woese (KOW) motif, a sequence of twenty-seven residues that has been conserved in transcription factors and ribosomal proteins from all three domains of life (Kyrpides *et al.*, 1996). Specifically, the KOW motif of the Mtr4 arch interacts with RNA substrates *in vitro* (Weir *et al.*, 2010). The arch is likely important for the TRAMP complex-independent activities of Mtr4, such as binding to ribosomal biogenesis proteins and involvement in the maturation of 5.8S rRNA, as previously mentioned. In fact, deletion of this characteristic structure indicates that, while it has RNA-binding capabilities, the arch does not have a role in TRAMP complex-dependent function (Jackson *et al.*, 2010; Weir *et al.*, 2010).

Within the TRAMP complex, Mtr4 preferentially interacts with polyadenylated transcripts (Bernstein *et al.*, 2008). Interestingly, Mtr4 seems to regulate the length of the poly(A) tail that is added by Trf4/5 to four or five adenosines (Jia *et al.*, 2012). This is consistent with the results of previous assays, which determined that the substrate binding site of the Mtr4 helical core is five residues (Bernstein *et al.*, 2010; Weir *et al.*, 2010). Furthermore, its helicase activity seems to be enhanced by Trf4-Air2 activity, although Trf4-Air2 activity is not enhanced by Mtr4 (Jia *et al.*, 2012).

Conservation of the TRAMP Complex and Its Subunits

Orthologs of TRAMP complex subunits are present in humans and have been shown to interact, indicating that this complex is conserved from fungi to mammals (Lubas *et al.*, 2011). The TRAMP complex homolog of *Schizosaccharomyces pombe*, another common fungal laboratory model, is akin to the *S. cerevisiae* complex in activity, substrate targeting, and subunit composition (Win *et al.*, 2006; Bühler *et al.*, 2007; Keller *et al.*, 2010). While the yeast TRAMP complex is found throughout the entire nuclear region, the human TRAMP complex is specifically found in the nucleolus and is mainly important for targeting rRNA (Lubas *et al.*, 2011). Interestingly, infection of human cells by RNA viruses can induce nuclear export of human Air1/2 and Mtr4 orthologs. Once in the cytoplasm, these TRAMP complex subunits can target viral RNA for degradation by the RNA exosome (Molleston *et al.*, 2016). Human Trf4/5 orthologs can also localize to the cytoplasm, indicating that the human TRAMP complex may continue to function outside of the nucleus in times of severe cellular stress.

While yeast Trf4/5 are the most characterized non-canonical poly(A) polymerases in terms of substrate-specificity, the Trf4 homolog of *Drosophila melanogaster* is known to at least target snRNAs (Nakamura *et al.*, 2008). Although their nuclear polyadenylation activity is maintained, Trf4/5 orthologs can also localize to the cytoplasm in *D. melanogaster*, *Caenorhabditis elegans*, and mammals (Millonigg *et al.*, 2014; Harnisch *et al.*, 2016; Shin *et*

al., 2017). PAPD5, and possibly also PAPD7, is a mammalian ortholog of Trf4. While the specific function of PAPD7 has not been elucidated, PAPD5 polyadenylates precursor and mature forms of mRNA, rRNA, and snoRNA (Shcherbik *et al.*, 2010; Berndt *et al.*, 2012; Sudo *et al.*, 2016; Shin *et al.*, 2017). Unlike yeast Trf4/5, PAPD5 can directly bind RNA but it may still require other cofactors to correctly identify targets for polyadenylation (Rammelt *et al.*, 2011).

The human protein ZCCHC7, which also contains the IWYRxY motif that is present within yeast Air1/2, has been designated as a human ortholog of Air1. Importantly, it interacts with human Trf4 ortholog PAPD5, despite the RNA-binding activity of PAPD5, which indicates that formation of the TRAMP complex may be conserved (Lubas *et al.*, 2011). A subsequent study revealed that ZCCHC7 localizes to the nucleoli of HeLa cells where it can directly interact with PAPD5, as well as with the possible additional human Trf4 ortholog, PAPD7 (Fasken *et al.*, 2011).

As in yeast, the human MTR4 protein associates with human Rrp6 and Rrp47 orthologs, PM/ScI-100 and C1D, and is essential for 5.8S rRNA processing (Schilders *et al.*, 2007). This role in 5.8S rRNA processing is also conserved in the protist, *Trypanosoma brucei*, as is its association with a Trf4/5 ortholog (Cristodero and Clayton, 2007). As previously stated, homologs of all TRAMP complex subunits interact in humans. In addition to its inclusion within the nucleolar human TRAMP complex, MTR4 can also be a subunit of the nuclear exosome-targeting (NEXT) complex (Lubas *et al.*, 2011) (**Figure 1.2**). The NEXT complex also contains ZCCHC8 and RBM7, which are scaffolding and RNA-binding subunits, respectively. This cofactor of the human nuclear RNA exosome is found in the nucleoplasm and is important for the degradation of several subsets of ncRNA, including PROMPTS and snoRNA species that are derived from pre-mRNA introns (Lubas *et al.*, 2011; Hrossova *et al.*, 2015). Recently, human MTR4 was also identified as a subunit of a novel nuclear RNA exosome cofactor, the poly(A) tail exosome targeting (PAXT) connection

(Figure 1.2). The composition of this cofactor is similar to the NEXT complex because in addition to MTR4, it is also comprised of putative scaffolding and RNA-binding proteins. However, its RNA-binding subunit, PABPN1, preferentially targets poly(A) tails. Consequentially, targets of the PAXT connection are more polyadenylated and therefore, generally longer than NEXT complex substrates (Meola *et al.*, 2016).

Mtr4 homologs have also been identified as components of various complexes in other fungal species (**Figure 1.2**). As previously mentioned, the Mtr4 ortholog of *S. pombe* assembles within the TRAMP complex. However, this species also contains an Mtr4 homolog, Mtl1, which is an arched RNA helicase and a component of the MTREC complex (Lee *et al.*, 2013). Like the TRAMP complex, the MTREC complex is a nuclear cofactor of the RNA exosome. Yet in *S. pombe*, the MTREC complex plays a more crucial role in the degradation of CUTs and meiotic mRNA than the TRAMP complex does (Zhou *et al.*, 2015). Interestingly, two copies of the *Neurospora crassa* Mtr4 ortholog are present within the FFC complex, which is an important component of this fungal organism's circadian clock. The *N. crassa* Mtr4 ortholog, FRH, has a role in RNA biogenesis. However, its ATPase activity is also critical for the hyperphosphorylation of the other FFC complex subunit, FRQ, which is an important clock protein (Lauinger *et al.*, 2014).

Diseases Linked to Dysfunctional Cofactors of the RNA Exosome

Since the RNA exosome is dependent upon various cofactors, it is currently unclear if some diseases are specifically caused by a dysfunctional RNA exosome, dysfunctional cofactor(s), or both. Moreover, the essentiality of the RNA exosome and some of its cofactors indicates that detrimental mutations have not yet been identified because they cause lethality before birth.

In humans, various mutations in two SKI complex subunits cause trichohepatoenteric (THE) syndrome. This disease is characterized by severe gastrointestinal symptoms, hair abnormalities, and general failure to thrive (Hartley *et al.*, 2010; Fabre *et al.*, 2012). A

missense mutation in *RBM7*, which encodes an RNA-binding component of the human NEXT complex, is associated with spinal motor neuropathy (Giunta *et al.*, 2016) (**Table 1.1**).

While humans express homologs of TRAMP complex subunits, they have not yet been implicated in any disorders. However, inducing TRAMP complex mutations in yeast can result in slow growth phenotypes and increased RNA accumulation. Therefore, it is reasonable to assume that mutating TRAMP complex subunits is deleterious in humans to some extent. In fact, the locus containing the human Trf4 homolog is often amplified in many types of tumors (Walowsky *et al.*, 1999).

SIGNIFICANCE

Investigating the Impact of RNA Processing and Degradation on Cellular Physiology

The entire lifespan of an RNA transcript must be tightly regulated, whether it encodes a protein or is a ncRNA that carries out other important cellular processes. The essentiality of the RNA exosome and some of its cofactors, as well as its ubiquitous cellular location, highlights the overall importance of maintaining proper function of the 3'-5' RNA processing and degradation pathway. This is reinforced by the variety of symptoms that are caused by mutations of both the RNA exosome and its cofactors. My work has included the development of yeast models to study human RNA exosome mutations that have been linked with disease phenotypes. Determining how these mutations specifically affect the structure and/or activity of the RNA exosome is crucial for developing future disease treatments.

Elucidating Interactions Within and Between the RNA Exosome and TRAMP Complex

Although the RNA exosome was discovered nearly two decades ago, the mechanisms by which it identifies and differentiates its substrates for processing or degradation remain unknown. Moreover, the specific interaction sites between the RNA exosome and many of its cofactors, including the TRAMP complex, have not yet been fully described. Upon its discovery within the last decade, the majority of research on the TRAMP

complex has focused on identifying its substrates. A novel aspect of my project is characterizing how its subunits assemble into a functional complex. Defining and determining the importance of TRAMP complex subunit interactions is essential for eventually gaining a complete understanding of this complex and moreover, its relationship with the RNA exosome.

CHAPTER 2

Materials and Methods

This chapter contains material from Fasken MB*, Losh JS*, Leung SW, Brutus S, Avin B, Vaught JC, Potter-Birriel J, Craig T, Conn GT, Mills-Lujan K, Corbett AH, van Hoof

A. Insight into the RNA exosome complex through modeling pontocerebellar hypoplasia type 1b disease mutations in yeast. *Genetics*. 2017; 205: 221-37 (*these authors contributed equally to this work). Permission from the Genetics Society of America is not needed if reproducing an article for a dissertation (genetics.org/content/permissions).

This chapter also contains material from Losh JS*, King AK*, Bakelar J, Taylor L, Loomis J, Rosenzweig JA, Johnson SJ, van Hoof A. **Interaction between the RNA-dependent ATPase and poly(A) polymerase subunits of the TRAMP complex is mediated by short peptides and important for snoRNA processing.** *Nucleic Acids Research*. 2015; 43(3): 1848-58 (*these authors contributed equally to this work). This is an Open Access article distributed under the terms of the Creative Commons Attribution License (<http://creativecommons.org/licenses/by/4.0/>), which permits unrestricted reuse, distribution, and reproduction in any medium, provided the original work is properly cited.

MATERIALS

Plasmids

Unless otherwise noted, all plasmids listed in **Table 2.1** contain an endogenous promoter and a 3' flanking region to maintain native expression levels. All plasmids contain a selectable marker that complements auxotrophy or provides antibiotic resistance to yeast transformants. Additionally, all plasmids have an *amp^R* gene, which provides ampicillin resistance to bacterial transformants.

Name	Insert	Marker	Reference
pAG32	empty vector	<i>HYGB</i>	(Goldstein and McCusker, 1999)
pGAL-HO	<i>GAL</i> promoter, <i>HO</i>	<i>URA3</i>	N. Kim lab
pRS413	empty vector	<i>HIS3</i>	(Sikorski and Hieter, 1989)
pRS415	empty vector	<i>LEU2</i>	(Sikorski and Hieter, 1989)
pRS416	empty vector	<i>URA3</i>	(Sikorski and Hieter, 1989)
p411GAL1	empty vector	<i>MET15</i>	K. Morano lab
Yep52/-26CBP1	<i>CBP1</i>	<i>LEU2</i>	(Mayer and Dieckmann, 1989)
pAV188	<i>his3-nonstop</i> reporter	<i>LEU2</i>	(van Hoof <i>et al.</i> , 2002)
pAV476	TAP tag	<i>LEU2</i>	A. van Hoof lab
pAV854	<i>trf5Δ98-117-TAP</i>	<i>LEU2</i>	This study
pAV885	<i>TRF5-TAP</i>	<i>LEU2</i>	This study
pAV928	<i>RRP40-2xMyc</i>	<i>LEU2</i>	This study
pAV929	<i>rrp40-G8A-2xMyc</i>	<i>LEU2</i>	This study
pAV930	<i>rrp40-W195A-2xMyc</i>	<i>LEU2</i>	This study
pAV935	<i>rrp40-S87A-2xMyc</i>	<i>LEU2</i>	This study
pAV936	<i>rrp40-S87A/V95P-2xMyc</i>	<i>LEU2</i>	This study
pAV937	<i>rrp40-W195R-2xMyc</i>	<i>LEU2</i>	This study
pAV991	<i>RRP4-2xMyc</i>	<i>LEU2</i>	This study
pAV1059	<i>TRF4-TAP</i>	<i>LEU2</i>	This study
pAV1063	<i>AIR2</i>	<i>HIS3</i>	This study
pAV1073	<i>trf4Δ115-134-TAP</i>	<i>LEU2</i>	This study
pAV1105	<i>TRF5</i> promoter, TAP tag	<i>LEU2</i>	This study
pAV1106	<i>trf5ΔNΔC-TAP</i>	<i>LEU2</i>	This study
pAV1107	<i>trf4Δ115-134-TAP</i>	<i>URA3</i>	This study
pAV1119	<i>trf4-DADA-TAP</i>	<i>LEU2</i>	This study
pAV1121	<i>trf4-DADA-Δ115-134-TAP</i>	<i>LEU2</i>	This study
pAV1132	<i>trf5-DADA-TAP</i>	<i>LEU2</i>	This study
pAV1134	<i>trf5-DADA-Δ98-117-TAP</i>	<i>LEU2</i>	This study
pAV1170	<i>trf5ΔN</i>	<i>LEU2</i>	This study
pAV1172	<i>trf5ΔC-TAP</i>	<i>LEU2</i>	This study
pAV1176	<i>TRF4</i> promoter, TAP tag	<i>LEU2</i>	This study
pAV1182	<i>rrp4-G58V-2xMyc</i>	<i>LEU2</i>	This study
pAV1183	<i>rrp4-G226D-2xMyc</i>	<i>LEU2</i>	This study
pAV1185	<i>trf4ΔNΔC-TAP</i>	<i>LEU2</i>	This study
pAV1188	<i>trf4ΔN</i>	<i>LEU2</i>	This study
pAV1210	<i>trf4ΔC-TAP</i>	<i>LEU2</i>	This study
pAV1256	<i>TRF4-TAP</i>	<i>URA3</i>	This study
pAV1262	<i>trf4ΔNΔC-TAP</i>	<i>URA3</i>	This study

Yeast Strains

All *S. cerevisiae* strains designated in **Table 2.2** as BY4741 or BY4742 are originally derived from these two commonly used strains, which were designed to be more conducive for plasmid selection (Brachmann *et al.*, 1998). All strains listed in **Table 2.2** are haploid.

Yeast extract-peptone dextrose (YPD) rich medium was used when growing yeast in liquid culture or on plates. Yeast extract-peptone was also supplemented with galactose for growing strains expressing genes under the control of a *GAL* promoter. Synthetic complete (SC) media lacking specific amino acids was used for selective growth.

Table 2.2 Yeast strains used in this study		
Name	Genotype	Reference
BY4741	<i>MATa, his3Δ1, leu2Δ0, met15Δ, ura3Δ0</i>	(Bachmann <i>et al.</i> , 1998)
BY4742	<i>MATα, his3Δ1, leu2Δ0, lys2Δ0, ura3Δ0</i>	(Bachmann <i>et al.</i> , 1998)
DTY8	<i>MATa, LEU2, URA3, his1-</i>	K. Morano lab
DTY9	<i>MATα, LEU2, URA3, his1-</i>	K. Morano lab
SV260	BY4741, <i>trf4Δ::natMX4, trf5Δ::kanMX6 [TRF4, URA3]</i>	(Holub <i>et al.</i> , 2012)
yAV284	BY4741, <i>ski7Δ::NEO</i>	Dharmacon™
yAV1103	BY4742, <i>rrp4Δ::NEO [RRP4, URA3]</i>	A. van Hoof lab
yAV1135	BY4742, <i>rrp44Δ::NEO [rrp44-endo, LEU2]</i>	A. van Hoof lab
yAV1144	BY4741, <i>rrp6Δ::NEO</i>	A. van Hoof lab
yAV1284	BY4741, <i>rrp44Δ::natMX4 [rrp44-exo, LEU2]</i>	A. van Hoof lab
yAV1335	BY4741, <i>trf4Δ::natMX4, trf5Δ::kanMX6 [TRF5-TAP, LEU2]</i>	This study
yAV1336	BY4741, <i>trf4Δ::natMX4, trf5Δ::kanMX6 [trf5Δ98-117-TAP, LEU2]</i>	This study
yAV1368	<i>MATa, his3Δ1, leu2Δ0, ura3Δ0, MET15, rrp40Δ::NEO [RRP40, URA3]</i>	This study
yAV1369	<i>MATa, his3Δ1, leu2Δ0, ura3Δ0, MET15, rrp40Δ::NEO [RRP40, URA3] [rrp40-W195A-2xMyc, LEU2]</i>	This study, plated on 5-FOA before use
yAV1370	<i>MATa, his3Δ1, leu2Δ0, ura3Δ0, MET15, rrp40Δ::NEO [RRP40, URA3] [rrp40-G8A-2xMyc, LEU2]</i>	This study, plated on 5-FOA before use
yAV1371	<i>MATa, his3Δ1, leu2Δ0, ura3Δ0, MET15, rrp40Δ::NEO [RRP40, URA3] [RRP40-2xMyc, LEU2]</i>	This study, plated on 5-FOA before use
yAV1396	<i>MATa, his3Δ1, leu2Δ0, ura3Δ0, MET15, rrp40Δ::NEO [RRP40, URA3] [rrp40-S87A-2xMyc, LEU2]</i>	This study, plated on 5-FOA before use
yAV1397	<i>MATa, his3Δ1, leu2Δ0, ura3Δ0, MET15, rrp40Δ::NEO [RRP40, URA3] [rrp40-S87A/V95P-2xMyc, LEU2]</i>	This study, plated on 5-FOA before use
yAV1398	<i>MATa, his3Δ1, leu2Δ0, ura3Δ0, MET15, rrp40Δ::NEO [RRP40, URA3] [rrp40-W195R-2xMyc, LEU2]</i>	This study, plated on 5-FOA before use
yAV1587	<i>MATa, his3Δ1, leu2Δ0, ura3Δ0, MET15, rrp40Δ::NEO [RRP40, URA3] [rrp40-W195F-2xMyc, LEU2]</i>	This study, plated on 5-FOA before use
yAV1588	<i>MATa, his3Δ1, leu2Δ0, ura3Δ0, MET15, rrp40Δ::NEO [RRP40, URA3] [rrp40-D152A-2xMyc, LEU2]</i>	This study, plated on 5-FOA before use
yAV1686	BY4741, <i>trf4Δ::natMX4, trf5Δ::kanMX6 [TRF4-TAP, LEU2]</i>	This study
yAV1688	BY4741, <i>trf4Δ::natMX4, trf5Δ::kanMX6 [trf4Δ115-134-TAP, LEU2]</i>	This study
yAV1803	BY4741, <i>trf4Δ::natMX4, trf5Δ::kanMX6 [trf4Δ115-134-TAP, URA3] [trf5Δ98-117-TAP, LEU2]</i>	This study
yAV1824	BY4741, <i>[trf5ΔN ΔC-TAP, LEU2]</i>	This study
yAV1826	BY4741, <i>trf4Δ::natMX4, trf5Δ::kanMX6 [trf5ΔNΔC-TAP, LEU2]</i>	This study
yAV1877	BY4741, <i>trf4Δ::natMX4, trf5Δ::kanMX6 [TRF4, URA3] [trf4-DADA-TAP, LEU2]</i>	This study
yAV1878	BY4741, <i>trf4Δ::natMX4, trf5Δ::kanMX6 [TRF4, URA3] [trf4-DADA-Δ115-134-TAP, LEU2]</i>	This study
yAV1879	BY4741, <i>trf4Δ::natMX4, trf5Δ::kanMX6 [TRF, URA3] [trf5-DADA-TAP, LEU2]</i>	This study

yAV1880	BY4741, <i>trf4Δ::natMX4, trf5Δ::kanMX6</i> [TRF4, URA3] [<i>trf5-DADA-Δ98-117-TAP, LEU2</i>]	This study
yAV1970	BY4741, [<i>trf5ΔN, LEU2</i>]	This study
yAV1972	BY4741, [<i>trf5ΔC-TAP, LEU2</i>]	This study
yAV1974	BY4741, <i>trf4Δ::natMX4, trf5Δ::kanMX6</i> [<i>trf5ΔN, LEU2</i>]	This study
yAV1976	BY4741, <i>trf4Δ::natMX4, trf5Δ::kanMX6</i> [<i>trf5ΔC-TAP, LEU2</i>]	This study
yAV2014	BY4741 [<i>RRP4-2xMyc, LEU2</i>]	This study
yAV2015	BY4741 [<i>rrp4-G58V-2xMyc, LEU2</i>]	This study
yAV2016	BY4741 [<i>rrp4-G226D-2xMyc, LEU2</i>]	This study
yAV2017	BY4742, <i>rrp4Δ::NEO</i> [<i>RRP4-2xMyc, LEU2</i>]	This study
yAV2020	BY4741 [<i>trf4ΔNΔC-TAP, LEU2</i>]	This study
yAV2022	BY4741 [<i>trf4ΔN, LEU2</i>]	This study
yAV2024	BY4741, <i>trf4Δ::natMX4, trf5Δ::kanMX6</i> [<i>trf4ΔN, LEU2</i>]	This study
yAV2036	BY4741 [<i>trf4ΔC-TAP, LEU2</i>]	This study
yAV2038	BY4741, <i>trf4Δ::natMX4, trf5Δ::kanMX6</i> [<i>trf4ΔC-TAP, LEU2</i>]	This study
yAV2040	BY4741, <i>trf4Δ::natMX4, trf5Δ::kanMX6</i> [<i>trf4ΔNΔC-TAP, LEU2</i>]	This study
yAV2074	BY4741, <i>trf4Δ::natMX4, trf5Δ::kanMX6, air2Δ::hphMX4</i> [TRF4, URA3]	This study
yAV2077	BY4741, <i>trf4Δ::natMX4, trf5Δ::kanMX6, air2Δ::hphMX4</i> [TRF5-TAP, LEU2]	This study
yAV2079	BY4741, <i>trf4Δ::natMX4, trf5Δ::kanMX6, air2Δ::hphMX4</i> [<i>trf5Δ98-117-TAP, LEU2</i>]	This study
yAV2081	BY4742, <i>rrp4Δ::NEO</i> [RRP4, URA3] [<i>rrp4-G58V-2xMyc, LEU2</i>]	This study
yAV2082	BY4742, <i>rrp4Δ::NEO</i> [RRP4, URA3] [<i>rrp4-G226D-2xMyc, LEU2</i>]	This study
yAV2118	BY4741, <i>trf4Δ::natMX4, trf5Δ::kanMX6, air2Δ::hphMX4</i> [TRF4, URA3] [AIR2, HIS3]	This study
yAV2119	BY4741, <i>trf4Δ::natMX4, trf5Δ::kanMX6, air2Δ::hphMX4</i> [TRF4, URA3] [TRF4-TAP, LEU2]	This study, plated on 5-FOA before use
yAV2178	BY4741, <i>air1Δ::NEO</i>	Dharmacon™
yAV2180	BY4742, RRP40	(Gillespie <i>et al.</i> , 2017)
yAV2182	BY4742, <i>rrp40-G8A</i>	(Gillespie <i>et al.</i> , 2017)
yAV2183	BY4742, <i>rrp40-G148C</i>	(Gillespie <i>et al.</i> , 2017)
yAV2184	BY4742, <i>rrp40-W195R</i>	(Gillespie <i>et al.</i> , 2017)
yAV2222	BY4741, <i>trf4Δ::natMX4, trf5Δ::kanMX6, air2Δ::hphMX4</i> [TRF4, URA3] [TRF5-TAP, LEU2] [AIR2, HIS3]	This study
yAV2242	BY4742, <i>air1Δ::NEO</i>	Dharmacon™
yAV2288	BY4741, <i>trf4Δ::natMX4, trf5Δ::kanMX6</i> [TRF4-TAP, URA3] [TRF5-TAP, LEU2]	This study
yAV2289	BY4741, <i>trf4Δ::natMX4, trf5Δ::kanMX6</i> [<i>trf4ΔNΔC-TAP, URA3</i>] [<i>trf5ΔNΔC-TAP, LEU2</i>]	This study

Oligonucleotides

Oligonucleotides designed for this work and listed in **Table 2.3** were ordered from Sigma-Aldrich®. Lyophilized oligonucleotides were resuspended in autoclaved deionized water at a 50µM stock concentration.

Table 2.3 Oligonucleotides used in this study		
Name	Target	5'-3' Sequence
Cloning Oligonucleotides		
oAV557	TAP tag	CGCAAGCTTTGCCGGTAGAGGTGTGGTCAATAAGAGCGAC
oAV868	<i>TRF5</i> F	GCGGCGGCGGCCGCGCCATCATGGGTGCTGCTGCCTTTG
oAV869	<i>TRF5</i> R	GCGGCGCTGCAGCAAGAGCCTGGCCTTTAGAGAGCC
oAV870	<i>trf5Δ98-117</i> F	GCGGCGACTAGTTCTTTTGCTAGATTCTGCCCTTTGTTCC
oAV871	<i>trf5Δ98-117</i> R	GCGGCGACTAGTGAACAAATAAAGGAAGATGATGATG
oAV1327	<i>TRF4</i> prom F	TATTATGCGGCCGCTCACCTTTATCCCAAATTAG
oAV1328	<i>trf4Δ115-134</i> R	GCGGCGACTAGTCTCATCCCCGTGCACTGCTA
oAV1329	<i>trf4Δ115-134</i> F	GCGGCGACTAGTGCCGAACAGGAAGAGGAGAG
oAV1330	<i>TRF4</i> R	GCGGCGCTGCAGCAAGGGTATAAGGATTATATCC
oAV1377	<i>TRF5</i> prom F	TATTATGCGGCCGCCACAAAGTACTACATCTATGGTCT
oAV1378	<i>TRF5</i> prom R	GCGGCGACTAGTCCAATAAACTCCGCCCTCGTTTG
oAV1379	<i>trf5ΔNΔC</i> F	GCGGCGACTAGTGTCGTCTATGGAGTATCCTTGGATAAGAAATCATTGTCATTCCG
oAV1380	<i>trf5ΔNΔC</i> R	GCGGCGCTGCAGGTTGTCGTGAAATCTCTCTTTTG
oAV1409	<i>trf4-DADA</i> F	GCCTGGTTCCGCTATTGCTTGCCTGG
oAV1410	<i>trf4-DADA</i> R	GCTCGTTACCACGCAAGCAATAGCGGAAC
oAV1411	<i>trf5-DADA</i> F	GCCGGGTTCTGCCATTGCCTGTGTGCG
oAV1412	<i>trf5-DADA</i> R	CGACACAGGCAATGGCAGAACCCGG
oAV1482	<i>trf5ΔN</i> R	GCGGCGCTGCAGGTTAAAGAGCCTGGCCTTTAGAGAG
oAV1483	<i>trf5ΔC</i> F	GCGGCGACTAGTGTCGTCTATGACAAGGCTCAAAGCAAAATATTCA
oAV1504	<i>TRF4</i> prom R	GCGGCGACTAGTCAAGTATAGTTCCTTGCTTATTC
oAV1505	<i>trf4ΔNΔC</i> F	GCGGCGACTAGTTGAAATATGGATTATCCATGGATTTTAATCATGATCACTCC
oAV1506	<i>trf4ΔNΔC</i> R	GCGGCGCTGCAGGATCCTTGAATCTCTTGCCTTTCCACGATATTTG
oAV1507	<i>trf4ΔN</i> R	GCGGCGCTGCAGGTTAAAGGGTATAAGGATTATATCC
oAV1508	<i>trf4ΔC</i> F	GCGGCGACTAGTTGAAATATGGGGGCAAAGAGTGTAACAGCC
oAV1513	<i>rrp4-G58V</i> F	CTCAAATTGTGACGCCAGTTGAGCTGGTCACTGATG
oAV1514	<i>rrp4-G58V</i> R	CATCAGTGACCAGCTCAACTGGCGTCACAATTTGAG
oAV1515	<i>rrp4-G226D</i> F	GGCAACATAACCGTAGTTCTCGATGTCAATGGTTACATATGG
oAV1516	<i>rrp4-G226D</i> R	CCATATGTAACCATTGACATCGAGAACTACGGTTATGTTGCC
oAV1544	<i>air2Δ::hphMX4</i> F	GAATTAACCTTACCTGTACAACGATAGCAGCTTACATCACTTCTCGCAGTCAGCTTGCCTTGTCCCCGCCG
oAV1555	<i>air2Δ::hphMX4</i> R	GAAAATATAATGTAACCAAGAACAGCTTGTTAAAGGGCTTCCTATTTAAAGGATGAATTCGAGCTCGTTTTTC
oAV1572	<i>air1Δ::MET15</i> F	CATTCTCACATGAGGAATACAAAGGAAGCGGACCACGGAGCTAAGATATTGCCATCCTCATGAAAACTGTG
oAV1573	<i>air1Δ::MET15</i> R	GTTTGCTGCAATGAGAATGGAAAAAATTAAAAAAATCTACATATAATCCTTGTGAGAGAAAGTAGG
oAV1627	<i>air1Δ::hphMX4</i> F	CATTCTCACATGAGGAATACAAAGGAAGCGGACCACGGAGCTAAGATATTAGCTTGCTTGTCCCCGCCG

oAV1628	<i>air1Δ::hphMX4 R</i>	GTTTGCTGCAATGAGAATGGAAAAAAAAATTAAAAAACTC ACATATAATCGATGAATTCGAGCTCGTTTTTC
oAV1657	<i>RRP40</i> alleles	GCATTGGGAAAAGCCATATACG
oAV1658	<i>RRP40</i> alleles	GAAAAACAGGCCAACTTTGCAAGTGGG
Northern Oligonucleotides		
oAV224	SRP	GTCTAGCCGCGAGGAAGG
oAV777	5.8S rRNA	TTTCGCTGCGTTCCTCATC
oAV849	<i>snR33</i>	AGGAACCGACTCAAACCGG
oAV908	<i>pre-snR33</i>	AAGTTTTGCAAATCGATTGTCC
oAV910	<i>snR128</i>	TCCTACCGTGGAACTGCG
oAV911	<i>pre-snR128</i>	GATACTACAGTATACGATCACTC
oAV1608	<i>CBP1</i>	CTCGGTCCTGTACCGAACGAGACGAGG
qRT-PCR Oligonucleotides		
<i>ACT1</i> qtFor Morano lab	<i>ACT1</i> F	TTTGGGTTTGAATCTGCCGGTATTGAC
<i>ACT1</i> qtRev Morano lab	<i>ACT1</i> R	CTTTCGGCAATACCTGGGAACATGG
oAV1225	<i>NBL001c</i> F	AACTACCTAAGAAAAGCATC
oAV1226	<i>NBL001c</i> R	TCGATTTCAATTCGACTGC

METHODS

Plasmid Cloning

The majority of plasmid cloning was performed by first designing primers to a specific region of interest, performing a polymerase chain reaction (PCR), and isolating purified product. Purified product was obtained by performing a plasmid cleanup or extracting from an agarose gel with a Zymoclean™ Gel DNA Recovery Kit by Zymo Research. Digested plasmids and products were ligated at ratios of 1:3 or 1:5. The QuikChange® Lightning Site-Directed Mutagenesis Kit by Agilent Technologies was used to induce point mutations in existing plasmids. After performing bacterial transformations, as described below, newly cloned plasmids were isolated with a Wizard® Plus SV Minipreps DNA Purification System and sequenced.

Bacterial Transformation

Ligated product was added to chilled, chemically competent *E. coli*. Previously created plasmid stock or water was added to chemically competent *E. coli* as positive or negative controls for transformation, respectively. Reactions were placed on ice and then briefly incubated at 42°C. Cells were returned to ice for twenty minutes before plating onto rich medium containing 100 mg/mL ampicillin. Plates were incubated at 37°C for no longer than twenty-four hours.

Yeast Transformation

For high efficiency reactions, yeast strains were transformed as previously described (Gietz and Schiestl, 1995). However, the majority of transformations were performed by first resuspending a small amount of yeast into a tube containing 500µL PLATE (40% polyethylene glycol, 0.1M LiAc, 10mM Tris HCl, pH 7.5, 1mM EDTA). Boiled single-stranded carrier DNA and 1µg experimental DNA were added to the reaction, which was incubated

overnight at room temperature. Cells were then pelleted, resuspended in autoclaved deionized water, and plated onto selective medium.

When attempting to knockout *AIR1*, the *Candida albicans* transformation electroporation protocol from the laboratory of Michael Lorenz at UTHealth was modified for yeast transformation. Cell pellets were resuspended in 10mL of 1X TE/LiOAc solution and incubated for one hour at 30°C. 250µL 1M dithiothreitol (DTT) was added and the incubation was continued for an additional thirty minutes. Cells were pelleted and washed with autoclaved deionized water. Next, cells were pelleted, washed, and resuspended in 5mL 1M sorbitol. Cells and 1µg experimental DNA were pipetted into a cuvette and electroporated at 1800 volts in an Eppendorf Electroporator® 2510. 50µL 1M sorbitol was added to the electroporated cells before pelleting and resuspending in liquid rich medium. After a recovery incubation for four hours at 30°C, cells were pelleted, resuspended in autoclaved deionized water, and plated onto selective medium.

Yeast DNA Isolation

Genomic yeast DNA was isolated with the Zymo Research YeaStar™ Genomic DNA kit. Plasmids expressed in yeast were isolated with the Zymo Research Zymoprep™ Yeast Plasmid Miniprep II kit.

Yeast Homologous Recombination

To delete *AIR2*, long oligonucleotides were designed with homology to both the *hphMX4* cassette and regions just up- and downstream of the target coding site. The *hphMX4* cassette contains the *hph* open reading frame (ORF) from *Klebsiella pneumoniae*, which provides resistance to hygromycin B. Its constitutive expression is ensured by a yeast *TEF1* promoter and terminator within the cassette. PCR was used to amplify the *hphMX4* cassette that included flanking regions homologous to the sites bordering *AIR2*. The PCR products were used to transform *trf4Δ*, *trf5Δ* cells complemented with plasmids allowing for

Trf4, Trf5, or *trf5* Δ ⁹⁸⁻¹¹⁷ protein expression. Transformation reactions were plated onto medium containing hygromycin B at a final concentration of 300 μ g/L. Genomic DNA was extracted from transformants that grew in the presence of hygromycin B. PCR analysis of these DNA samples confirmed the presence of the *hphMX4* cassette and the loss of *AIR2*.

This homologous recombination assay was similarly used when attempting to delete *AIR1* in *trf4* Δ , *trf5* Δ , *air2* Δ strains complemented with plasmids allowing for the expression of various Trf4/5 proteins. Performing homologous recombination of *AIR1* with *hphMX4* did not result in growth on media containing hygromycin B. Due to the variety of genetic markers already used in the experimental strain set, *MET15* was selected as an alternative option for swapping out *AIR1*, as these strains were all genetically *met15* Δ . Therefore, successful homologous recombination would have allowed for growth on medium lacking methionine and cysteine. Additionally, I transformed these strains with an [*AIR2*, *HIS3*] plasmid to control for any synthetic lethality that might arise from deleting *AIR1* in this background, although *air1* Δ , *air2* Δ cells have been previously reported as viable (Inoue *et al.*, 2000). No transformants that were able to grow on medium lacking methionine and cysteine were obtained. The yeast transformation was repeated with a high efficiency protocol, which still did not result in growth on this medium. In addition to *trf4* Δ , *trf5* Δ , *air2* Δ strains, wild-type and *trf4* Δ , *trf5* Δ strains were also transformed in case *air2* Δ was somehow preventing an *AIR1* knockout. This did not result in growth on medium lacking methionine and cysteine, nor did attempting to transform cells via electroporation. Redesigning the oligonucleotides for the initial PCR still did not result in viable transformants. It remains unclear as to why *AIR1* cannot be switched out for the *hphMX4* cassette or *MET15*.

Yeast Plasmid Shuffle Assay

The genotypic background of strains used in this assay was *leu2Δ, ura3Δ*. The allele of interest was inserted into a plasmid with a *LEU2* gene marker. This plasmid was used to transform cells already expressing the essential gene on a plasmid with a *URA3* gene marker. Transformants were selected on solid medium lacking leucine and uracil, before replica plating onto medium containing 5.74 mM 5-fluoroorotic acid (5-FOA). *URA3* cells express an enzyme that converts 5-FOA to a toxic metabolite, 5-fluorouracil (5-FU), which results in lethality. Growth on 5-FOA reveals that the allele of interest on the *LEU2* plasmid can complement the essentiality of the original gene.

Yeast Mating

When mating, two strains were struck perpendicularly in an “x” formation onto rich medium. After one or two days of growth at 30°C, cells were collected from the middle of the “x”. The presence of diploids was assessed by streaking these cells onto selective medium. The resulting colonies, which presumably contained diploids generated from mating events, were struck onto medium containing potassium acetate, which induces sporulation. Plates were incubated for about five days at 30°C. Sporulated yeast were resuspended in 100μL autoclaved deionized water and exposed to 10μL glucosylase, an enzyme that breaks down the ascus, for several hours. Ascus digestion was terminated by pelleting and resuspending the yeast in autoclaved deionized water. The cell suspension was aspirated out and the tubes were washed four times with autoclaved deionized water. 1mL of 0.02% Triton X-100 solution was added in order to collect the hydrophobic spores attached to the walls of the tubes. Tubes were sonicated in order to disperse the spores throughout the solution before plating onto rich and selective media.

The mating type of a strain was determined by crossing it with known mating type tester strains, DTY8 and DTY9, which are *MATa* or *MATα*, respectively (**Table 2.2**). Most

strains created in this study are *HIS1*, *his3Δ1* but the mating type tester strains are *his1-*, *HIS3*. Successful mating results in growth on media lacking histidine. Therefore, if the mating resulted in growth, the mating type of a newly created strain was determined to be the opposite type of the tester strain.

When attempting to delete *AIR1*, a *MATa air1Δ, met15Δ* strain from the Dharmacon™ Yeast Knockout Collection was mated with a *MATα* strain containing wild-type *AIR1* and *MET15* alleles. This did not yield *air1Δ, MET15* cells that could be mated with the *MATa trf4Δ, trf5Δ, air2Δ* strains generated via homologous recombination, as all progeny were determined to be *MATa*.

To change the mating type of a strain, cells were transformed with pAV1222, which encodes HO, the yeast mating type switching enzyme, under the control of a galactose-inducible promoter (**Table 2.1**). Transformants were grown at 30°C in liquid rich medium containing galactose. Liquid cultures were then plated onto solid rich medium containing dextrose. Lack of available galactose turns off the expression of the HO enzyme but in order to ensure its inactivity, the plasmid shuffle assay was performed to remove pAV1222. The mating types of colonies were determined by crossing with DTY8 and DTY9, as described above. When attempting to delete *AIR1*, this technique was used on a *MATa air1Δ, met15Δ* strain, which resulted in *MATα* cells that could be mated with *MATa trf4Δ, trf5Δ, air2Δ* background strains. However, transforming the *air1Δ, met15Δ* cells with a *MET15* marker plasmid did not result in growth on medium lacking methionine and cysteine. The medium recipe was determined to be correct, as other laboratory strains known to contain a wild-type *MET15* allele grew on it as expected. No published studies could provide information into why linking *air1Δ* with *MET15* may not be possible.

Finally, a *MATα air1Δ, MET15* strain was ordered from the Dharmacon™ Yeast Knockout Collection and crossed with the *MATa trf4Δ, trf5Δ, air2Δ* strains generated via

homologous recombination. Interestingly, this did not result in any progeny that had retained resistance to hygromycin B. Therefore, none of the progeny were *air2Δ*. As previously mentioned, a double deletion of *AIR1* and *AIR2* is not known to be synthetic lethal. Therefore, it is not immediately evident as to why both of these genes could not be successfully knocked out in concert with deletions of *TRF4* and *TRF5*, although it is possible that combined loss of Air1/2 and Trf4/5 protein expression is synthetic lethal.

Yeast Growth Assays

Serial dilution assays were used to determine growth phenotypes of strains and to test for genetic complementation. Strains were grown overnight at 30°C in liquid medium. Cells were then sub-cultured and concentrations were normalized to $OD_{600} = 0.6$. Cultures were then serially diluted by a factor of five in a 96-well plate and spotted onto solid rich or selective medium. Yeast peptone dextrose (YPD) rich medium was used as a positive control for growth. Selective medium, containing antibiotics or lacking certain amino acids, was used according to the selectable markers expressed by a tested set of strains. When assessing if PCH1b-associated mutations affect mitochondrial activity, glycerol was added to medium at a final concentration of 3%. When testing for the effect of drug stress on TRAMP complex formation, 5-FU was added at concentrations of 50μM, 100μM, or 200μM. Plates were incubated at 30°C, the optimal yeast growth temperature, as well as at room temperature or 37°C to differentiate growth phenotypes at a variety of temperatures. Growth assays that included newly created, untested strains were also incubated at 15°C to assess for cold sensitivity. Plates were incubated at 42°C when measuring the effect of heat stress on various strains. Plates were imaged with a ProteinSimple AlphaImager® Mini after one to seven days of growth, depending on the specific assay.

Liquid growth assays were used to similarly test growth phenotypes of strains but provided a more sensitive measurement. After growing strains overnight at 30°C in selective

liquid medium, cell concentrations were normalized and subsequently diluted to $OD_{600} = 0.01$ in the same type of medium. Each strain was tested in triplicate. The serial dilutions were performed in a 24-well plate, which was sealed with a breathable film. Growth at 30°C or 37°C was monitored and recorded for up to twenty-four hours at OD_{600} in a BioTek Synergy™ Mx microplate reader with Gen5 v2.04 software. The average growth of the technical triplicates was calculated and graphed with Microsoft® Excel.

Yeast *his3-nonstop* Reporter Assay

This assay was performed as previously described in cells with a *his3Δ* background (Schaeffer *et al.*, 2008). For this assay, strains were first transformed with pAV188, a *his3-nonstop* reporter plasmid (**Table 2.1**; van Hoof *et al.*, 2002). Transformants were serially diluted, spotted onto minimal medium lacking histidine, and incubated at 30°C or 37°C. Cells without RNA degradation deficiencies can efficiently clear *his3-nonstop* transcripts, which does not allow for growth on medium lacking histidine. Cells with RNA degradation deficiencies cannot clear these transcripts, resulting in histidine biosynthesis and growth on this medium. Plates were imaged after one, two, and three days of growth with a ProteinSimple Alphamager® Mini.

Yeast Protein Isolation

Cells were grown in liquid media, pelleted, and frozen at -80°C. Frozen cell pellets were washed in 500μL of TP (20mM Tris HCl, pH 7.9, 0.5M EDTA, 10% glycerol, 50mM NaCl, 2μg/μL 500x protease inhibitor stock) and centrifuged at 12,000 rpm for one minute. The pelleted was resuspended in 200μL TP and 100μL of glass beads were added. Samples were vortexed for one minute, followed by incubation on ice for one minute. After repeating this vortexing and ice incubation four times to ensure cell lysis, samples were centrifuged at 7,000 rpm for seven minutes at 4°C.

Sample concentration was determined by performing Bradford assays. Cell extracts were diluted in autoclaved deionized water and loaded in duplicate into a 96-well plate. Standard wells were loaded with 0, 5, 10, 15 or 20 μ L of 100 μ g/mL BSA. After adding 150 μ L Bradford reagent to all wells, plates were read on a BioTek Synergy™ Mx microplate reader with Gen5 v2.04 software.

The supernatant was transferred to a new tube and 6X protein loading buffer (0.35 mM Tris HCl, pH 6.8, 36% glycerol, 10% SDS, 5% β -mercaptoethanol, 0.012% bromophenol blue) was added for SDS-PAGE gel electrophoresis. The amount of 6X protein loading buffer added was calculated by dividing the volume of the supernatant in the tube by six.

Western Blotting

Protein samples in 6X protein loading buffer were incubated at 65°C to denature them before loading into an 8% SDS-PAGE gel. After electrophoresis, proteins resolved on the gel were transferred to a nitrocellulose membrane. Staining with Coomassie Brilliant Blue R-250 dye from Thermo Fisher Scientific or SWIFT™ dye from G-Biosciences was performed on gels or membranes, respectively. A 10mL 5% solution of non-fat milk in TBST (1X TBS, 0.1% Tween 20) was used for both membrane blocking and antibody dilution. For detection of TAP-tagged proteins, membranes were blotted overnight at 4°C with primary polyclonal antibody, α -Protein A (1:100,000 working concentration), and for an hour at room temperature with secondary antibody, Goat α -Rabbit IgG-HRP (1:5,000 working concentration). For detection of the Pgk1 loading control, membranes were blotted overnight at 4°C with primary monoclonal antibody, α -Pgk1 (1:10,000 working concentration), and for an hour at room temperature with secondary antibody, Goat α -Mouse IgG-HRP (1:5,000 working concentration). After each antibody exposure, membranes were washed three times for five minutes in 10mL TBST. Membranes were incubated in a GE Amersham™ ECL™

Prime Western Blotting Detection Reagent kit and imaged on a GE ImageQuant™ LAS 4000 Mini.

Yeast RNA Isolation

Cells were grown in liquid media, pelleted, and frozen at -80°C. Total RNA was collected similarly to a previously described phenol-chloroform method (Caponigro *et al.*, 1993). Prior to use, phenol and phenol-chloroform solutions were equilibrated with LET (100mM LiCl, 20mM EDTA, 25mM Tris, pH 8.0). Yeast cell walls were disrupted by vortexing in phenol with 100µL glass beads. Multiple wash and centrifugation steps were performed to isolate the RNA-containing aqueous phase, which was then frozen at -80°C in 1mL 100% ethanol and 40µL 3M NaAc. The precipitated RNA was then pelleted by centrifugation at 15,000 rpm for thirty minutes. After vacuum drying the RNA pellet, it was resuspended in 200µL diethylpyrocarbonate (DEPC)-treated water and quantified with a GE NanoVue™ Plus Spectrophotometer.

Isolation with hot phenol was performed to obtain RNA for RNA-Seq, similarly to a previously described protocol (He *et al.*, 2008). Frozen cell pellets were resuspended in 500µL RNA buffer A (1.67% NaOAc, 0.5M EDTA, deionized water) before adding 500µL of a phenol/RNA buffer A solution, which was heated to 65°C. Samples were incubated at 65°C for a total of four minutes, with a ten second vortex step each minute. Samples were then centrifuged at 15,000 rpm for four minutes. The aqueous layer was collected and fresh 500µL phenol/RNA buffer A solution was added. Incubating, vortexing, and centrifuging was repeated. The re-isolated aqueous layer was added to a new tube and vortexed with 500µL of a phenol-chloroform solution, equilibrated with TE (1M Tris, pH 8.0, 0.5M EDTA, deionized water). After centrifugation for four minutes at 15,000 rpm, the aqueous layer was pipetted into a new tube, mixed with 1mL 100% ethanol, and incubated at -80°C. The precipitated RNA was pelleted and washed in 1mL 70% ethanol before resuspension in

100 μ L DEPC-treated water. Samples were incubated at 65°C, vortexed, and incubated on dry ice a total of six times before quantification on a GE NanoVue™ Plus Spectrophotometer.

Northern Blotting

After RNA isolation, samples were run on a denaturing gel. This gel was either formaldehyde agarose or urea polyacrylamide, depending on the length of transcripts that would be probed. After being run on an agarose or polyacrylamide gel, RNA was transferred to either a nitrocellulose or a nylon membrane, respectively, and crosslinked with a Stratagene UV Stratalinker® 1800. Oligonucleotides designed to probe the specific transcripts of interest were 5' labelled with ATP- γ -³²P, using T4 polynucleotide kinase. Crosslinked membranes were hybridized with the radioactively-labelled nucleotides and exposed to phosphor screens. Phosphorimaging of the screens was done with an Amersham STORM PhosphorImager™ or a GE Typhoon™ FLA 7000.

qRT-PCR

After treating samples with DNase using the Ambion® TURBO DNA-free™ kit, quantitative reverse transcriptase-PCR (qRT-PCR) was carried out with the SYBR® Green RNA-to-Ct™ 1-Step kit from Applied Biosystems, using oligonucleotides designed for specific transcripts (**Table 2.3**). Oligonucleotides specific for CUTs were designed as previously described (Wyers *et al.*, 2005). qRT-PCR reactions were performed with an Applied Biosystems® 7500 Real Time PCR System. Transcripts were normalized to an *ACT1* control, measured with oligonucleotides from the laboratory of Kevin Morano at UTHealth (**Table 2.3**). Microsoft® Excel was used to calculate and graph values.

Transcriptome Sequencing

After isolating RNA with the hot phenol method, sample quality was assessed via formaldehyde agarose gel electrophoresis. Transcriptome sequencing (RNA-Seq) was performed on an Illumina HiSeq2500™ by LC Sciences in Houston, Texas, USA. Poly(A)⁺

RNA was isolated from duplicate cultures of *trf4* Δ , *trf5* Δ double deletion strains complemented with either *TRF5* or *trf5* Δ 98-117 plasmids. This poly(A)⁺ RNA was then converted to a sequencing library. Each library was sequenced and yielded between ten and fourteen million reads of fifty nucleotides. The Bowtie open-source software package was used to map these reads to the annotated yeast genes (ftp://ftp.ensembl.org/pub/release-77/fasta/saccharomyces_cerevisiae/dna/). Genes that were significantly up- or down-regulated in strains expressing mutant variants of Trf4/5 proteins were identified using the previously described edgeR open-source software package (Robinson *et al.*, 2010).

Similar analysis was performed with duplicate cultures of *trf4* Δ , *trf5* Δ double deletion strains complemented with plasmids allowing for the expression of either wild-type or mutant variants of both Trf4/5 proteins. These mutant variants are lacking either the necessary site for interaction with Mtr4 (*trf4* Δ 115-134, *trf5* Δ 98-117) or both N- and C-termini (*trf4* Δ N Δ C, *trf5* Δ N Δ C). RNA-Seq was performed at the Nex-Gen Core at the University of Texas Medical Branch at Galveston. The poly(A)⁺ RNA was converted to sequencing libraries, each yielding between twenty-six million to thirty-eight million paired-end reads of seventy-five nucleotides. The TopHat open-source software package was used to map these reads to the yeast genome (ccb.jhu.edu/software/tophat/index.shtml). The Cufflinks open-source software package was used to determine differential gene expression (cole-trapnell-lab.github.io/cufflinks/). Hits were further classified by analysis with open-access tools provided by the Gene Ontology (GO) Consortium (geneontology.org). Data values were plotted with Microsoft[®] Excel.

Multiple Sequence Alignment

Sequences were obtained from the Fungal Orthogroups Repository (broadinstitute.org/regev/orthogroups/). Alignment of these sequences was generated with the publicly accessible EMBL-EBI Clustal Omega program (ebi.ac.uk/Tools/msa/clustalo/).

The desired file format was obtained by inputting the sequence alignment into the publicly accessible SIB BoxShade server (ch.embnet.org/software/BOX_form.html).

CHAPTER 3

Assessing Human PCH1b-Associated Mutations with Yeast Models

This chapter is based upon Fasken MB*, Losh JS*, Leung SW, Brutus S, Avin B, Vaught JC, Potter-Birriel J, Craig T, Conn GT, Mills-Lujan K, Corbett AH, van Hoof A.

Insight into the RNA exosome complex through modeling pontocerebellar hypoplasia type 1b disease mutations in yeast. *Genetics*. 2017; 205: 221-37 (*these authors

contributed equally to this work). Permission from the Genetics Society of America is not needed if reproducing an article for a dissertation (genetics.org/content/permissions).

INTRODUCTION

Pontocerebellar hypoplasia (PCH) is a group of autosomal recessive disorders caused by mutations in one of several genes (**Table 3.1**). Amino acid substitutions in *EXOSC3*, the gene encoding the human ortholog of the yeast RNA exosome cap subunit Rrp40, have been linked with PCH subtype 1b (PCH1b) (Wan *et al.*, 2012) (**Figure 3.1, cyan**). Similarly, PCH1c is caused by mutations in *EXOSC8*, which encodes the human ortholog of the yeast RNA exosome core ring subunit, Rrp43 (Boczonadi *et al.*, 2014) (**Figure 3.1, pink**). However, most PCH subtypes are caused by mutations in genes encoding tRNA splicing endonuclease subunits that function in tRNA processing, a selenocysteinyl tRNA charging enzyme, or a mitochondrial arginyl-tRNA synthetase (Edvardson *et al.*, 2007; Budde *et al.*, 2008; Agamy *et al.*, 2010; Namavar *et al.*, 2011; Hanada *et al.*, 2013; Schaffer *et al.*, 2014; Breuss *et al.* 2016) (**Table 3.1, green rows**). Most recently, PCH7 was linked to mutations in an exonuclease that is important for snRNA maturation (Lardelli *et al.*, 2017).

Yet, a few PCH subtypes are associated with genes that have no obvious role in RNA processing (**Table 3.1, orange rows**). These mutations are found in genes encoding vaccinia-related kinase, chromatin modifying protein 1A, and adenosine monophosphate deaminase 2 (Renbaum *et al.*, 2009; Mochida *et al.*, 2012; Akizu *et al.*, 2013). Additionally, PCH subtypes have been linked with mutations in genes encoding components of endosome or synaptic vesicle transport machinery (Feinstein *et al.*, 2014; Ahmed *et al.*, 2015). While the link between these genes and PCH is not immediately evident, the downstream effects of the essential catalytic activity of the RNA exosome are undoubtedly important for most, if not all, aspects of cellular physiology. Understanding how these unrelated genetic mutations cause PCH disorders with common traits requires the study of the functional defects that lead to disease.

Table 3.1 Subtypes of pontocerebellar hypoplasia (PCH)			
PCH Subtype	Associated Gene	Function of Encoded Protein	Reference
1a	<i>VRK1</i>	Serine/threonine-protein kinase	(Renbaum <i>et al.</i> , 2009)
1b	<i>EXOSC3</i>	Cap subunit of RNA exosome	(Wan <i>et al.</i> , 2012)
1c	<i>EXOSC8</i>	Core subunit of RNA exosome	(Boczonadi <i>et al.</i> , 2014)
2a	<i>TSEN54</i>	Subunit of tRNA splicing endonuclease	(Budde <i>et al.</i> , 2008)
2b	<i>TSEN2</i>	Subunit of tRNA splicing endonuclease	(Budde <i>et al.</i> , 2008)
2c	<i>TSEN34</i>	Subunit of tRNA splicing endonuclease	(Budde <i>et al.</i> , 2008)
2d	<i>SEPSECS</i>	Selenocysteinyl-tRNA charging	(Agamy <i>et al.</i> , 2010)
2e	<i>VPS53</i>	Endosome transport	(Feinstein <i>et al.</i> , 2014)
2f	<i>TSEN15</i>	Subunit of tRNA splicing endonuclease	(Breuss <i>et al.</i> , 2016)
3	<i>PCLO</i>	Synaptic vesicle cycling	(Ahmed <i>et al.</i> , 2015)
4	<i>TSEN54</i>	Subunit of tRNA splicing endonuclease	(Budde <i>et al.</i> , 2008)
5	<i>TSEN54</i>	Subunit of tRNA splicing endonuclease	(Namavar <i>et al.</i> , 2011)
6	<i>RARS2</i>	Mitochondrial arginyl-tRNA synthesis	(Edvardson <i>et al.</i> , 2007)
7	<i>TOE1</i>	snRNA maturation	(Lardelli <i>et al.</i> , 2017)
8	<i>CHMP1A</i>	Chromatin modification	(Mochida <i>et al.</i> , 2012)
9	<i>AMPD2</i>	Adenosine monophosphate deamination	(Akizu <i>et al.</i> , 2013)
10	<i>CLP1</i>	Pre-tRNA processing	(Hanada <i>et al.</i> , 2013) (Schaffer <i>et al.</i> , 2014)

Table 3.1 Subtypes of pontocerebellar hypoplasia (PCH). While this rare autosomal recessive disorder is characterized by atrophy of the pons and cerebellum, it is further divided into subtypes based on additional phenotypes and/or associated genes. While many PCH subtypes are associated with genes that are clearly important for RNA processing (green rows), the genetic basis of other subtypes does not appear to be directly linked with this mechanism (orange rows).

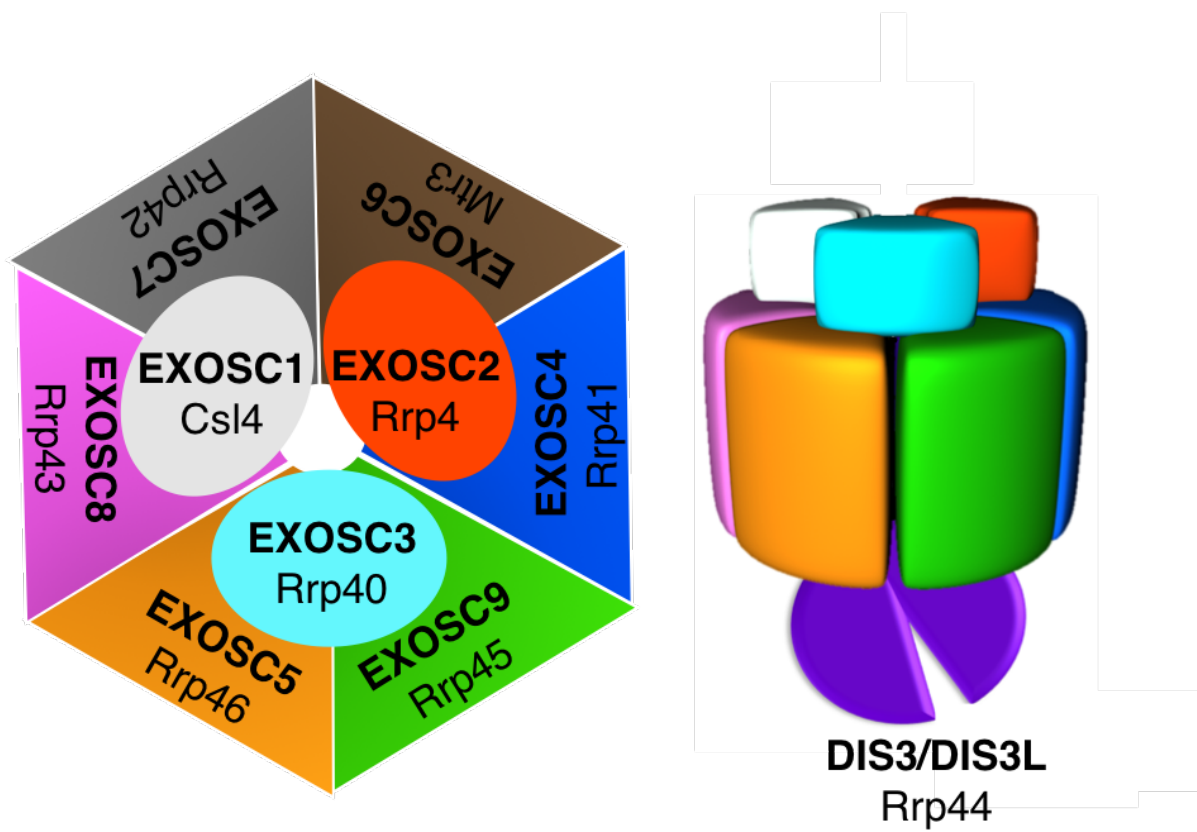


Figure 3.1 Human and yeast nomenclature of RNA exosome subunits. The structure of the RNA exosome is conserved throughout eukaryotes. Yeast subunits (previously introduced in **Figure 1.1**) directly correlate to human orthologs, whose names are provided in bold.

Pontocerebellar Hypoplasia Subtype 1b (PCH1b) and EXOSC3

While severe atrophy of the pons and cerebellum is the common feature of all PCH subtypes, Individuals affected with PCH1b also exhibit Purkinje cell abnormalities and spinal motor neuron degeneration (Wan *et al.*, 2012). Other PCH1b phenotypes include severe muscular atrophy, microcephaly, and retardation in both growth and mental development (Rudnik-Schöneborn *et al.*, 2013). Most patients do not live past childhood, even with symptomatic treatment. Elucidating the molecular mechanisms that underlie PCH1b is critical for developing new therapies.

The essential protein, EXOSC3/Rrp40 is one of the three cap subunits of the RNA exosome. It has an N-terminal domain, central S1 domain, and C-terminal KH domain (Oddone *et al.*, 2007). The latter two domains are putative sites of RNA binding. Moreover, the structure of these two domains forms a pocket, which has recently been identified as a binding site for Mpp6, a nuclear cofactor of the RNA exosome that delivers substrates for degradation (Milligan *et al.*, 2008; Falk *et al.*, 2017a). In addition to binding RNA or cofactors, the cap subunits also each interact with two subunits of the RNA exosome core ring. Specifically, EXOSC3/Rrp40 binds to core subunits EXOSC5/Rrp46 and EXOSC9/Rrp45 (**Figure 3.1, cyan, orange, green**) (Liu *et al.*, 2006).

It is currently unclear how the mutations in *EXOSC3* contribute to PCH1b, but it is unlikely that they cause a complete inactivation of the RNA exosome since this complex is both conserved and essential (Mitchell *et al.*, 1997). *EXOSC3* amino acid substitutions may cause PCH1b by several potential mechanisms. First, these mutations may affect a subset of RNA exosome functions. For example, only the mRNA degradation activity of the RNA exosome is inhibited in yeast cells that express mutant variants of Csl4, another subunit of the cap (van Hoof *et al.*, 2000b). It is also possible that PCH1b-associated changes in the EXOSC3 subunit could affect the ability of the RNA exosome to degrade normal, premature, or aberrant forms of tRNA. Second, the incorporation of a mutant EXOSC3 subunit into the

RNA exosome could reduce total activity of the complex. Third, the mutations could impair RNA exosome-independent functions of the EXOSC3 protein if such functions exist. However, this seems less likely than the possibilities listed above since mutations in another RNA exosome subunit gene, *EXOSC8*, result in PCH phenotypes as well (Boczanadi *et al.*, 2014).

PCH1b-Associated *EXOSC3* Mutations

Analysis of exons from multiple PCH1b individuals within a single family identified *EXOSC3* as the causative gene. This was confirmed by expanding the analysis to include patients from twelve more families (Wan *et al.*, 2012). As with other autosomal-recessive diseases, PCH1b occurs at a higher frequency in consanguineous families. Patients homozygous for the *EXOSC3-G31A* allele exhibit severe disease, while a homozygous *EXOSC3-D132A* allele results in a less severe phenotypes (**Table 3.2**). However, heterozygosity of *EXOSC3-D132A* with likely null alleles results in increased severity (Wan *et al.*, 2012; Biancheri *et al.*, 2013; Rudnik-Schöneborn *et al.*, 2013; Schwabova *et al.*, 2013; Eggens *et al.*, 2014) (**Table 3.2**). *EXOSC3-G31A* has not been found in combination with obvious null alleles, but it has been found in compound heterozygosity with an *EXOSC3-W238R* mutant allele (Wan *et al.*, 2012; Rudnik-Schöneborn *et al.*, 2013) (**Table 3.2**). Loss of *EXOSC3* has been modeled in zebrafish by knockdown with antisense morpholinos, which revealed brain abnormalities and decreased motility similar to human phenotypes (Wan *et al.*, 2012). Yet, the functional consequences of these specific point mutations in *EXOSC3* have not been analyzed in detail. Two additional mutations in *EXOSC3* have been identified but the associated phenotypes are less severe than those described in previous studies. These patients were only reported to exhibit mild pontocerebellar atrophy, if any (Zanni *et al.*, 2013; Halevy *et al.*, 2014).

Table 3.2 Major <i>EXOSC3</i> mutations in PCH1b patients				
Substitution	PCH1b Patient Genotype		Disease Severity	Patient Lifespan
G31A	G31A	Homozygous	Severe	4-17 months
D132A	D132A	Homozygous	Less severe	3-20 years
	D132A/null	Heterozygous	Severe	4-27 months
W238R	W238R/G31A	Heterozygous	Severe	7-8 months

Table 3.2 Major *EXOSC3* mutations in PCH1b patients. Previously reported genotypes, disease severity, and lifespan are presented to provide context for the functional consequences of the different amino acid substitutions (Wan *et al.*, 2012; Biancheri *et al.*, 2013; Rudnik-Schöneborn *et al.*, 2013; Schwabova *et al.*, 2013; Eggens *et al.*, 2014).

RESULTS

Yeast Can Be Employed as a Model System to Study PCH1b-Associated Mutations

To begin to address the molecular defects that underlie PCH1b, I collaborated with the laboratory of Dr. Anita Corbett at Emory University to create and analyze amino acid substitutions in yeast *RRP40* that correspond to the *EXOSC3* substitutions of PCH1b patients. We generated a protein sequence alignment of human *EXOSC3*, yeast *Rrp40*, and other eukaryotic orthologs. Human RNA exosome cap subunit *EXOSC2* and yeast ortholog *Rrp4* were also included in the alignment due to their functional similarity to *EXOSC3/Rrp40*. Archaea only have an *EXOSC2/Rrp4* ortholog, which was also included in our alignment (Buttner *et al.*, 2005; Lorentzen *et al.*, 2007) (**Figure 3.2 A**).

The human *EXOSC3* residues that are substituted in PCH1b are among the most conserved residues of this protein. Only ten residues of human *EXOSC3* have remained perfectly conserved and two of them, G31 and W238, are PCH1b-associated. Residue D132 is also conserved in most orthologs, but it has been replaced by a serine in yeast *Rrp40* and most other ascomycete orthologs (**Figure 3.2 A**).

We aimed to assess the functional consequences of these PCH1b-associated substitutions. Human *EXOSC3* protein does not substitute for the essential function of *Rrp40* protein in yeast (Brouwer *et al.*, 2001). Therefore, we first created mutations in the yeast *RRP40* gene that result in the expression of the following variants: *rrp40-G8A* (corresponding to *EXOSC3-G31A*), *rrp40-S87A* (corresponding to *EXOSC3-D132A*), and *rrp40-W195R* (corresponding to *EXOSC3-W238R*). In both humans and yeast, these PCH1b-associated residues are found in all three domains of *EXOSC3/Rrp40* (**Figure 3.2 B**).

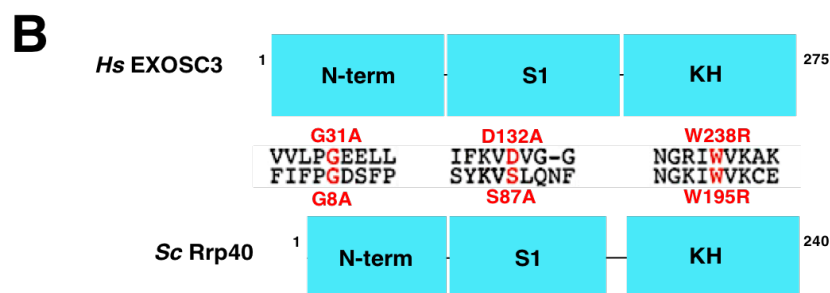
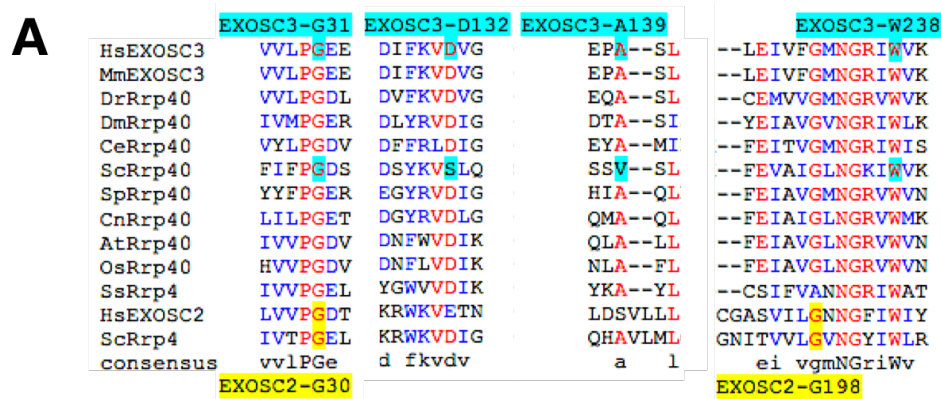


Figure 3.2 Protein sequence alignment of EXOSC3 orthologs. **(A)** This alignment was generated from the protein sequences of human EXOSC3, yeast Rrp40, EXOSC3/Rrp40 orthologs from other multi- and unicellular eukaryotes, human EXOSC2, yeast Rrp4, and archael Rrp4. There is significant sequence conservation around sites corresponding to those of PCH1b-associated mutations, as evidenced by the presence of identical residues (red) and similar residues (blue). Selected regions of the alignment reveal that the amino acids substituted in human EXOSC3 in PCH1b patients are conserved in yeast Rrp40 (highlighted in cyan). Amino acids substituted in human EXOSC2 in patients with a novel syndrome, SHRF, are conserved in yeast Rrp4 (highlighted in yellow). **(B)** Both EXOSC3 and Rrp40 contain three domains: an N-terminal domain, a central putative RNA-binding S1 domain, and a C-terminal putative RNA-binding KH domain. The position and flanking sequence of the major PCH1-associated amino acid substitutions in human EXOSC3 and the corresponding substitutions generated in yeast Rrp40 are indicated in red.

To create a yeast model, *LEU2* plasmids encoding for Myc-tagged wild-type Rrp40 protein or each mutant variant under the control of the endogenous *RRP40* promoter were generated and transformed into *rrp40Δ* cells that already contain [*RRP40*, *URA3*] plasmids. The plasmid shuffle was performed to select against the [*RRP40*, *URA3*] plasmids, resulting in the specific expression of *LEU2* plasmid constructs in the *rrp40Δ* background. This ensured that the sole copy of *RRP40* in the yeast model was either wild-type or one of the *rrp40* mutant alleles that correspond to PCH1b-associated mutations in *EXOSC3*.

PCH1b-Associated Mutations Likely Have Structural Consequences

To assess the potential interactions of the residues mutated in PCH1b patients, we examined previously published RNA exosome structures from both humans and yeast (Liu *et al.*, 2006; Makino *et al.*, 2013; Wasmuth *et al.*, 2014). These structures are publicly available through the Research Collaboratory for Structural Bioinformatics Protein Data Bank (rcsb.org/pdb/home/home.do). Based on these structures, the positions of the PCH1b-associated conserved residues (black, bold) in EXOSC3/Rrp40 (blue) are shown within the context of the RNA exosome (**Figure 3.3**). Strikingly, the residues are all in positions that could be important for interactions with other RNA exosome subunits, although they are not clustered together in primary sequence and they are located in different domains (**Figure 3.2 B**; Wan *et al.*, 2012). Specifically, Rrp40 residue G8 is packed against residues S129, M130, and V168 of Rrp46, a subunit of the RNA exosome core (**Figure 3.3**). Substituting any bulkier side chain at Rrp40 G8, such as the PCH1b-associated substitution to alanine, could interfere with the interaction of these two RNA exosome subunits. Similar positioning indicates that this may also occur in the case of EXOSC3 residue G31. Rrp40 residue S87 forms a hydrogen bond with Rrp40 Q89, which could be disrupted by the PCH1b-associated substitution to alanine (**Figure 3.3**). This hydrogen bond formation is also seen in the corresponding residues of the human RNA exosome structure. A disruption of this hydrogen bond could impair the folding of a loop located within the S1 domain of EXOSC3/Rrp40.

Unlike Rrp40 residues G8 and S87, Rrp40 W195 is not located at an RNA exosome subunit interface, but it could still be important for maintaining interactions between subunits. This residue is located in a pocket surrounded by a loop containing Rrp40 D152, which is positioned to make a salt bridge with residue K13 of Rrp45, a subunit of the RNA exosome core (**Figure 3.3**). These residues are similarly positioned in the human RNA exosome structure. The PCH1b-associated substitution to arginine at W195 could therefore alter the position of D152, subsequently weakening the interaction with Rrp45. In addition to possibly affecting the ability of Rrp40 to interact with other RNA exosome subunits, the location of PCH1b-associated substitutions could also affect RNA binding or interactions with RNA exosome cofactors.

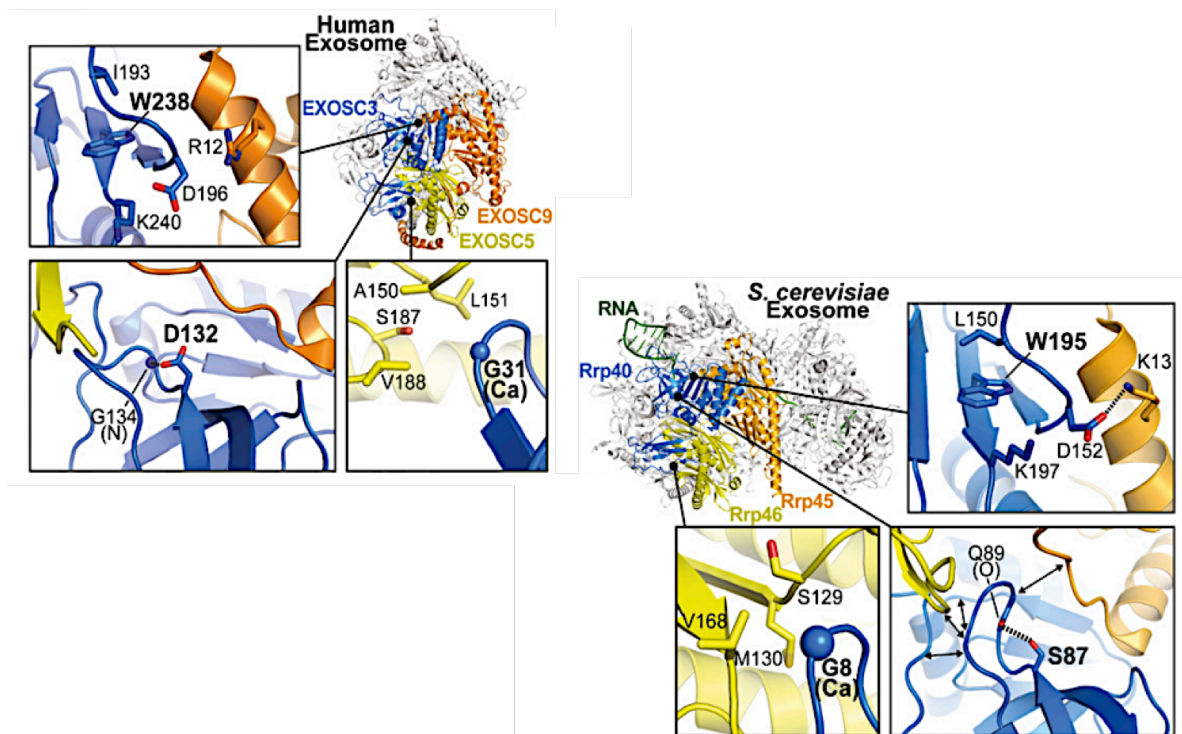


Figure 3.3 PCH1b-associated substitutions occur at EXOSC3 residues located near RNA exosome subunit interfaces. Structural models of the human RNA exosome (left) [PDB#2NN6 (Liu *et al.*, 2006)] and yeast RNA exosome (right) [PDB#4IFD (Makino *et al.*, 2013)] are depicted. The nine-subunit human RNA exosome structure highlights the EXOSC3 (blue), EXOSC5 (yellow), and EXOSC9 (orange) subunits. The yeast RNA exosome structure highlights the orthologous Rrp40 (blue), Rrp46 (yellow), and Rrp45 (orange) subunits. Zoomed-in views of three subunit interface regions show the locations of PCH1b-associated residues G31, D132, and W238 (bold). Additional zoomed-in views show the evolutionarily conserved Rrp40 residues G8, S87, and W195 (bold). EXOSC3 G31/Rrp40 G8 is located in a hydrophobic pocket at an interface with EXOSC5/Rrp46. EXOSC3 D132/Rrp40 S87 and the backbone of G134/Q89 are positioned to form a hydrogen bond that may organize the loop between strands β 3 and β 4, which is at the interface with both EXOSC5/Rrp46 and EXOSC9/Rrp45. EXOSC3 W238/Rrp40 W195 sits in a large pocket and could be important for positioning the loop that forms an interface with EXOSC9/Rrp45.

Expressing Some PCH1b-Associated Variants in Yeast Results in Growth Deficiency

In yeast, all of the RNA exosome subunits are encoded by essential genes (Allmang *et al.*, 1999a). To first test the functional consequences of PCH1b-associated substitutions, I assessed whether the *rrp40* mutant genes could complement the lethality of a yeast *rrp40* Δ mutant. For these studies, I examined *rrp40-G8A*, *rrp40-S87A*, and *rrp40-W195R* mutant strains. Since the substitution of tryptophan 195 to arginine in *rrp40-W195R* cells is a dramatic change, my collaborators and I decided to also change tryptophan 195 to alanine (*rrp40-W195A*). This removes the large hydrophobic residue without simultaneously introducing a positive charge. In addition, we created a very conservative change of tryptophan 195 to phenylalanine (*rrp40-W195F*), which retains the large hydrophobic residue.

I grew *rrp40* Δ cells expressing each substitution variant as the sole copy of the essential *RRP40* gene. These cells were serially diluted and spotted on plates, which were incubated at various temperatures. In this solid medium assay, *rrp40-W195R* and *rrp40-W195A* mutant cells gave rise to smaller colonies, indicative of a modest growth defect that is most noticeable at 37°C (**Figure 3.4 A**). To provide a more quantitative comparison of growth rates, I also performed growth assays in liquid cultures at 37°C. This analysis revealed that *rrp40-W195A* and *rrp40-W195R* cells grow at a slower rate than wild-type *RRP40* cells. Their doubling times increased by 13% and 20%, respectively, compared to *RRP40* cells (**Figure 3.4 B, C**). The other variants, *rrp40-G8A* and *rrp40-S87A*, grew in a manner indistinguishable from wild-type *RRP40* cells (**Figure 3.4 B**). The *rrp40-W195F* mutant also grew similarly to wild-type *RRP40* cells (**Figure 3.4 C**). At 30°C, the *rrp40-W195R* and *rrp40-W195A* mutant cells also reproducibly grew more slowly than the other mutants, although the difference was less pronounced than at 37°C (data not shown).

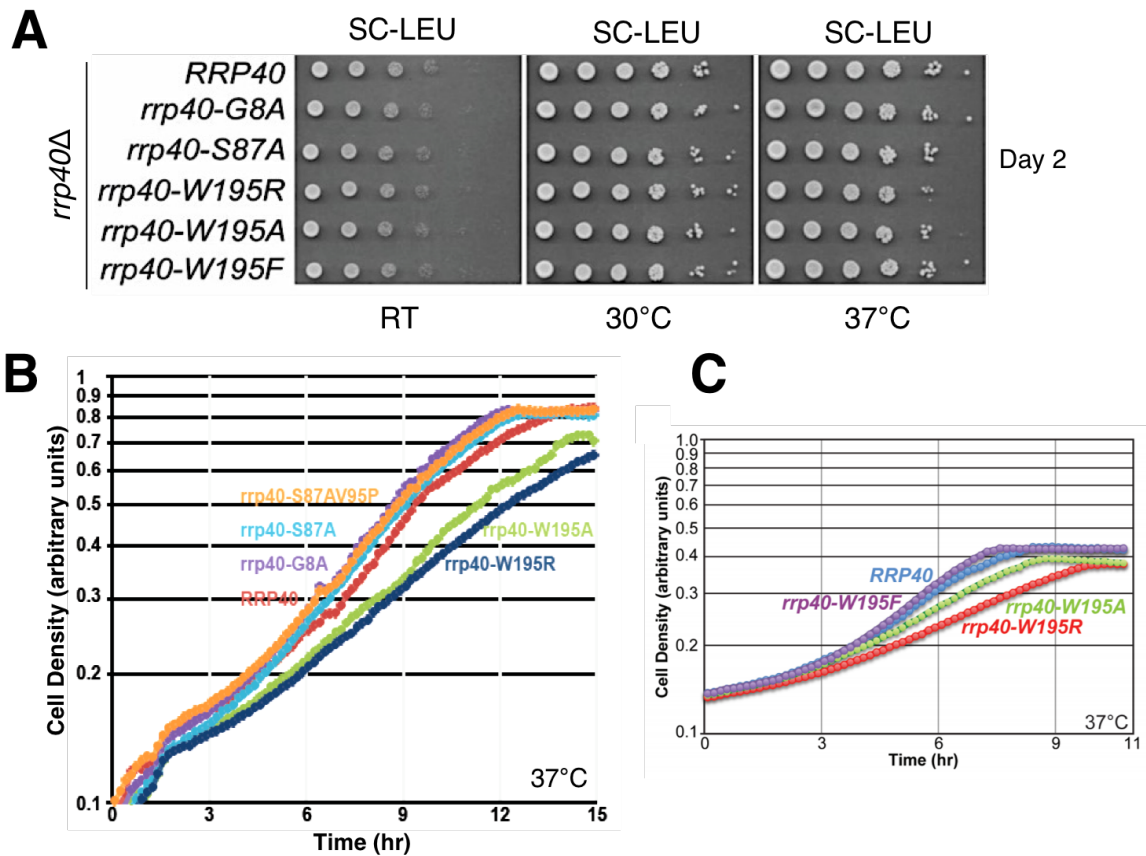


Figure 3.4 Yeast expressing *rrp40-W195R* or *rrp40-W195A* as the sole copy of Rrp40 exhibit impaired growth at 37°C. **(A)** The growth of *rrp40Δ* cells containing only wild-type *RRP40* or mutant *rrp40* plasmid was analyzed by performing serial dilutions, spotting onto selective solid medium, and incubation at the indicated temperatures. **(B)** The same strains were grown in triplicate in liquid selective medium at 37°C. Optical density was calculated every fifteen minutes. **(C)** Additional liquid growth assays were performed at 37°C, comparing the doubling times of cells expressing one of the three W195 variants to those expressing wild-type Rrp40 protein.

I took advantage of the fact that RNA exosome mutants are sensitive to the antimetabolite 5-fluorouracil (5-FU), an inhibitor of thymidine synthesis that impairs both DNA and RNA metabolism (Fang *et al.*, 2004; Lum *et al.*, 2004). To further assess the function of *rrp40-W195R* and *rrp40-W195A* proteins, I serially diluted and spotted the mutant strains on solid medium containing 25 μ M 5-FU. The plates were then incubated at several temperatures. The *rrp40-W195R* and *rrp40-W195A* strains exhibit reduced growth on 5-FU plates at 37°C, relative to wild-type *RRP40* cells (**Figure 3.5**). In contrast, the *rrp40-W195F* mutant shows growth similar to wild-type cells. These results demonstrate that no single amino acid substitution in Rrp40, which corresponds to a PCH1b-associated substitution in EXOSC3, causes a complete loss of Rrp40 protein function. Thus, at least some threshold level of EXOSC3 function is likely required for viability and development in humans. The results of **Figure 3.4** and **Figure 3.5** also show that substitutions removing the large hydrophobic W195 residue modestly impair cell growth.

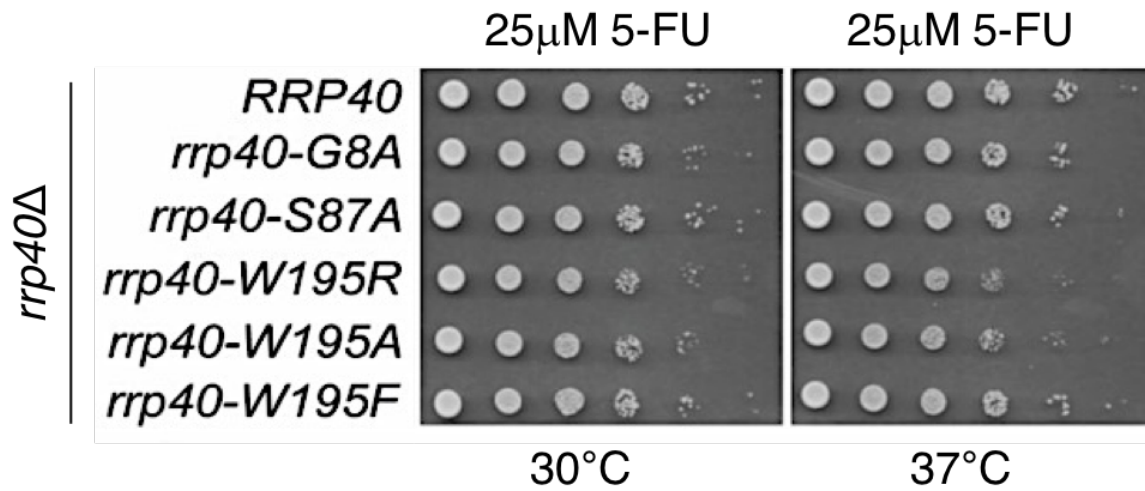


Figure 3.5 Yeast expressing *rrp40-W195R* or *rrp40-W195A* as the sole copy of Rrp40 exhibit impaired growth in the presence of 5-fluorouracil (5-FU). The growth of *rrp40Δ* cells containing only wild-type *RRP40* or mutant *rrp40* plasmid was analyzed by performing serial dilutions, spotting onto solid medium containing 25 μM 5-FU, and incubation at the indicated temperatures.

In addition to these five mutations, we generated *rrp40*Δ strains containing plasmids that encode either *rrp40-S87A/V95P* or *rrp40-D152A* mutant protein. A proline substitution at EXOSC3 residue A139 has been found in conjunction with the *EXOSC3-D132A* allele in a heterozygous PCH1b patient (Wan *et al.*, 2012). This residue is well-conserved and corresponds to valine, a similar hydrophobic amino acid, at position 95 in yeast Rrp40 (**Figure 3.2 A**). I included the *rrp40-S87A/V95P* strain in the liquid growth assays and found that this mutant grew similarly to wild-type *RRP40* cells (**Figure 3.4 B**).

While a mutation at EXOSC3 residue D196 has not been associated with PCH1b, we generated an alanine substitution at the corresponding D152 residue of Rrp40. As previously described, analysis of RNA exosome structures revealed that EXOSC3 W238 and Rrp40 W195 may have an important role in maintaining the interaction between EXOSC3/Rrp40 and EXOSC9/Rrp45 (**Figure 3.3**). It is possible that the presence of this bulky tryptophan residue is critical for positioning a nearby negatively charged aspartic acid in a conformation that allows for interaction with a positively charged residue on EXOSC9/Rrp45. Although we created strains lacking the tryptophan residue, we additionally replaced this aspartic acid to further analyze the importance of maintaining interaction between these RNA exosome subunits. I performed liquid growth assays to determine the effect of this mutation on cell growth. The growth of *rrp40-D152A* cells was significantly impaired in comparison to cells expressing wild-type Rrp40 or a mutant variant that retains a bulky hydrophobic residue at position 195 (**Figure 3.6**). This finding suggests that this aspartic acid residue is important for the Rrp40-Rrp45 interaction, which contributes to the structural integrity of the RNA exosome. Moreover, it further supports the hypothesis that this interaction is dependent upon the presence of a nearby bulky hydrophobic residue.

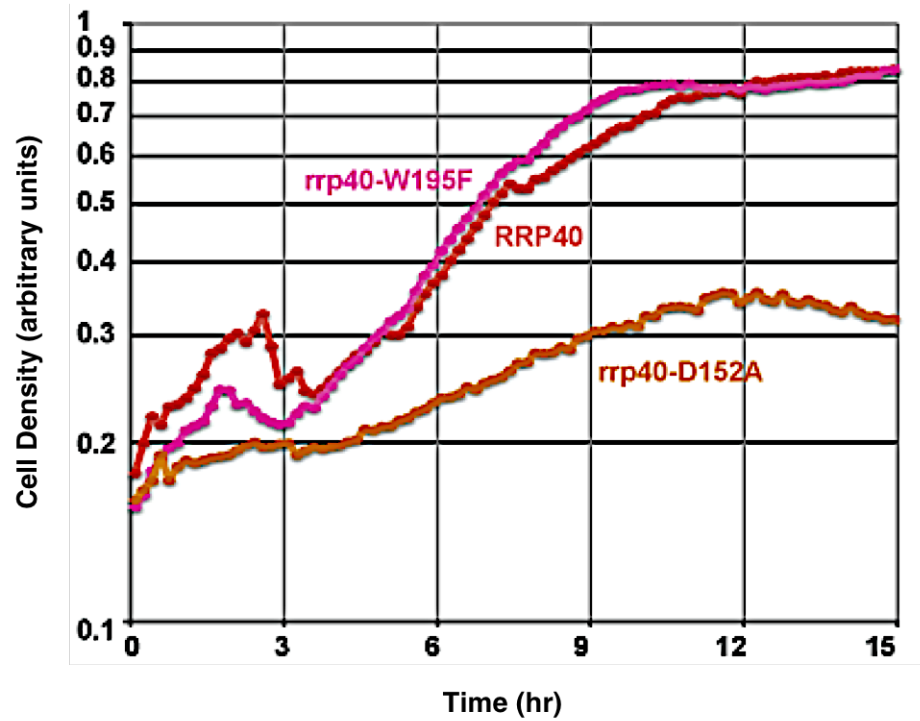


Figure 3.6 Yeast expressing *rrp40-D152A* as the sole copy of Rrp40 exhibit impaired growth at 37°C. The growth of *rrp40*Δ cells containing only wild-type *RRP40* or mutant *rrp40* plasmid in liquid selective medium was measured and compared. These strains were grown in triplicate and incubated at 37°C for the duration of the assay. Optical density was calculated every fifteen minutes.

PCH1b-Associated Mutations Could Affect Multiple Cellular Functions

It is unsurprising that one point mutation in a single RNA exosome subunit could cause such severe phenotypes since this complex is conserved, essential, and located in both the nucleus and the cytoplasm. Moreover, known PCH1b phenotypes are varied and irreversibly affect many types of tissues within a single patient. Therefore, possible effects of PCH1b-associated mutations on RNA exosome activity in the nucleus and cytoplasm, as well as subsequent effects on mitochondrial function, were assessed with the yeast model.

Assessing the Nuclear Activity of the Mutant RNA Exosome

To assess whether the slow growth observed for the *rrp40-W195R* mutant correlates with a change in RNA exosome function, my collaborators examined the steady-state level of several well-defined nuclear RNA exosome targets via quantitative RT-PCR. These selected transcripts were *ITS2* rRNA, *U4* snRNA, and the *NEL025C* CUT. *NEL025C* and *U4* RNA levels were modestly, but statistically significantly, increased in *rrp40-W195R* mutants at 37°C in comparison to a strain expressing wild-type Rrp40 protein. This is consistent with the changes in cellular growth revealed by my solid and liquid serial dilution assays. The level of *ITS2* transcripts was not significantly different in the mutant when compared to wild-type, suggesting that not all targets are equally affected by this PCH1b-associated mutation. Moreover, there was no significant difference in any of the RNA levels when comparing *rrp40-G8A* cells to wild-type *RRP40* cells (Falk, Losh *et al.*, 2017). This provides further evidence that RNA exosome function, specifically within the nucleus, is compromised in *rrp40-W195R* mutants.

Assessing the Cytoplasmic Activity of the Mutant RNA Exosome

I next assessed if expression of these *rrp40* mutant proteins affects the cytoplasmic functions of the RNA exosome. The rationale behind this was multifaceted. First, the cytoplasmic activity of the RNA exosome is not essential, as opposed to its nuclear functions (Jacobs Anderson and Parker, 1998). Second, mutations in a different subunit of the RNA

exosome cap (EXOSC1/Csl4) specifically inactivate its cytoplasmic function, but not its essential nuclear function (van Hoof *et al.*, 2000b). Finally, a clinical study of PCH proposed the hypothesis that PCH1b and PCH1c may result from a defect in cytoplasmic mRNA degradation by the RNA exosome (Boczonadi *et al.*, 2014).

To examine cytoplasmic function of the RNA exosome in *rrp40* mutants, I employed a *his3-nonstop* reporter assay. This assay exploits the observation that the yeast cytoplasmic RNA exosome is required for the degradation of mRNA transcripts that lack stop codons (van Hoof *et al.*, 2002). In cells with functional cytoplasmic RNA exosomes, the *his3-nonstop* reporter, which encodes the His3 protein and lacks stop codons, is degraded. Therefore, histidine is not biosynthesized in these cells so they cannot grow on media lacking this amino acid. In cells with defective cytoplasmic RNA exosomes, the *his3-nonstop* mRNA reporter is stabilized, biosynthesis of histidine proceeds, and the cells can grow on media lacking histidine. The *rrp40* Δ cells, expressing PCH1b-associated variants as the sole copy of Rrp40, were transformed with the *his3-nonstop* reporter plasmid. They were then serially diluted and spotted onto solid medium lacking histidine (His⁻) and control medium containing histidine (His⁺).

As a control for impaired cytoplasmic function, I also serially diluted and spotted a *ski7* Δ strain containing the *his3-reporter*, as Ski7 is a required cofactor of the cytoplasmic RNA exosome (van Hoof *et al.*, 2002). As expected, the *ski7* Δ control strain grew on His⁻ medium (**Figure 3.7**). In contrast, none of the experimental *rrp40* mutants grew on His⁻ medium, indicating that cytoplasmic RNA exosome-mediated nonstop mRNA decay proceeds normally in cells expressing these *rrp40* variants (**Figure 3.7**). These results suggest that amino acid substitutions linked to PCH1b do not block the function of the cytoplasmic RNA exosome, at least in yeast.

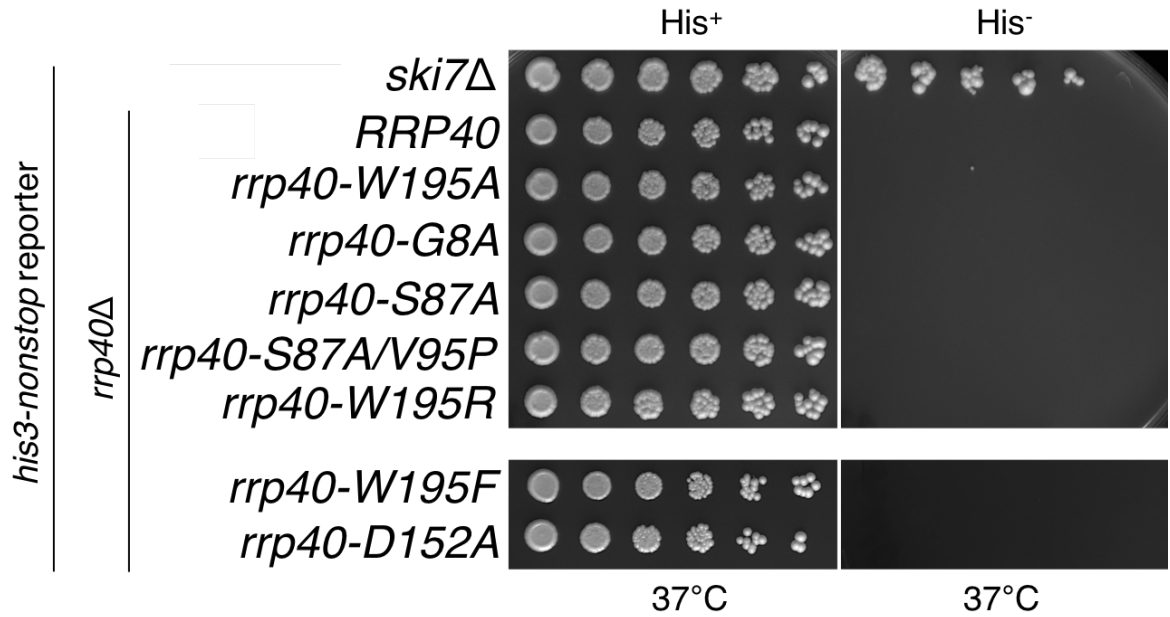


Figure 3.7 PCH1b-associated *rrp40* mutations do not impact cytoplasmic function of the RNA exosome. Yeast cells expressing *rrp40* variants as the sole copy of Rrp40 do not rescue a *his3-nonstop* reporter, which is rapidly degraded by the cytoplasmic RNA exosome, to restore growth on medium lacking histidine. As a control, deletion of *SKI7*, which encodes a key cofactor of the cytoplasmic RNA exosome, rescues the *his3-nonstop* reporter and thus confers growth on medium lacking histidine. The growth of *rrp40Δ* cells containing only wild-type *RRP40* or mutant *rrp40* plasmid was analyzed by performing serial dilutions, spotting onto solid medium containing histidine (His⁺) or lacking histidine (His⁻), and incubation at 37°C. The *rrp40-W195F* and *rrp40-D152A* strains were assayed identically to the other strains, but on a different day. Their ability to grow on medium lacking histidine was also compared to *ski7Δ* cells.

Assessing the Mitochondrial Activity in Cells Expressing PCH1b-Associated Mutations

A recently published case study described mitochondrial dysfunction in a patient with the PCH1b-associated allele, *EXOSC3-D132A*. Studies of the patient's muscular fibroblasts revealed that a significant amount of the mutant EXOSC3-D132A protein was accumulated in the cytoplasm. Copies of mitochondrial DNA (mtDNA) within the patient's muscle tissue were reduced to about a third of wild-type levels, yet no mutations in the mtDNA or mitochondrial genes were detected. RNA-Seq revealed that mRNA transcribed from genes encoding mitochondrial subunits was significantly increased in muscle tissue as well (Schottmann *et al.*, 2017). This transcript accumulation may be explained by RNA exosome dysfunction caused by the patient's *EXOSC3-D132A* mutation. Interestingly, the authors did not detect the same abnormalities in dermal fibroblasts (Schottmann *et al.*, 2017). This indicates that there may be a tissue-specific effect of the *EXOSC3-D132A* mutation, although it is unclear if this effect is direct or indirect.

To test if mitochondrial activity is impaired in the yeast model, I serially diluted and spotted strains expressing wild-type or mutant variants of Rrp40 onto solid medium containing glycerol instead of glucose as the carbon source. This glycerol-containing medium induces respiration in yeast, so lack of growth indicates that this mitochondrial process is negatively impacted. None of the strains, including cells expressing *rrp40-S87A* protein, which corresponds to EXOSC3-D132A, exhibited growth deficiencies on this medium at either 30°C or 37°C (**Figure 3.8**). This suggests that these mutations do not lead to mitochondrial impairment in yeast.

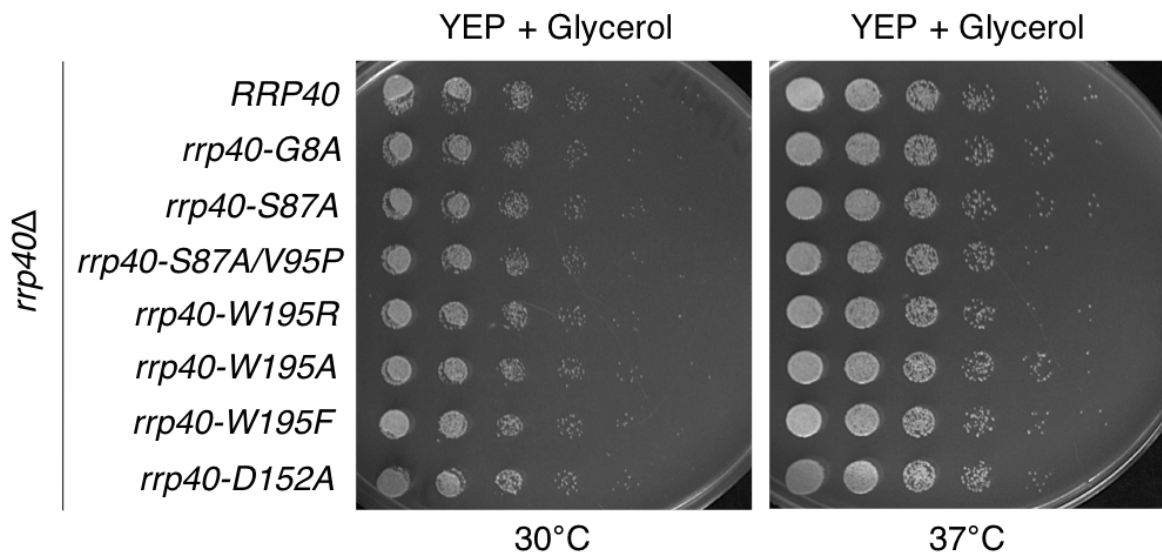


Figure 3.8 PCH1b-associated *rrp40* mutations do not impact mitochondrial respiration.

The growth of *rrp40Δ* cells containing only wild-type *RRP40* or mutant *rrp40* plasmid was analyzed by performing serial dilutions, spotting onto solid rich yeast medium containing glycerol as the sole carbon source, and incubation at the indicated temperatures.

Expression and Stability of EXOSC3/rrp40 Mutants Indicate Proteasomal Degradation

My collaborators performed several experiments to test whether PCH1-associated mutations impact protein levels and stability. Western blotting revealed that at 37°C, rrp40-G8A and rrp40-S87A expression was within twofold of wild-type Rrp40, while rrp40-W195R expression was reduced by about threefold (Fasken, Losh *et al.*, 2017). Expression of rrp40-W195A and rrp40-W195F variants were also reduced in comparison to wild-type Rrp40, but not as significantly. Therefore, my collaborators compared only the stability of the rrp40-W195R variant to that of wild-type Rrp40 via western blotting after cycloheximide treatment. Exponential decay curves revealed that at 30°C the rrp40-W195R variant is unstable with a half-life of ~116 minutes, in comparison to the Rrp40 half-life of ~222 minutes (Fasken, Losh *et al.*, 2017).

A potential explanation for the reduced stability of this variant could be that it does not assemble efficiently into the RNA exosome and therefore, is targeted for degradation by the proteasome. If this impaired assembly model was supported by subsequent assays, we hypothesized that the wild-type Rrp40 would outcompete a mutant variant for *in vivo* assembly into the RNA exosome. Whereas the previous western blotting assays were performed with *rrp40*Δ strains, which each expressed a Myc-tagged wild-type or mutant variant of Rrp40, my collaborators expressed Myc-tagged wild-type or mutant variants in a strain already expressing TAP-tagged wild-type Rrp40 to address this hypothesis. Quantitation of protein levels revealed that only the mutants with W195 substitutions were expressed at significantly lower levels than wild-type Rrp40 (Fasken, Losh *et al.*, 2017). Moreover, the levels of the W195 variants were even more reduced than when they had been expressed in *rrp40*Δ cells. My collaborators performed a similar cycloheximide treatment assay to test the stability of the rrp40-W195R variant when co-expressed with wild-type Rrp40. Exponential decay curves showed that the half-life of the mutant dropped to only ~6 minutes (Fasken, Losh *et al.*, 2017). These results suggest that these W195

variants, especially rrp40-W195R, cannot compete efficiently with wild-type Rrp40 for assembly into the RNA exosome.

To assess if this rapid degradation of rrp40-W195R is mediated by the proteasome, my collaborators compared the stability of this mutant in either a wild-type background or in a strain with a dysfunctional proteasome. Exponential decay curves revealed that rrp40-W195R was stable over the course of thirty-five minutes in cells with impaired proteasome function. However, this protein was very unstable in wild-type cells, with a short half-life of ~5 minutes (Fasken, Losh *et al.*, 2017). These results indicate that the rrp40-W195R variant is degraded by the proteasome and suggest that cells can selectively discriminate and target this variant for degradation when wild-type Rrp40 is available.

My collaborators next performed native-PAGE gel analysis to determine if this reduction in rrp40-W195R stability truly indicates reduced assembly into the RNA exosome. This assay compared levels of mutant or wild-type Rrp40 in cells with either normal or abnormal proteasome function. A high amount of wild-type Rrp40 in both strain backgrounds migrated as a single complex of ~600 kDa. Moreover, the amounts of rrp40-G8A and rrp40-S87A that migrated as a ~600 kDa complex were similar to wild-type Rrp40 in both strain backgrounds. However, only a low amount of rrp40-W195R migrated as a single complex of ~600 kDa in both strain backgrounds (Fasken, Losh *et al.*, 2017). Importantly, the native-PAGE lysates were analyzed by denaturing SDS-PAGE, which showed that the level of rrp40-W195R increased in the proteasome mutant background when compared to wild-type cells (Fasken, Losh *et al.*, 2017). Therefore, the reduced amount of migrated rrp40-W195R on the native gel was not simply due to low protein levels. These results suggest that the rrp40-W195R variant associates less efficiently with the RNA exosome than wild-type Rrp40 or even other PCH1b-associated variants.

To determine whether the results obtained using our yeast model extend to EXOSC3 in mammalian cells, my collaborators generated mutations in mouse *EXOSC3* that

correspond to PCH1b-associated substitutions and those analyzed in our yeast model. They assessed only two of the variants in mice, EXOSC3-G31A and EXOSC3-W237R, which correspond to EXOSC3-G31A/rrp40-G8A and EXOSC3-W238R/rrp40-W195R, respectively. Plasmids allowing for the expression of Myc-tagged wild-type or variant proteins were transfected into a mouse N2a neuronal cell line, which already expresses endogenous EXOSC3 protein (Klebe and Ruddle, 1969). Western blotting revealed that EXOSC3-G31A variant was reduced twofold relative to wild-type mouse EXOSC3, whereas EXOSC3-W237R showed a fourfold reduction (Fasken, Losh *et al.*, 2017). These results suggest that the mouse EXOSC3-W237R variant is unstable in the presence of wild-type EXOSC3, similar to the results from rrp40-W195R analysis in our yeast model. Therefore, mammalian cells may have conserved our proposed mechanism of discrimination between wild-type and variant EXOSC3 subunits during RNA exosome assembly.

PCH1b-Associated Mutations Do Not Affect the Degradation of *CBP1* mRNA

As previously stated, PCH is a genetically heterogeneous group of diseases. Mutations in genes encoding various enzymes involved in tRNA processing have been linked to PCH type 2, 4, 5, 6, and 10, although these mutations do not always result in tRNA defects (Edvardson *et al.*, 2007; Budde *et al.*, 2008; Agamy *et al.*, 2010; Namavar *et al.*, 2011; Hanada *et al.*, 2013; Schaffer *et al.*, 2014) (**Table 3.1**). Specifically, PCH4 and PCH5, as well as PCH2 subtypes a, b, c, and f, are caused by mutations in the tRNA splicing endonuclease (TSEN) complex. This is a conserved four-subunit enzyme that promotes intron removal from precursor tRNA and mutations in each subunit have been linked to PCH disease (Budde *et al.*, 2008; Battini *et al.*, 2014; Breuss *et al.*, 2016). Interestingly, PCH2 subtypes present similar, if not identical, symptoms to PCH1b and PCH1c, despite being caused by mutations in the TSEN complex instead of in the RNA exosome. However, like the RNA exosome, the TSEN complex is also an RNase.

While the main function of the TSEN complex is tRNA intron removal, it has an additional function, at least in yeast. The complex, known as the Sen complex in yeast, cuts *CBP1* mRNA. Cbp1 protein is required for the mitochondrial production of cytochrome b, an important component of the electron transport chain. The cleaved *CBP1* transcript is then degraded by the cytoplasmic RNA exosome (Tsuboi *et al.*, 2015). Products of Sen complex cleavage are not typically degraded via cooperative activity of the RNA exosome (Wu and Hopper, 2014). Therefore, this finding indicates a possible link between the similar pathology of PCH1 and PCH2. Perhaps transcripts important for neural and brain development are cleaved and degraded by a cooperative Sen complex-RNA exosome pathway (**Figure 3.9**). Consequently, PCH-associated mutations in either complex may disrupt this process, resulting in similar phenotypes.

A visiting summer undergraduate student, Keta Patel, assisted me with transforming several yeast strains with a plasmid encoding *CBP1*. Two alternative transcripts, differing at the 3' end, arise from this gene in response to metabolic signals (Mayer and Dieckmann, 1989). Transforming yeast with this plasmid allows for the overexpression of both *CBP1* transcripts. The strains used for this transformation included cells endogenously expressing PCH1-associated *rrp40-G8A*, *rrp40-G148C*, or *rrp40-W195R* mutant variants, gifted to us by the laboratory of Guillaume Chanfreau at the University of California, Los Angeles (Gillespie *et al.*, 2017). We also transformed a wild-type strain, as well as a *ski7Δ* strain that is defective in *CBP1* mRNA degradation. After isolating RNA from these transformants, I performed northern blotting to assess if the *CBP1* mRNA that is cleaved by the Sen complex accumulates due to PCH1-associated mutations. Expression of the mutant variants does not result in the accumulation of Sen complex-cleaved mRNA (**Figure 3.10**). This indicates that PCH1b-associated mutations do not disrupt the ability of the RNA exosome to clear the products of Sen complex cleavage.

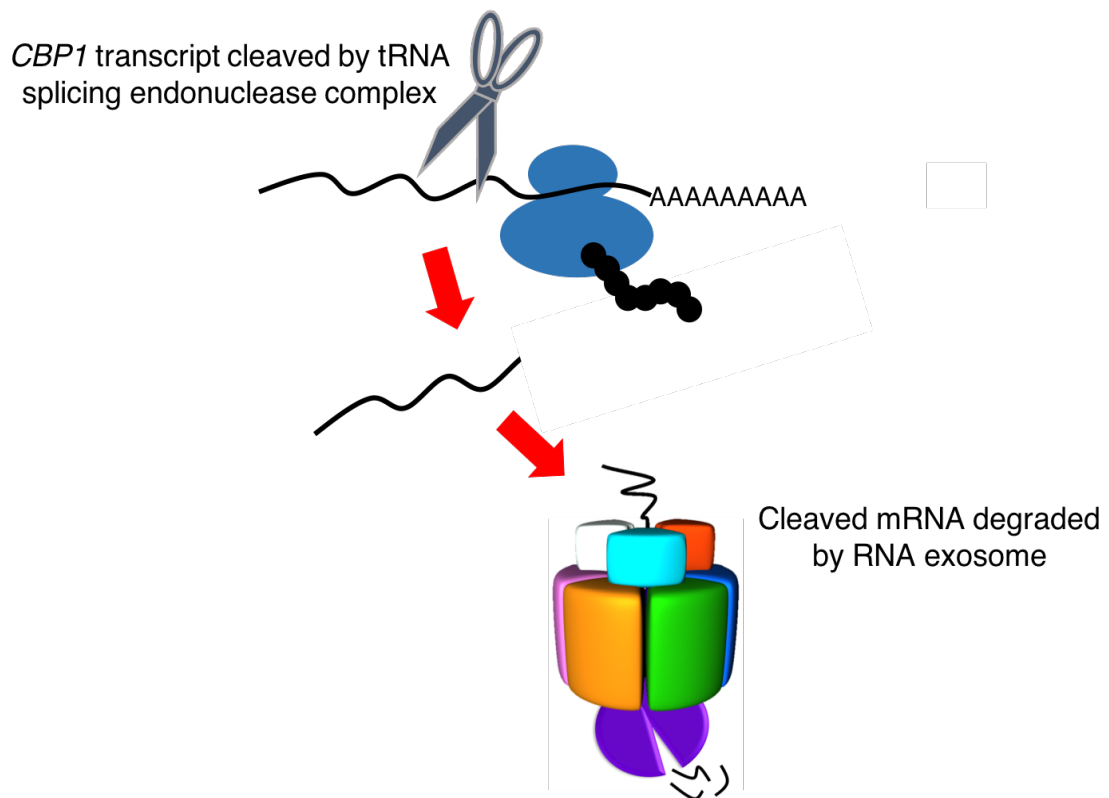


Figure 3.9 Model for cooperation between the tRNA splicing endonuclease complex and the RNA exosome. The tRNA splicing endonuclease (TSEN) complex, or Sen complex in yeast, (scissors) cleaves *CBP1* transcripts. While most products of TSEN complex cleavage are degraded by the 5'-3' RNA degradation pathway, *CBP1* mRNA is a substrate of the RNA exosome. If these two complexes partner together to clear cleaved *CBP1* mRNA, as well as other transcripts, this may provide a molecular basis for the phenotypic similarity exhibited between patients with TSEN complex or RNA exosome mutations.

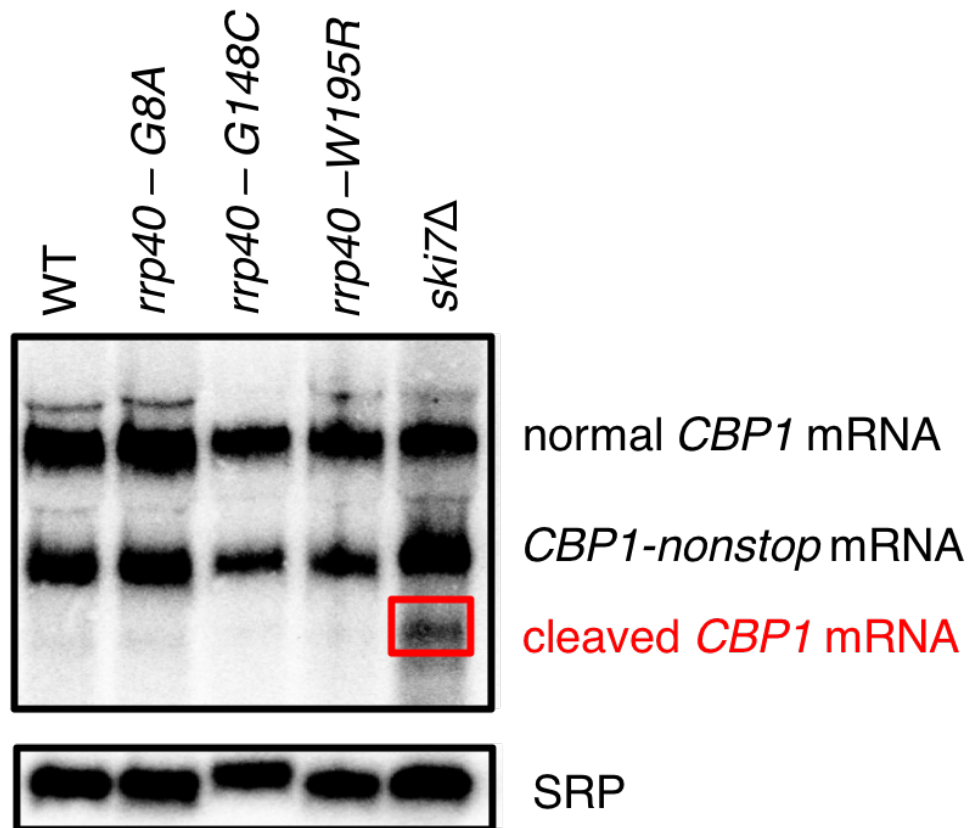


Figure 3.10 PCH1b-associated mutations do not interfere with the degradation of cleaved *CBP1* mRNA. Probes specific for the indicated species were used for northern blotting. The ribonucleoprotein, signal recognition particle (SRP), was included as a loading control. Both normal and non-stop transcripts were present in wild-type cells and in cells endogenously expressing PCH1b-associated variants of Rrp40. *ski7*Δ cells were included as a negative control for cytoplasmic RNA exosome function. All strains, except for *ski7*Δ, were able to degrade cleaved *CBP1* mRNA.

Human Mutations in Other RNA Exosome Subunits Can Be Similarly Modeled in Yeast

Substitutions in a second RNA exosome cap subunit, EXOSC2, which corresponds to yeast Rrp4, have been linked to a novel syndrome (**Figure 3.1, red**). This syndrome is characterized by decreased stature, hearing loss, retinitis pigmentosa, distinctive facial appearance, premature aging, intellectual disability, and hyperthyroidism (Di Donato *et al.*, 2016). It has recently been named SHRF, an acronym derived from the first four phenotypes listed. These symptoms have little overlap with PCH1b or any of the other PCH subtypes, which is surprising due to the conserved structural and functional similarity of EXOSC2/Rrp4 and EXOSC3/Rrp40. As stated previously in this chapter, my collaborators and I included EXOSC2 and Rrp4 in our protein sequence alignment of EXOSC3, Rrp40, and other eukaryotic orthologs when beginning this study. We found that the *EXOSC2-G30V* mutation, which is associated with SHRF, is located in the analogous position to the PCH1b-associated *EXOSC3-G31A* mutation (**Figure 3.2 A, yellow highlight**). This glycine residue is conserved between EXOSC2 and EXOSC3 paralogs, as well as within both yeast and human sequences, which suggests that it may be functionally important. For example, structural studies indicate that this mutation could negatively affect the ability of EXOSC2 protein to interact with residues of EXOSC4, a subunit of the RNA exosome core ring (**Figure 3.1, blue**) (Di Donato *et al.*, 2016). The *EXOSC2-G198D* mutation is also associated with SHRF and could affect EXOSC2 protein structure or function due to the location of this substitution within the KH domain, which is a region of RNA-binding (Di Donato *et al.*, 2016). While some patients are homozygous for the *EXOSC2-G30V* allele, *EXOSC2-G198D* has currently only been reported with *EXOSC2-G30V* in heterozygotes (Di Donato *et al.*, 2016).

A visiting summer undergraduate student, Jillian Vaught, assisted me with modeling these two mutations in yeast. We performed site-directed mutagenesis to generate *rrp40-G58V* and *rrp40-G226D* alleles, which are analogous to human *EXOSC2-G30V* and

EXOSC2-G198D alleles, respectively. These newly created plasmids were used to transform *rrp4Δ* cells holding [*RRP4*, *URA3*] plasmids, as *RRP4* is essential for viability. Plasmids encoding either mutant allele contained a *LEU2* marker, which allowed for selection against [*RRP4*, *URA3*] plasmids when the cells were plated on media containing 5-FOA. This plasmid shuffle assay resulted in the sole expression of mutant *rrp4* protein. As a control for growth, I also transformed *rrp4Δ* cells with a [*RRP4*, *LEU2*] plasmid. Growth of serial dilutions revealed that expression of *rrp4*-G58V as the sole copy of the essential *RRP4* protein is lethal, whereas *rrp4*-G226D expression does not significantly impair cell growth (**Figure 3.11 A**). Western blot analysis performed by my collaborators revealed that both mutant variants are expressed in the *rrp4Δ* background (data not shown). These results indicate that, while both mutant proteins are expressed, only the *rrp4*-G226D variant is functional. I additionally performed a *his3-nonstop* reporter assay, as previously described, to test if the *rrp4*-G226D allele affected cytoplasmic RNA exosome activity. Cells expressing this mutant did not grow on media lacking histidine, indicating that the *rrp4*-G226D mutation does not affect the cytoplasmic function of this complex (**Figure 3.11 B**).

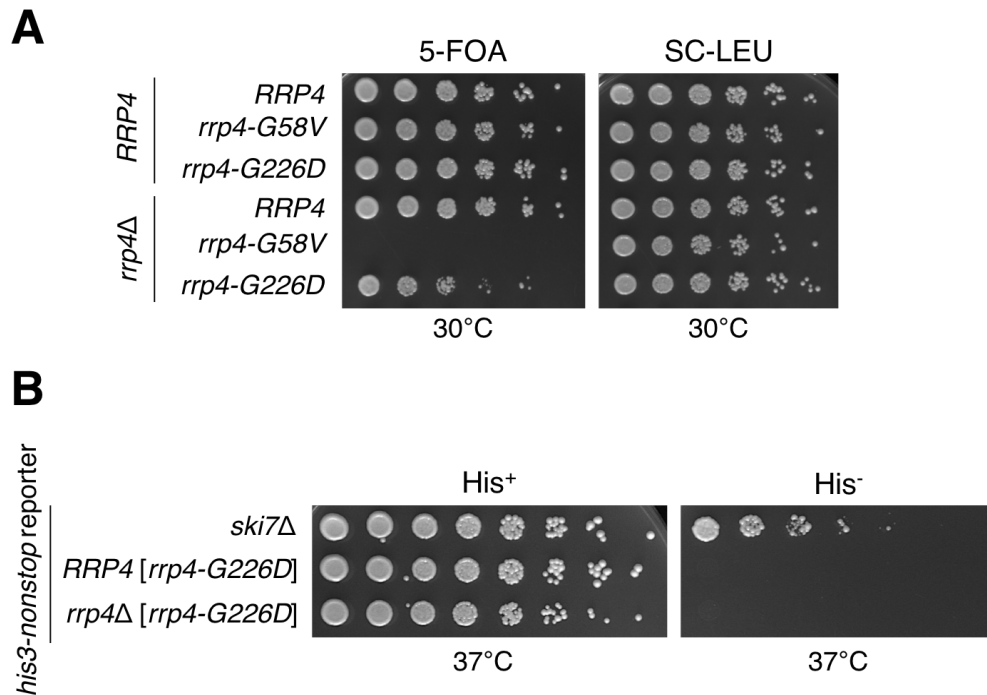


Figure 3.11 Expression of *rrp4-G58V* as the sole copy of Rrp4 in yeast is lethal but *rrp4-G226D* is not. **(A)** The growth of wild-type or *rrp4Δ* cells containing wild-type RRP4 or mutant *rrp4* plasmid was analyzed by performing serial dilutions, spotting onto selective solid medium, and incubation at 30°C. To select against the [*RRP4*, *URA3*] plasmid, the plasmid shuffle assay was performed by plating serial dilutions onto medium containing 5.74 mM 5-fluoroorotic acid (5-FOA). In an *rrp4Δ* background, sole expression of *rrp4-G58V* protein is synthetic lethal, while sole expression of *rrp4-G226D* protein only slightly impacts growth. **(B)** Yeast cells expressing *rrp4-G226D*, in either a wild-type or *rrp4Δ* background, do not rescue a *his3-nonstop* reporter, which is rapidly degraded by the cytoplasmic RNA exosome, to restore growth on medium lacking histidine. As a control, deletion of *SKI7*, which encodes a key cofactor of the cytoplasmic RNA exosome, rescues the *his3-nonstop* reporter and thus confers growth on medium lacking histidine. The growth of *rrp4-G226D* cells was analyzed by performing serial dilutions, spotting onto solid medium containing histidine (His⁺) or lacking histidine (His⁻), and incubation at 37°C.

CONCLUSIONS AND FUTURE DIRECTIONS

The results of this study provide insight into the functional impact of amino acid substitutions linked to PCH1b. Although a number of PCH1b-associated substitutions alter evolutionarily conserved residues present in the EXOSC3/Rrp40 protein, most of these mutations do not appear to alter RNA exosome function to a detectable degree in the yeast assays employed by myself and collaborators. This was not highly surprising, given the essentiality of the RNA exosome and its activities (Mitchell *et al.*, 1997; Allmang *et al.*, 1999b; Allmang *et al.*, 2000; van Dijk *et al.*, 2007; Chlebowski *et al.*, 2010). This finding also indicated that these PCH1b-associated mutations do not cause complete loss of the EXOSC3/Rrp40 protein. However, the W195R substitution in Rrp40, corresponding to W238R in EXOSC3, causes a reproducible reduction in yeast cell growth, RNA exosome function, and Rrp40 protein levels. These results provide insight into the possible mechanisms of RNA exosome dysfunction and also suggest that the relative severity of such mutations can be assessed using yeast.

Notably, PCH1b patients that are compound heterozygous for the W238R and G31A *EXOSC3* mutations have severe disease phenotypes and have not been reported to live beyond one year (Wan *et al.*, 2012). Moreover, no PCH1b patient genotypes that are homozygous for the *EXOSC3-W238R* allele have been reported. Given the impact of the W195R substitution on Rrp40 protein function, homozygosity for the *EXOSC3-W238R* allele could severely impair the RNA exosome to an extent that is incompatible for life. In addition to the *EXOSC3* mutations that we have modeled in yeast, dozens of other nonsynonymous mutations in this gene have been identified via genome sequencing (<http://www.ncbi.nlm.nih.gov/SNP/>). Therefore, yeast models could be useful for the analysis of the functional impact of *EXOSC3* substitutions and could provide important information for both the diagnosis of PCH1b patients and genetic counseling of heterozygous carriers.

PCH1b-Associated Mutations Reside at Possible Interaction Sites with other Proteins

A comparison of published EXOSC3 and Rrp40 structures revealed that the residues that are mutated in PCH1b patients are positioned at interfaces with other subunits of the RNA exosome. Moreover, PCH1b-associated substitutions appear to weaken, if not completely disrupt, the existing interactions between EXOSC3/Rrp40 and nearby proteins. In addition to interfering with subunit binding within the RNA exosome, PCH1b-associated mutations could also negatively affect interactions between EXOSC3/Rrp40 and cofactors of the RNA exosome. In fact, a recent structural study determined that Mpp6 specifically interacts with Rrp40 when attaching to the RNA exosome in yeast (Wasmuth *et al.*, 2017). This conserved cofactor, known as MPP6 in humans, delivers transcripts to the nuclear RNA exosome that need to be degraded (Schilders *et al.*, 2005; Milligan *et al.*, 2008). Interestingly, expression of the EXOSC3-W238R protein appears to be unfavorable for interaction with MPP6. Specifically, RNA exosomes containing this mutant subunit do not co-immunoprecipitate efficiently with MPP6 (Falk *et al.*, 2017a). This indicates that the expression of EXOSC3-W238R protein negatively affects interaction with MPP6 or the integrity of the RNA exosome. As mentioned, the RNA exosome has many nuclear and cytoplasmic cofactors. However, it is not known if all of them specifically bind to EXOSC3/Rrp40. Additional immunoprecipitation assays could be performed to determine which other RNA exosome cofactors, if any, bind to wild-type EXOSC3/Rrp40 in comparison to PCH1b-associated EXOSC3/rrp40 mutants.

A recent study found that recessive mutations in *EXOSC9* result in PCH-like phenotypes (Donkervoort *et al.*, 2017). *EXOSC9*, or Rrp45 in yeast, is one of the two core subunits of the RNA exosome that interacts with the EXOSC3/Rrp40 cap subunit. As previously discussed, my collaborators and I hypothesize that the *EXOSC3-W238R/rrp40-W195R* mutation weakens the interaction between EXOSC3/Rrp40 and EXOSC9/Rrp45 (**Figure 3.3, Figure 3.6**). Fibroblast analysis of a patient expressing mutant EXOSC9-L14P

protein revealed reduced levels of wild-type EXOSC3 and EXOSC8 protein (Donkervoort *et al.*, 2017). This indicates that mutations in just one subunit of the RNA exosome can lead to a general decrease in the stability of the complex. Similar analysis could be performed with fibroblasts obtained from PCH1b patients in order to determine if the expression of mutant EXOSC3 protein results in a reduction in the expression of other RNA exosome subunits and therefore, a possible reduction in the total number of complete RNA exosome complexes.

The PCH1b-Associated *rrp40-W195R* Mutation Affects Protein Stability and Function

In comparison to other PCH1b-associated substitutions examined in this study, significant alteration of protein stability was only detected for the *rrp40-W195R* and *rrp40-W195A* variants, which both lack the native bulky hydrophobic tryptophan residue at position 195. Moreover, the *rrp40-W195F* variant that my collaborators and I have generated maintains a bulky hydrophobic residue and did not show defects in growth or stability. This indicates that a bulky hydrophobic residue at position 195 of Rrp40 is important for protein stability and function.

Assessing the impact of the *rrp40-W195R* mutant on the nuclear function of the RNA exosome has revealed that this mutation results in elevated levels of known RNA exosome target transcripts. Shortly after our work was published, an additional study showed that expression of *rrp40-W195R* results in a significant impairment of pre-rRNA and pre-tRNA processing (Gillespie *et al.*, 2017). My initial assessment of the possible effects of PCH1b-associated mutations on cytoplasmic RNA exosome activity did not reveal any significant phenotypes. However, I only evaluated the degradation of a single non-stop transcript. As previously stated, the structure of the RNA exosome is identical in both the nucleus and the cytoplasm. Therefore, it is unclear if PCH1b-associated mutations could affect the stability or function of this complex in one, but not both, of these cellular compartments. However, as mentioned in the previous section, EXOSC3-W238R negatively impacts interaction with the

nuclear RNA exosome cofactor, MPP6. This indicates that perhaps this PCH1b-associated mutation does selectively affect nuclear functions of the RNA exosome machinery. It is also possible that PCH1b-associated mutations severely affect the processing activity of the RNA exosome, but only moderately affect its ability to degrade.

The RNA Exosome May Have a Mechanism to Discriminate Mutant Subunits

The results obtained from analyses of the *rrp40*-W195R and *rrp40*-W195A mutant proteins yielded a surprising finding that could help further the understanding of RNA exosome assembly and quality control (**Figure 3.12**). In an *rrp40* Δ background, protein expression and stability of these variants are decreased in comparison to wild-type Rrp40 protein. However, their expression and stability are further decreased in a strain background that already expresses wild-type Rrp40. Additionally, *rrp40*-W195R does not associate as efficiently with the RNA exosome as wild-type Rrp40 (**Figure 3.12 A, B**). This finding suggests a model where cells assemble functional RNA exosomes by distinguishing between wild-type Rrp40 and its mutant forms (**Figure 3.12 C**).

Several possible mechanisms for RNA exosome assembly could explain how cellular machinery determines preference for wild-type Rrp40. Although RNA exosome assembly factors have not yet been identified, there could be chaperones which help ensure the optimal formation of this ten-subunit complex. In this scenario, the rate of variant subunit assembly into the RNA exosome may be decreased relative to the that of wild-type subunits. An alternative possibility is that assembly of RNA exosome subunits could be reversible at a significant rate (**Figure 3.12 C**). Defects in interactions with other RNA exosome subunits, which appear to be caused by PCH1b-associated mutations, could increase the rate of Rrp40 disassembly from the complex. Therefore, in the presence of wild-type Rrp40, a variant subunit could be replaced and subsequently degraded by the proteasome.

Although very little is known about RNA exosome stability and quality control, a study of two *T. brucei* RNA exosome subunits showed that overexpressing tagged versions led to

proteasome-dependent turnover of the endogenously expressed subunits (Estévez *et al.*, 2003). Based on this work and a previous study, which showed that neither subunit was detected independently of glycerol density gradient fractions containing the RNA exosome, it was proposed that these RNA exosome subunits are subject to rapid degradation when not incorporated into the complex (Estévez *et al.*, 2001; Estévez *et al.*, 2003). Another finding that supports our model of RNA exosome subunit stoichiometry-dependent turnover comes from a recent study that reported two *EXOSC8* mutations in PCH1c patients, *EXOSC8-A2V* and *EXOSC8-S272T*. *EXOSC8* knockdown or mutations that reduced steady-state protein levels lead to a simultaneous decrease in *EXOSC3* protein levels (Boczonadi *et al.*, 2014). Consistent with these observations on the *T. brucei* and human RNA exosomes, our results in both yeast and mammalian cells suggest that a conserved mechanism exists to ensure formation and/or maintenance of optimal RNA exosome complexes. Further studies will be required to confirm and understand how the RNA exosome can apparently discriminate between wild-type and mutant subunits.

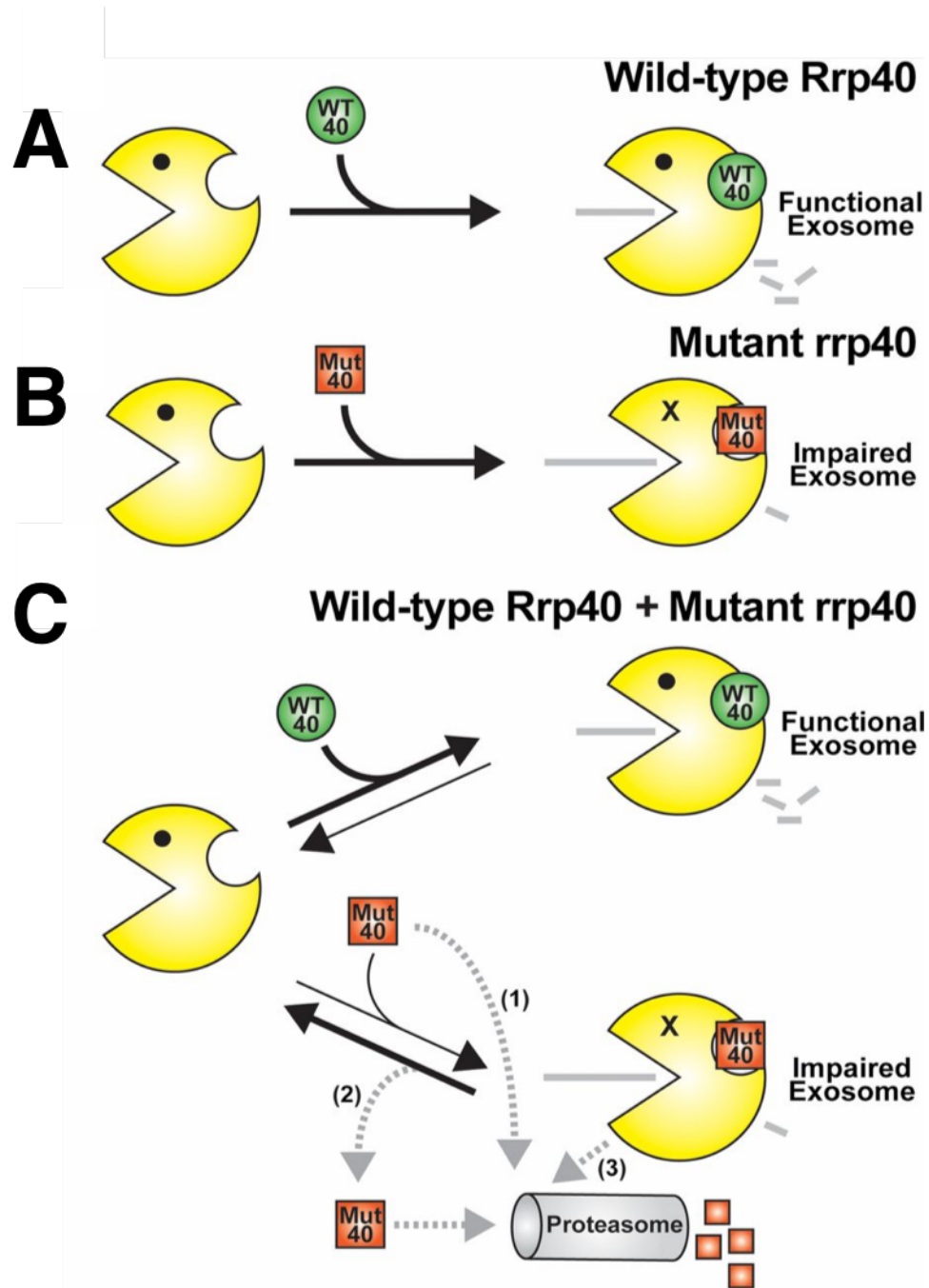


Figure 3.12 Model for RNA exosome assembly and function. **(A)** When cells express wild-type Rrp40 (WT 40, green circle) as the only copy of Rrp40, the RNA exosome (yellow Pac-Man) assembles properly to produce a fully functional complex. **(B)** When cells express variant *rrp40*-W195R (Mut 40, orange square) as the only copy of Rrp40, the RNA exosome shows impaired function, as evidenced by a modest decrease in cell

growth, altered substrate levels, and subunit instability. **(C)** When cells express both wild-type Rrp40 and the rrp40-W195R variant, the mutant is highly unstable and degraded in a proteasome-dependent manner. As indicated by the black arrows depicting RNA exosome assembly and disassembly, the rrp-W195R protein may be assembled into the RNA exosome less efficiently than the wild-type protein. Alternatively, the RNA exosome containing the mutant subunit could be disassembled more rapidly than complexes containing wild-type Rrp40. Several possible routes for the degradation of the mutant subunit exist (grey dashed arrows): (1) The mutant subunit could be directly degraded without ever becoming incorporated into the RNA exosome, (2) the mutant subunit could be targeted for degradation after the RNA exosome has been disassembled, or (3) the entire RNA exosome containing the mutant subunit could be targeted for degradation. Further studies will be required to distinguish between these possible mechanisms for rapid, proteasome-mediated turnover of the rrp40-W195R variant.

Various PCH Subtypes May Have a Molecular Link to One Another

The laboratory of Dr. Anita Hopper at Ohio State University has modeled a PCH2-associated mutation, *TSEN2-Y309C*, in yeast. Yeast expressing the equivalent mutation, *sen2-F230C*, do not exhibit significant growth deficiency in comparison to wild-type cells (Dhungel, 2012). As previously mentioned, PCH2 patients do not always exhibit tRNA defects (Budde *et al.*, 2008). It is possible that PCH2 mutations tweak activity of the TSEN complex such that it can still cleave tRNA, but cannot recognize mRNA, including *CBP1* transcripts. This faulty recognition hypothesis is further supported by the fact that tRNA folds into a cloverleaf structure, but *CBP1* mRNA does not, indicating that even a wild-type TSEN complex detects its targets differently.

My northern blotting analysis revealed that PCH1b-associated mutations do not affect the degradation of cleaved *CBP1* transcripts. However, a yeast strain co-expressing *sen2-F230C* and PCH1b-associated *rrp40* mutants could be generated to test if the PCH2-associated mutation interferes with *CBP1* mRNA cleavage and if the impacts of such an effect could be relieved by RNA exosomes containing PCH1b-associated mutations. Northern blotting for cleaved *CBP1* transcripts, as previously described, would be repeated with RNA isolated from these cells.

Mutations in RNA Exosome Subunits Result in Different Tissue-Specific Defects

A key question is: how do defects in the critically important and ubiquitously expressed RNA exosome result in a variety of tissue-specific phenotypes? This is particularly intriguing because studies on human fibroblasts and zebrafish embryos have revealed that mutations in the RNA exosome cap gene, *EXOSC3*, affect mostly spinal neurons and Purkinje cells but mutations in the RNA exosome core genes, *EXOSC8* and *EXOSC9*, also affect oligodendroglia and motor neurons (Wan *et al.*, 2012; Boczonadi *et al.*, 2014; Donkervoort *et al.*, 2017). Mutations in a different RNA exosome cap gene, *EXOSC2*, cause SHRF, which is not similar to PCH disease despite the functional and structural

similarity of EXOSC2 and EXOSC3 subunits (Di Donato *et al.*, 2016). It is possible that PCH-associated mutations in *EXOSC3* or *EXOSC8*, as well as disease-related mutations in *EXOSC2*, trigger subtle functional changes that impact specific subsets of RNA exosome targets. These RNA subsets could be different for the two PCH subtypes and SHRF. For PCH1b, altered RNA exosome substrate targeting could be initially identified by RNA-Seq, using RNA isolated from our yeast strains expressing disease-associated *rrp40* mutant protein. However, subsequent RNA-Seq assessment of altered substrate targeting by the RNA exosome would need to be performed with RNA isolated from neuronal cells expressing PCH1b-associated EXOSC3 variants.

The Yeast Model Can Be Used to Assess Mutations in Other RNA Exosome Subunits

Two human disease-linked *EXOSC2* mutations were modeled in yeast, similarly to the PCH1b-associated *EXOSC3* mutations. The synthetic lethality of the *rrp4-G58V* allele was surprising, since homozygous expression of the orthologous human allele, *EXOSC2-G30V*, is not lethal. This highlights the fact that while yeast modeling can provide valuable initial insight into uncharacterized molecular mechanisms, modeling analysis must be expanded to diploid metazoan cells to provide an accurate reflection of human gene expression. However, due to the severity of symptoms resulting from *EXOSC2-G30V* gene expression and the conservation of this residue, its lethality in the yeast model is not totally unexpected. My collaborators have recently substituted the Rrp4 G58 residue for an alanine, resulting in a viable strain. While this is a less drastic mutation, the creation of this *rrp4-G58A* strain will allow for protein expression and stability assays, as well as assessment of the various RNA exosome functions that may be affected by a point mutation at this residue.

Human disease-linked mutations in other RNA exosome subunits could also be similarly modeled in yeast. As stated above, *EXOSC9* mutations also cause PCH-like symptoms (Donkervoort *et al.*, 2017). Therefore, the effects of these mutations could be initially tested via the assays described in this study in order to gain initial insight into their

molecular implications. In conclusion, the work presented here provides a rapid screening approach that exploits yeast to provide insight into characteristics of the RNA exosome that could be impacted by mutations associated with PCH1b and other similar disorders.

CHAPTER 4

Identifying the Importance of Maintaining TRAMP Complex Assembly

This chapter is based upon Losh JS*, King AK*, Bakelar J, Taylor L, Loomis J, Rosenzweig JA, Johnson SJ, van Hoof A. **Interaction between the RNA-dependent ATPase and poly(A) polymerase subunits of the TRAMP complex is mediated by short peptides and important for snoRNA processing.** *Nucleic Acids Research*. 2015; 43(3): 1848-58 (*these authors contributed equally to this work). This is an Open Access article distributed under the terms of the Creative Commons Attribution License (<http://creativecommons.org/licenses/by/4.0/>), which permits unrestricted reuse, distribution, and reproduction in any medium, provided the original work is properly cited.

This chapter also contains material from Losh JS, van Hoof A. **Gateway arch to the RNA exosome.** *Cell*. 2015; 162: 940-1. License number 4196040308742 has been obtained from Elsevier Inc. If a license is for use in a thesis/dissertation, it may be submitted to the institution in print or electronic form (elsevier.com/solutions/sciencedirect/support/rights-and-permissions).

INTRODUCTION

The heterotrimeric *Trf4/5 Air1/2 Mtr4* polyadenylation (TRAMP) complex was first characterized in *S. cerevisiae* as a cofactor of the RNA exosome (LaCava *et al.*, 2005). The TRAMP complex is thought to aid the RNA exosome in the degradation of many types of protein-coding and non-coding transcripts. *Trf4/5* are noncanonical poly(A) polymerases, *Air1/2* are zinc knuckle RNA binding proteins, and *Mtr4* is an RNA helicase. While this eukaryotic complex is conserved, the duplicated *TRF4/TRF5* and *AIR1/AIR2* genes arose during a whole-genome duplication in an ancestor of *S. cerevisiae* (Kellis *et al.*, 2004; Byrne and Wolfe, 2005). Therefore, most other eukaryotic genomes contain only one ortholog of each. It has previously been shown that the human homologs of each subunit interact, suggesting that TRAMP complex formation is conserved between fungi and animals (Lubas *et al.*, 2011).

In yeast, *Mtr4* is encoded by an essential gene but the other TRAMP complex subunits are not individually essential (de la Cruz *et al.*, 1998; Giaever *et al.*, 2002). However, a *trf4Δ, trf5Δ* strain is inviable and an *air1Δ, air2Δ* strain is extremely slow growing (Castaño *et al.*, 1996; Inoue *et al.*, 2000). These growth phenotypes suggest that all three subunits of the TRAMP complex perform critical functions. Yet, the importance of their assembly into this complex is not currently understood, especially since both TRAMP complex-dependent and –independent activities have been attributed to each subunit (de la Cruz *et al.*, 1998; Inoue *et al.*, 2000; Vaňáčová *et al.*, 2005; Houseley and Tollervey, 2006; Bernstein *et al.*, 2008; Gellon *et al.*, 2008; San Paolo *et al.*, 2009; Jackson *et al.*, 2010; Weir *et al.*, 2010; Fasken *et al.*, 2011; Jia *et al.*, 2011; Holub *et al.*, 2012).

Studying the TRAMP complex-dependent activities of each subunit, as well as the known interaction sites between the subunits, have allowed me to develop an initial model of the TRAMP complex conformation and function (**Figure 4.1**). First, the second, third, and fourth zinc knuckles of the *Air1/2* subunit bind an RNA that needs to be degraded by the

RNA exosome. This subunit must hold the RNA in place, as Trf4/5 do not possess RNA-binding capabilities. The Trf4/5 subunit then begins to add a poly(A) tail to the 3' end of the substrate. This growing poly(A) tail is fed into the substrate binding site of the Mtr4 helical core. Mtr4 then unwinds the polyadenylated RNA into a linear structure that is more conducive for being loaded into the central channel of the RNA exosome, where it can be degraded in the 3' to 5' direction.

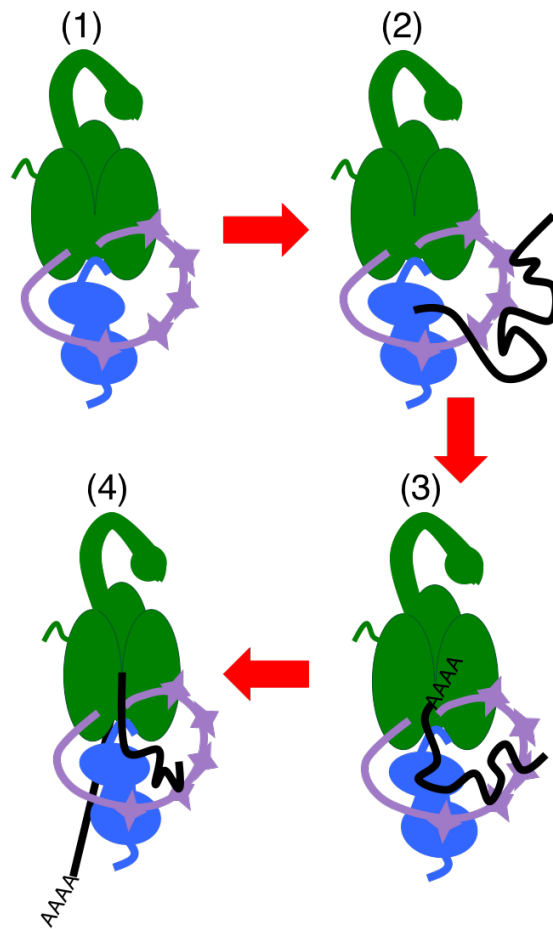


Figure 4.1 Model for TRAMP complex conformation and function. (1) The Air1/2 subunit (purple) has previously been shown to bind to the central domain of the Trf4/5 subunit (Holub *et al.*, 2012) (blue). The work presented in this chapter has identified a region of the unstructured Trf4/5 N-terminus that interacts directly with Mtr4 (green). (2) Several zinc knuckles (stars) of Air1/2 are able to bind an RNA. This substrate is likely positioned so that it comes into contact with the catalytic domain of Trf4/5. (3) The Trf4/5 subunit adds a short poly(A) tail to the substrate. Due to direct interaction between Trf4/5 and Mtr4, as well as the predilection that Mtr4 has for poly(A) sequences, the newly polyadenylated substrate is then able to be inserted into the Mtr4 helical domain. (4) Mtr4 unwinds the substrate into a more linear formation so that it can be more easily threaded into the central channel of the RNA exosome, where it will be degraded.

Adding nucleotides to the 3' end of an RNA to facilitate the removal of nucleotides in the 3' to 5' direction is somewhat counterintuitive. However, several roles of TRAMP complex-mediated polyadenylation in the RNA exosome-dependent degradation pathway have been proposed. First, the catalytic subunit of the RNA exosome, Rrp44, is accessed through a narrow central channel formed by the subunits of the RNA exosome cap and core ring (Bonneau *et al.*, 2009; Malet *et al.*, 2010). Therefore, RNA exosome-dependent degradation is thought to require a long unstructured region, which may be provided by TRAMP complex-mediated polyadenylation. Under this hypothesis, the unstructured poly(A) tail would have to be a long enough to traverse the channel. Specifically, this would be about thirty nucleotides in length. Long 3' tails have been detected in RNA exosome mutants and the TRAMP complex can synthesize long poly(A) tails *in vitro* (LaCava *et al.*, 2005; Vaňáčková *et al.*, 2005; Allmang *et al.*, 1999b; van Hoof *et al.*, 2000a). However, a typical 3' tail synthesized by the TRAMP complex is an average length of four nucleotides and, thus, not long enough to completely pass through the central channel of the RNA exosome (Wlotzka *et al.*, 2011; Jia *et al.*, 2011). An indication that long unstructured 3' tails are not required for RNA exosome-mediated degradation comes from the observation that the RNA exosome appears to be fully capable of degrading cytoplasmic substrates independently of a poly(A) polymerase. This includes substrates that contain very stable secondary structures like G-quadruplexes (van Hoof *et al.*, 2002; Meaux and van Hoof, 2006).

An alternative hypothesis is that tails synthesized by Trf4/5 may be more important for targeting substrates to Mtr4, rather than for insertion into RNA exosome. Interestingly, Mtr4 preferentially interacts with polyadenylated RNA (Bernstein *et al.*, 2010; Jia *et al.*, 2012; Taylor *et al.*, 2014). Under both of these hypotheses, an RNA would initially interact with the poly(A) polymerase subunit of the TRAMP complex before being handed off to the RNA exosome.

However, a third possibility is that polyadenylation by Trf4/5 occurs in response to a block or stall during normal RNA processing by the RNA exosome. Physical interaction between the RNA exosome, Mtr4, and Trf4/5 may facilitate the polyadenylation of a product destined for degradation. This polyadenylation may enhance subsequent re-engagement of the RNA exosome and Mtr4 machinery. TRAMP complex-dependent tails are added at multiple positions, including within the region corresponding to the mature RNA, consistent with the idea that the TRAMP complex can act on partially degraded RNA (Schneider *et al.*, 2012). Yet while these various hypotheses address the role of the poly(A) tail, they do not readily explain why a helicase (Mtr4) and a poly(A) polymerase (Trf4/5) assemble into a complex.

Previously Known Subunit Interaction Sites Within the TRAMP Complex

The first TRAMP complex subunit interaction to be identified was that of the central domain of Trf4 with the fifth zinc knuckle of Air1/2, as well as with the linker region between the fourth and fifth zinc knuckles (Holub *et al.*, 2012). Due to sequence conservation, the central domain of Trf5 is highly similar to Trf4. Therefore, Trf5 likely interacts with Air1 in the same manner. Yet while Trf4 interacts with both Air1/2, only a Trf5-Air1 interaction has been exhibited (Wyers *et al.*, 2005; Houseley and Tollervey, 2006). This results in three possible conformations of the TRAMP complex: Trf4-Air1-Mtr4, Trf4-Air2-Mtr4, and Trf5-Air1-Mtr4 (**Figure 1.3 B**). Human orthologs of Trf4/5 and Air1/2 interact *in vitro*, but the specific binding sites have not been assessed (Sudo *et al.*, 2016). However, the interactions are likely similar to those identified in yeast due to domain conservation.

The termini of Air2 were first shown to be important for maintaining an interaction with Mtr4 *in vitro* (Holub *et al.*, 2012). My collaborators in the laboratory of Dr. Sean Johnson at Utah State University tested the binding of the first twenty-nine residues of the Air2 N-terminus to Mtr4 via fluorescence anisotropy. In addition to wild-type Mtr4, they also included Mtr4 variants lacking either the N-terminus or its characteristic arch since those two

regions are known to be important for interactions with other proteins or substrates. The N-terminus of Air2 bound all three Mtr4 variants with similar affinity ($K_d \sim 6.9 \mu\text{M}$ with Mtr4^{WT}, $K_d \sim 6.6 \mu\text{M}$ with Mtr4^{Δ74}, $K_d \sim 7.3 \mu\text{M}$ with Mtr4^{archless}) (Losh, King *et al.*, 2015). Subsequent structural analysis has further indicated that the N-terminus of Air1/2 can directly contact Mtr4 (Falk *et al.*, 2014). Human orthologs of Mtr4 and Air1/2 were recently shown to bind *in vitro*, although this study did not tease apart the specific sites of interaction (Sudo *et al.*, 2016).

Initial Identification of the Mtr4-Trf4/5 Interaction Site

The TRAMP complex was initially identified in a yeast two-hybrid screen for proteins that are able to interact with Mtr4 (LaCava *et al.*, 2005). All of the Trf5 clones identified in this screen included residues 53-199, which suggested that this part of the protein contains a binding site for Mtr4. Although this region of Trf5 is largely disordered, multiple sequence alignment revealed that Trf5 residues 98-117 are significantly conserved. Moreover, this analysis identified analogous Trf4 residues 115-134 (Losh, King *et al.*, 2015) (**Figure 4.2**). Since small, conserved motifs in largely disordered regions are often protein-protein interaction sites, my collaborators and I hypothesized that this may be the major, if not the only, site of interaction with Mtr4. The initial identification of this conserved putative Mtr4-Trf4/5 interaction site was particularly intriguing, as these are the two enzymatic subunits of the TRAMP complex.

My laboratory colleague, Dr. Alejandra Klauer King, began a deeper analysis of this site by starting with the initially identified region of Trf5 residues 53-199 and generating further truncations. She performed multiple truncations from both ends of this region and tested for a maintained interaction with Mtr4 via yeast two-hybrid analysis. Her results were consistent with our hypothesis that Trf5 residues 98-117 are a major site of Mtr4 interaction (Losh, King *et al.*, 2015).

```

Trf5Scer      096 -----KRNNSLEDNQDFIAFSDSSEDETEQIKEDDDERSSSFLLTDEHEVSKLTS-
Trf5Spar      096 -----KRGHSLEDNHDFIAFSDSSEEEKEQIKEDEDESSFLLADQYKSTFSS--
Trf5Smik      096 -----KGDHSLEDNHDFIAFSDTSSEDEKEQKRGEDEEKCDFLSLNQYEISTFGS--
Trf5Sbay      096 -----KNGNSLEDNHDFIAFSESSGDEE-EEERVTEEKSVLLVHDQYEISTVTS--
Trf5Skud      096 -----EKRNSLEDNQDFIPFSDSSEDEQGEEEGNSEGVSGFLMPDQYEITKNNT--
Trf5Cgla      110 -----ISGGKLEDNDDFIAFSSSEDENSGA-ENNESEDYLSGNTSSD-----
Trf5Kpol      084 -----NLEDSLKDNDDFIAVSSTSSEDE-----YDDISEDEDTDGNSS-----
Trf5Scas      125 -----LLQLNKLANNDDFIPFSASSEDEDEDEDEGPLNPTINDYGETLANR-
Trf4Scer      113 -----DEKD-LANNDDFISLSASSEDEQAEQ-EEEREKQLEIKKEKQK-----
Trf4Spar      113 -----NEKD-LANNDDFISLSASSEDEQAEQ-EEERQKEELEVKKKKQK-----
Trf4Smik      113 -----DEKD-LANNDDFISLSASSEDEHAEQ-EEERQKE-----EKQK-----
Trf4Sbay      113 -----NEND-LANNDDYIALSASSEDEDAKQKEEKQKKEEILKRKQK-----
Trf4Skud      114 -----SERD-LANNDDFISLSASSEDEDAKKEEERQKKEAELLRIRQK-----
Trf4Kpol      054 -----LRSD-IDTNNDFIAFSDSSEDEKENDDINEKESK-----DEDA-----
Trf4Scas      111 -----LQNNKLEDNQDFIAFSASSSSEDEKDIQEKQALEVDEQ--VTKEPT-----
Trf4Cgla      044 -----IDNNQIDENNDFIAFSESSGGE---DGDEAEQQPQ--AEEEE-----
TrfKlac       117 -----IGNNSLDANEDFIAFDLSEPEDEHENGFEEHSEPETAGKEEIE-----
TrfAgos       126 -----AAANALDDNQDFIGFSDSEEVASGE---ENGADAYA-VEDAE-----
TrfZrou       037 -----NGSLDGNDDFIAFDSSSEDEGGK----EEQE-----TESVE-----
TrfKthe       101 -----QDNALDDNQDYISLSMSSSEEEQESE---EEAPDEAGGEHPGGD-----
TrfKwal       100 -----EENALEDNQDYISLSMSSDAADVSS---EEEGHSDNVGSDDDY-----
TrfSklu       134 -----NQNALDNNEDFIPFAVSSSEEEDEEK---DEHGTYDDYDDEYPSKEEE-
TrfDhan       097 -----KFVNNELAKNQDFIEFGFSSSEEDAPERNDYDDYSDGVLSDDESGTI----
TrfCgui       096 -----KMEYNELSKNQDFIEFGFSSSE---EANKYDDYSDDGIISDDQSGNR----
TrfClus       089 -----AAPPNDLTNNNDYIRLGLSSSEDE-----EAEDLSDDGVLSDDESGSR----
TrfCtro       105 -----ITTETNELAKNEDFIGFGFSSTDEEE---SEGEE-----SEND-----
TrfCalb       103 -----KTPENELANNEDFIGFGFSSSEDDSEIISNSDNDL-----SNGDY----
TrfCpar       099 -----ESNELTTNQDFIQGFSSSEDEDE--HDEEHD-----SQNTN----
TrfLelo       140 TSSTSTNLPEANDLAKNDDFIEFGFLSSSEDEDEDEDRDDGNGGINSVAEEIDDTSR----
TrfYlip       168 --SPPPPPVDPSEWNMNEDFVGFDFSDGEDEEDEEPEEPVRSRRTIEEVDDASS----
TrfSoct       139 -----KPKPEPKNAVDENADYIGFDWNSDEDVNDTSKDETND-----SGPNNIPGMQ
Cid14Spom    141 -----KTNPVHDKAVENNSDFIKFDWNSDEDEDSVSNDKSKNNESLKKSSKNEIPGFMRQ
TrfSjap      144 -----KSIGDASVEGNADFIKFDSTDDEEEDKEDETSRR-----EEKSAIPAFMQK

```

Figure 4.2 Protein sequence alignment of fungal Trf4/5 orthologs. This alignment was generated from the Trf4/5 protein sequences of twenty-five ascomycete species. While the genomes of some species, including *S. cerevisiae*, contain two paralogs of this protein, others contain only one form. There is significant sequence conservation of the putative site of Mtr4 interaction, as evidenced by the presence of identical residues (red) and similar residues (blue). This short region of about 20 residues is located with the N-terminus. This is the only N-terminal region that is significantly conserved. The work presented in this chapter describes the identification and characterization of the *S. cerevisiae* Trf4/5 sites that are necessary for direct interaction with Mtr4 (bold). Specifically, these are Trf5 residues 98-117 and Trf4 residues 115-134.

Dr. King also found that residues 98-117 interact with both wild-type Mtr4 and an Mtr4 variant missing the characteristic arch domain. To ensure the presence of a direct interaction, Dr. Sean Johnson's lab performed fluorescence anisotropy with the Trf5 20-mer region and Mtr4 variants, as previously described in this chapter for the assessment of the Mtr4-Air1/2 interaction. The Trf5 20-mer bound to all three Mtr4 variants with similar affinity ($K_d \sim 10.7 \mu\text{M}$ with Mtr4^{WT}, $K_d \sim 11.3 \mu\text{M}$ with Mtr4^{Δ74}, $K_d \sim 6.0 \mu\text{M}$ with Mtr4^{archless}). Interestingly, both the yeast two-hybrid and fluorescence anisotropy assays indicated that the interaction affinity between the Trf5 20-mer and Mtr4 increases upon the deletion of the Mtr4 arch. Although not confirmed, it is possible that removal of the arch results in a conformational change of the Mtr4 core so that it is better positioned for this interaction. The results of these assays support the conclusion that this 20-mer region of Trf5 binds to the Mtr4 core (Losh, King *et al.*, 2015).

To determine if Trf5 residues 98-117 are required or simply sufficient for interaction with Mtr4, Dr. King assessed the binding of a Trf5 variant lacking residues 98-117 (trf5Δ98-117) with Mtr4, via yeast two-hybrid. This construct failed to interact with Mtr4. For a more definitive analysis, Dr. King generated TAP-tagged versions of full-length Trf5 and trf5Δ98-117 and expressed them in yeast from their endogenous promoters. The TAP-tagged proteins were purified and tested for co-purification with endogenous Mtr4 by western blotting, using antibodies raised against Mtr4. Endogenous Mtr4 was readily detectable in the purification of full-length Trf5, but not in the purification of trf5Δ98-117 (Losh, King *et al.*, 2015). From these results, we conclude that residues 98-117 are important for interaction with Mtr4 and moreover, preventing this interaction impairs formation of the TRAMP complex *in vivo*.

Dr. King then tested if trf5Δ98-117 protein could function as the sole source of Trf4/5. Surprisingly, the *trf5Δ98-117* allele fully complemented the lethality of a *trf4Δ*, *trf5Δ* strain

when performing a plasmid shuffle assay (Losh, King *et al.*, 2015). An additional member of my laboratory, Minseon Kim, created a strain expressing the *trf4* Δ 115-134 allele and found that it can also complement *trf4* Δ , *trf5* Δ synthetic lethality. We had previously determined this region to be the corresponding site of interaction with Mtr4 on Trf4 (Losh, King *et al.*, 2015) (**Figure 4.2**). To maintain control over experimental designs, all the generated alleles that are discussed in the following sections of this chapter are expressed in a *trf4* Δ , *trf5* Δ background, unless otherwise stated.

Based on these initial results, we concluded that maintaining a stable association with Mtr4 is not needed for the essential function of Trf4/5 or for cellular viability. However, these assays are not able to reveal effects on TRAMP complex function that may be caused by disrupting the direct interaction between its two catalytic subunits. Moreover, these results do not reveal if abolishing the Mtr4-Trf4/5 interaction completely disrupts the formation and/or activity of the TRAMP complex or if there are other protein-protein interactions that help it maintain at least some compositional integrity. Therefore, I have aimed to characterize the functional importance of interactions between TRAMP complex subunits in order to further elucidate the functions and possible essentiality of the TRAMP complex itself.

RESULTS

Disrupting the Mtr4-Trf4/5 Interaction Results in the Accumulation of RNA Exosome Substrates

Upon generating the *trf4* Δ , *trf5* Δ [*trf5* Δ 98-117] strain, which has a disrupted Mtr4-Trf5 interaction, I first tested whether impairing TRAMP complex formation affects specific TRAMP complex functions. As their name implies, cryptic unstable transcripts (CUTs) are not readily detectible in wild-type cells, but they accumulate in mutants with impaired TRAMP complex or RNA exosome activity (Wyers *et al.*, 2005). These complexes are believed to be responsible for the polyadenylation and subsequent degradation of CUTs,

respectively. I measured the accumulation of a specific CUT, *NBL001c*, via qRT-PCR since these RNA species are often difficult to detect with northern blotting. I used sequence-specific primers during the reverse transcription step that would allow for the detection of defects in either polyadenylation or subsequent degradation. As expected, CUT levels increased when eliminating the exoribonuclease activity of the catalytic subunit of the RNA exosome, Rrp44, or the additional nuclear 3'-5' ribonuclease, Rrp6 (*rrp44-exo* and *rrp6Δ* strains, respectively). In contrast, a strain lacking the endoribonuclease activity of Rrp44 (*rrp44-endo*) did not exhibit increased CUT accumulation (**Figure 4.3**). Similarly, I detected CUT accumulation in a *trf4Δ*, *trf5Δ* strain complemented with a plasmid that allows for the expression of full-length Trf5. This strain is lacking Trf4, which has been previously shown to be important for preventing CUT accumulation (Wyers *et al.*, 2005; Houseley *et al.*, 2007; Fasken *et al.*, 2011). Notably, the CUT steady-state levels in the *trf4Δ*, *trf5Δ* strain complemented with the *trf5Δ98-117* plasmid were similar to those measured in the *trf4Δ*, *trf5Δ* strain complemented with the *TRF5* plasmid (**Figure 4.3**). Therefore, impairing the Mtr4-Trf5 interaction may not affect the steady-state level of this transcript.

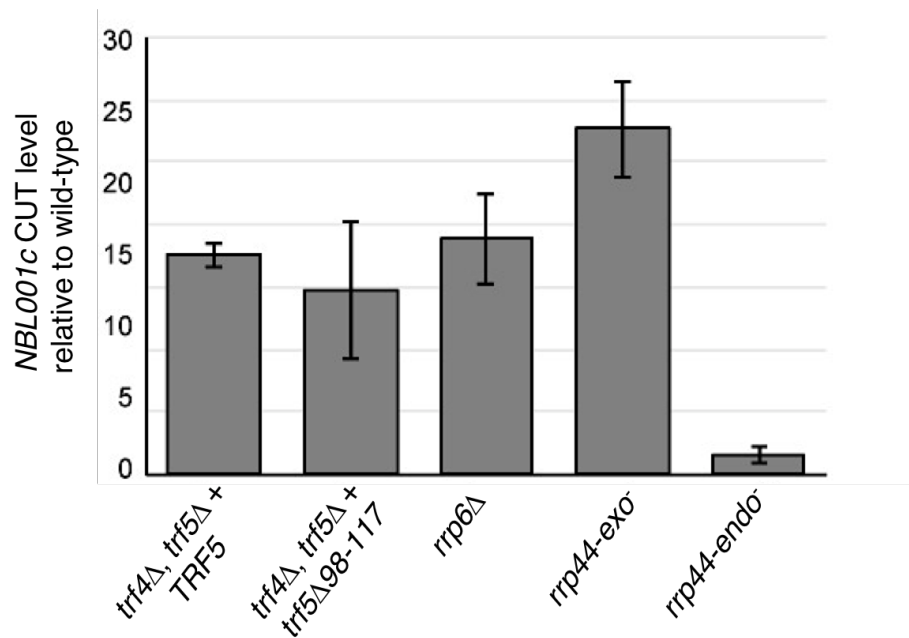


Figure 4.3 Disrupting stable TRAMP complex formation does not affect the degradation of a cryptic unstable transcript. After isolating RNA from these yeast strains, qRT-PCR analysis was used to determine the level of cryptic unstable transcripts (CUTs) in biological replicates. The level of CUTs detected in each strain is plotted relative to the level detected in a wild-type strain, after normalizing to a control *ACT1* transcript by the $\Delta\Delta C_t$ method. RNA samples isolated from *rrp6Δ* and *rrp44-exo* strains were included as positive controls for CUT accumulation. RNA isolated from the *rrp44-endo* strain was included as a negative control for CUT accumulation. While both *trf4Δ*, *trf5Δ* strains lack Trf4 expression, cells expressing *trf5Δ98-117* additionally lack the Mtr4-Trf5 interaction. However, the CUT levels are similar between the *TRF5* and *trf5Δ98-117* strains.

Mutations in subunits of the TRAMP complex or the RNA exosome have also been shown to result in 3' extended, polyadenylated snoRNA species. Thus, I next examined the effect of *trf5* Δ ⁹⁸⁻¹¹⁷ protein expression on the accumulation of the two main classes of snoRNA molecules. Specifically, I measured the accumulation of *snR128* and *snR33*, which are representatives of C/D box snoRNA and H/ACA box snoRNA, respectively. These species are detected as smears, instead of discrete products, which is indicative of their polyadenylation. Northern blotting allows for the visualization of these variously sized polyadenylated products, whereas qRT-PCR does not.

As previously reported, 3' extended species accumulate in *rrp44-exo* and *rrp6* Δ strains, which both lack 3'-5' exoribonuclease activity (Allmang *et al.*, 1999b; van Hoof *et al.*, 2000a; Schneider *et al.*, 2009; Klauer and van Hoof, 2013). I did not detect significant accumulation of these snoRNA species in an *rrp44-endo* strain, which lacks Rrp44 endoribonuclease activity (**Figure 4.4 A**). Polyadenylated snoRNA has also been reported in *trf4* mutants (Grzechnik and Kufel, 2008). Consistent with this, I detected accumulation of these species in a *trf4* Δ , *trf5* Δ strain complemented with a wild-type *TRF5* plasmid. However, the level of accumulation was lower than that of the *rrp44-exo* and *rrp6* Δ strains. Importantly, the *trf4* Δ , *trf5* Δ strain complemented with the *trf5* Δ ⁹⁸⁻¹¹⁷ plasmid reproducibly accumulated more 3' extended snoRNA than the *trf4* Δ , *trf5* Δ strain complemented with the wild-type *TRF5* plasmid. As similarly described for RNA exosome mutants, the steady-state level of mature snoRNA was not significantly increased in the *trf5* Δ ⁹⁸⁻¹¹⁷ strain when compared to the other strains (Allmang *et al.*, 1999b; van Hoof *et al.*, 2000a) (**Figure 4.4 A**). This was expected, as mature snoRNA is not a substrate for RNA exosome-mediated processing. Moreover, it may not accumulate in significant levels if the pathway for RNA exosome-mediated degradation is inhibited. Thus, impairing the Mtr4-Trf5 interaction

specifically interferes with the normal processing or degradation of the 3' extended forms of these snoRNA species.

I additionally performed northern blotting analysis with *trf4* Δ , *trf5* Δ strains complemented with a wild-type *TRF4* plasmid or a *trf4* Δ 115-134 plasmid to assess if there is also an effect on RNA degradation when disrupting the Mtr4-Trf4 interaction (**Figure 4.4 B**). Similar to *trf5* Δ 98-117 cells, *trf4* Δ 115-134 cells significantly accumulate polyadenylated snoRNA. Although previously tested, I additionally included RNA from *TRF5* or *trf5* Δ 98-117 strains. Both Trf5 strains accumulated more extended snoRNA than both Trf4 strains. However, this increased accumulation of 3' extended snoRNA in the *TRF5* and *trf5* Δ 98-117 strains may be partially due to the deletion of *TRF4*, which has been reported as the more highly expressed paralog in a wild-type yeast background (Ghaemmaghami *et al.*, 2003; Kulak *et al.*, 2014). It is also possible that TRAMP complexes containing Trf5 are more likely to target the specific snoRNA species that I probed for. However, a previous study of Trf4/5 substrate specificity indicated that while both proteins can polyadenylate 3' extended snoRNA for RNA exosome-mediated degradation, Trf4 is more likely to target these species (San Paolo *et al.*, 2009).

I additionally included a *trf4* Δ , *trf5* Δ strain complemented with both *TRF4* and *TRF5* plasmids as a control for plasmid expression. As expected, the presence of both wild-type Trf4/5 in this strain lessened the severity of 3' extended snoRNA accumulation. Finally, I included a *trf4* Δ , *trf5* Δ strain complemented with both *trf4* Δ 115-134 and *trf5* Δ 98-117 plasmids. This strain and its phenotypes will be discussed later in this chapter.

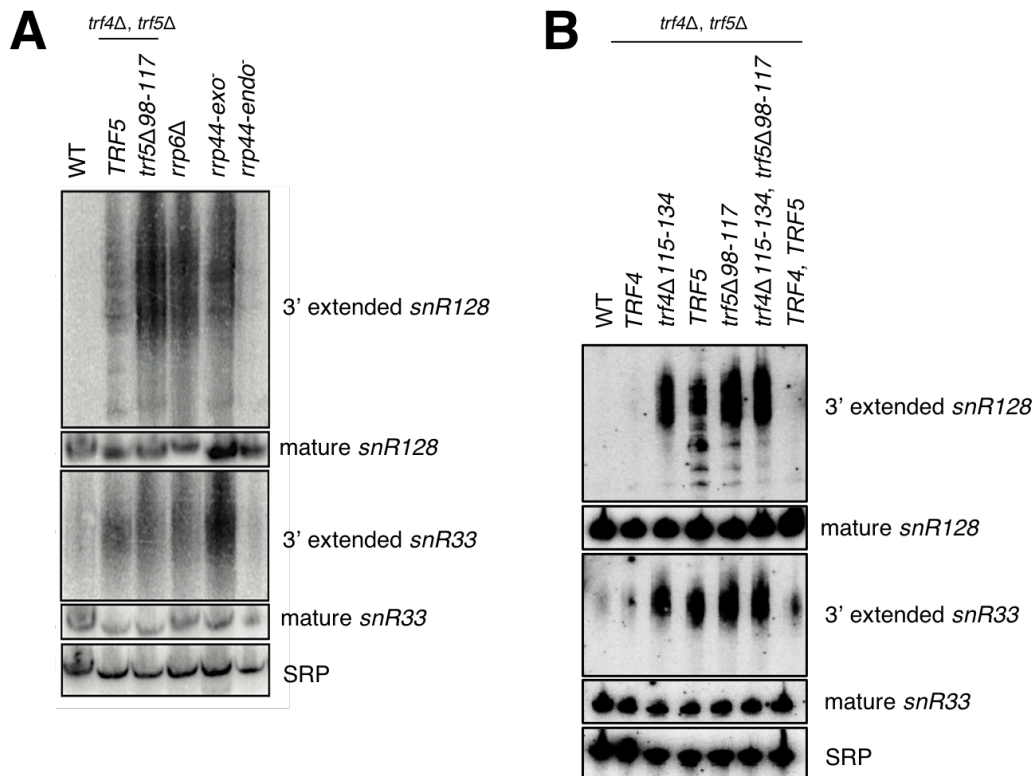


Figure 4.4 Disrupting stable TRAMP complex formation results in increased levels of 3' extended snoRNA species. Probes specific for the 3' extended and mature forms of snoRNA were used for northern blotting. 3' extended snoRNA is detected as a smear, which indicates its polyadenylation. These snoRNA species are representatives of the two main classes of snoRNA, C/D box (*snR128*) and H/ACA box (*snR33*). The ribonucleoprotein, signal recognition particle (SRP), was included as a loading control. **(A)** RNA isolated from *rrp6Δ* and *rrp44-exo⁻* cells was included as a positive control for polyadenylated snoRNA accumulation, while RNA isolated from *rrp44-endo⁻* cells was included as a negative control. While both *trf4Δ, trf5Δ* strains lack Trf4 protein expression, cells expressing *trf5Δ98-117* additionally lack the Mtr4-Trf5 interaction. Increased levels of 3' extended snoRNA in the *trf5Δ98-117* strain indicate that the Mtr4-Trf5 interaction is important for the clearance of these species. Steady-state levels of mature snoRNA are

not significantly different between strains. **(B)** Whereas retaining wild-type Trf4 expression in a *trf4* Δ , *trf5* Δ strain does not result in the accumulation of polyadenylated snoRNA, disrupting the Mtr4-Trf4 interaction does, as is similarly seen when disrupting the Mtr4-Trf5 interaction. Moreover, expressing both variants of Trf4/5 that are unable to interact with Mtr4 results in similar levels of accumulation. A *trf4* Δ , *trf5* Δ strain complemented with both wild-type *TRF4* and *TRF5* plasmids was included as a control for expression.

The Mtr4-Trf4/5 Interaction is Specifically Important for snoRNA Biogenesis

I analyzed RNA from *trf4* Δ , *trf5* Δ cells complemented with either *TRF5* or *trf5* Δ 98-117 plasmids for a more global analysis of the implications resulting from a disrupted Mtr4-Trf4/5 interaction. Transcriptome sequencing of poly(A)⁺ RNA was performed on duplicate RNA samples from each strain. This analysis revealed that the set of most significantly affected genes (false discovery rate (FDR) = 0.01) included seventy-one that were more abundant in the *trf5* Δ 98-117 mutant and only five that were less abundant. The set of overexpressed genes was predominated by known TRAMP complex substrates, including forty-three snoRNA genes (**Table 4.1**). Specifically, this set was comprised of genes encoding for thirty-two C/D box snoRNA species, eighteen H/ACA box snoRNA species, seven rRNA species, five other ncRNA species, five transposons, two mRNA transcripts, one dubious ORF, and one other snoRNA. This additional snoRNA, which has a role in pre-rRNA cleavage during 5.8S rRNA processing, is not categorized as a C/D box or H/ACA box species (Chu *et al.*, 1994).

Table 4.1 Genes identified by RNA-Seq as overexpressed in cells lacking the Mtr4-Tr5 interaction				
Gene	Fold-change (log2)	P-Value	FDR	Comments
<i>RDN58</i>	4.3	4.5E-126	1.6E-122	rRNA
<i>YLR154W-E</i>	4.1	6.7E-107	1.4E-103	overlaps with rRNA
<i>SCR1</i>	4.6	8.6E-056	1.3E-52	RNA component of SRP
<i>snR128</i>	2.3	2.7E-043	3.3E-40	C/D box snoRNA
<i>RDN5</i>	2.5	1.0E-040	9.2E-38	rRNA
<i>YLR154W-F</i>	3.0	8.6E-037	6.5E-34	overlaps with rRNA
<i>snR67</i>	5.1	6.1E-028	4.1E-25	C/D box snoRNA
<i>RDN25</i>	2.0	9.7E-028	5.4E-25	rRNA
<i>snR40</i>	4.2	7.9E-025	4.0E-22	C/D box snoRNA
<i>snR6</i>	5.1	8.1E-024	3.8E-21	<i>U6</i> snoRNA
<i>snR76</i>	3.9	4.6E-020	2.0E-17	C/D box snoRNA
<i>RDN18</i>	1.9	1.6E-019	6.3E-17	rRNA
<i>snR87</i>	2.9	1.2E-016	4.1E-14	C/D box snoRNA
<i>snR66</i>	2.4	6.5E-016	2.1E-13	C/D box snoRNA
<i>snR18</i>	4.1	6.6E-016	2.1E-13	C/D box snoRNA
<i>snR24</i>	4.6	1.6E-012	4.9E-10	C/D box snoRNA
<i>snR34</i>	1.5	8.7E-012	2.4E-09	H/ACA box snoRNA
<i>snR60</i>	1.7	8.9E-012	2.4E-09	C/D box snoRNA
<i>EFM3</i>	1.5	9.5E-012	2.4E-09	just 3' of H/ACA box <i>snR3</i> snoRNA
<i>snR71</i>	2.6	9.6E-012	2.4E-09	C/D box snoRNA
<i>snR17b</i>	3.0	1.6E-011	3.9E-09	<i>U3</i> snoRNA
<i>YGR161C-D</i>	1.2	5.9E-011	1.4E-08	TY1 transposon
<i>snR3</i>	1.5	2.7E-010	6.1E-08	H/ACA box snoRNA
<i>snR37</i>	1.2	4.3E-010	9.2E-08	H/ACA box snoRNA
<i>snR77</i>	1.4	1.2E-009	2.4E-07	C/D box snoRNA
<i>snR57</i>	3.1	2.3E-009	4.7E-07	C/D box snoRNA
<i>snR56</i>	1.1	6.3E-009	1.2E-06	C/D box snoRNA
<i>snR68</i>	3.0	6.4E-009	1.2E-06	C/D box snoRNA
<i>snR52</i>	3.6	7.1E-009	1.3E-06	C/D box snoRNA
<i>YJL047C-A</i>	1.6	9.5E-009	1.7E-06	overlaps with C/D box <i>snR60</i> snoRNA
<i>snR73</i>	4.2	1.1E-008	2.0E-06	C/D box snoRNA
<i>snR64</i>	1.4	1.4E-008	2.3E-06	C/D box snoRNA
<i>snR61</i>	2.5	1.8E-008	2.9E-06	C/D box snoRNA
<i>snR47</i>	1.8	4.9E-008	7.6E-06	C/D box snoRNA
<i>snR45</i>	1.7	5.6E-008	8.5E-06	C/D box snoRNA
<i>snR10</i>	0.9	6.3E-008	9.2E-06	H/ACA box snoRNA
<i>RPR1</i>	4.1	1.1E-007	1.5E-05	RNA component of RNase P
<i>snR85</i>	3.3	1.2E-007	1.7E-05	H/ACA box snoRNA

<i>YOL157C</i>	2.0	1.3E-007	1.8E-05	encodes isomaltase enzyme
<i>NME1</i>	3.7	3.5E-007	4.7E-05	RNA component of RNase MRP
<i>snR13</i>	1.3	4.1E-007	5.3E-05	C/D box snoRNA
<i>snR46</i>	1.1	5.6E-007	7.2E-05	H/ACA box snoRNA
<i>snR82</i>	1.3	6.0E-007	7.5E-05	H/ACA box snoRNA
<i>snR48</i>	4.5	8.4E-007	1.0E-04	C/D box snoRNA
<i>snR32</i>	0.9	1.9E-006	2.2E-04	H/ACA box snoRNA
<i>snR74</i>	4.5	2.3E-006	2.7E-04	C/D box snoRNA
<i>snR35</i>	1.2	2.8E-006	3.2E-04	H/ACA box snoRNA
<i>YOR040W</i>	1.5	3.6E-006	4.1E-04	just 3' of H/ACA box <i>snR9</i> snoRNA
<i>snR9</i>	1.1	6.4E-006	7.0E-04	H/ACA box snoRNA
<i>LIN1</i>	0.8	1.1E-005	1.2E-03	just 3' of C/D box <i>snR71</i> snoRNA
<i>RDN37</i>	1.9	1.4E-005	1.5E-03	rRNA
<i>snR51</i>	1.4	1.6E-005	1.7E-03	C/D box snoRNA
<i>YOR343W-A</i>	3.1	1.8E-005	1.8E-03	TY2 transposon
<i>PRP31</i>	1.4	1.8E-005	1.8E-03	U4/U6-U5 snRNP complex component
<i>snR54</i>	3.1	2.5E-005	2.4E-03	C/D box snoRNA
<i>snR78</i>	3.9	2.5E-005	2.4E-03	C/D box snoRNA
<i>BDF2</i>	0.8	2.8E-005	2.6E-03	involved in transcription initiation
<i>snR42</i>	1.0	2.8E-005	2.6E-03	H/ACA box snoRNA
<i>snR80</i>	1.3	2.9E-005	2.7E-03	H/ACA box snoRNA
<i>MMS2</i>	1.2	3.0E-005	2.7E-03	just 3' of H/ACA box <i>snR10</i> snoRNA
<i>POP6</i>	1.1	3.0E-005	2.7E-03	just 3' of H/ACA box <i>snR46</i> snoRNA
<i>snR4</i>	0.8	4.5E-005	3.9E-03	C/D box snoRNA
<i>snR19</i>	2.8	4.6E-005	4.0E-03	<i>U1</i> snRNA
<i>YIL082W-A</i>	8.5	5.7E-005	4.8E-03	TY3 transposon
<i>snR69</i>	3.1	5.8E-005	4.8E-03	C/D box snoRNA
<i>snR8</i>	1.2	1.0E-004	0.008	H/ACA box snoRNA
<i>YPL222C-A</i>	6.3	1.1E-004	0.008	dubious ORF
<i>YGR161C-C</i>	8.2	1.1E-004	0.008	TY1 transposon
<i>YDR316W-A</i>	8.2	1.1E-004	0.008	TY1 transposon
<i>snR58</i>	2.5	1.1E-004	0.008	C/D box snoRNA
<i>ODC2</i>	0.8	1.2E-004	0.009	just 3' of H/ACA box <i>snR35</i> snoRNA

Table 4.1 Genes identified by RNA-Seq as overexpressed in cells lacking the Mtr4-Tr5 interaction. RNA was isolated from biological replicates of *trf4* Δ , *trf5* Δ cells complemented with either *TRF5* or *trf5* Δ *98-117* plasmids. Samples were enriched for poly(A)⁺ RNA, which was then converted into a sequencing library. Mapping reads to the yeast genome revealed seventy-one genes that are overexpressed in the *trf5* Δ *98-117* strain, in comparison to *TRF5* cells. This set is predominated by snoRNA genes.

Mature snoRNA species are processed from primary transcripts in a variety of ways. The seventy-one RNA-Seq hits listed in **Table 4.1** include examples of monocistronically encoded snoRNA transcripts that are either only 3' processed (*snR8*; **Figure 4.5 A**) or are additionally processed at their 5' end by the nuclear Rat1 exoribonuclease and Rnt1 endoribonuclease (*snR87*; **Figure 4.5 B**). As opposed to the RNA exosome-dependent pathway of 3'-5' RNA degradation, these two ribonucleases are part of the 5'-3' RNA degradation pathway. A snoRNA that is processed from a spliced intron is also included in the RNA-Seq hits (*snR18*; **Figure 4.5 C**). For this, and other intron-encoded snoRNA species, there was a clear increase in reads that mapped to the snoRNA and the part of the intron found at its 3' end. There was no effect on the flanking protein-coding exons. Similarly, other mRNA genes (*RPL11A*; **Figure 4.5 E**) were not affected. Finally, the RNA-Seq hits contain an example of seven snoRNA transcripts that are transcribed as one polycistronic precursor (*snR72-78*; **Figure 4.5 D**). For each of these transcripts, there is a clear increase in the read density for both the snoRNA and the region just 3' of it. Strikingly, among the other genes that were detected as overexpressed, there are seven genes that are located just 3' to one of the overexpressed snoRNA genes (**Table 4.1**). The inclusion of these genes in the RNA-Seq hits is likely due to the presence of 3' extended polyadenylated snoRNA. All of these changes were clearly reproducible in the duplicate transcriptome sequencing samples (**Figure 4.5 F**). Thus, no particular type of snoRNA appears to be overrepresented among the RNA-Seq hits. Therefore, disrupting the Mtr4-Trf5 interaction appears to have a general negative effect on snoRNA biogenesis.

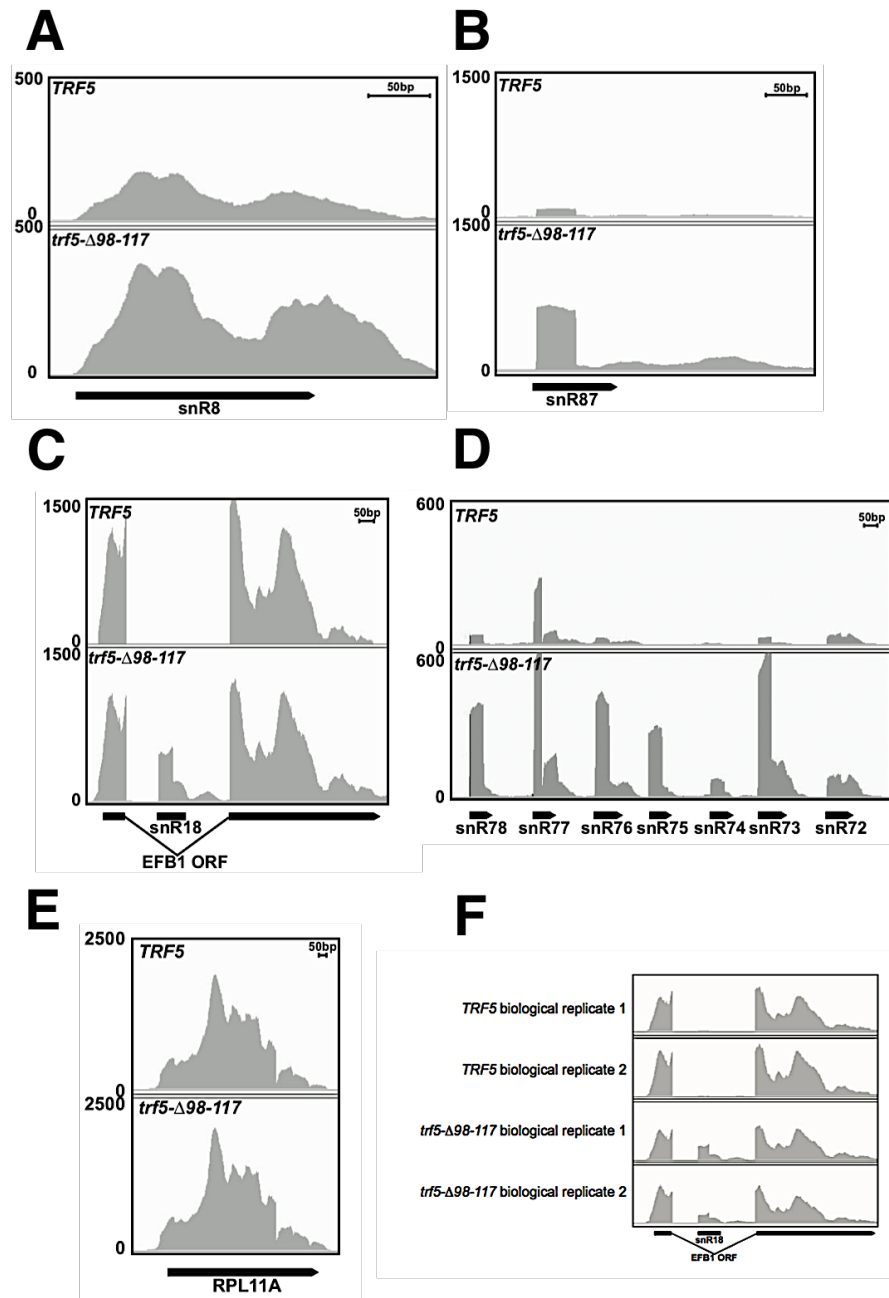


Figure 4.5 Disrupting stable TRAMP complex formation results in a variety of snoRNA processing defects. The set of genes that are overexpressed in cells lacking the Mtr4-Trf5 interaction include examples of snoRNA species that are processed in different ways from primary transcripts. A comparison of differential expression between both strains is provided for **(A)** *snR8*, a monocistronically encoded H/ACA box snoRNA that is not 5' processed, **(B)** *snR87*, a monocistronically encoded C/D box snoRNA that is 5' processed

by Rnt1 and Rat1, **(C)** *snR18*, a C/D box snoRNA that is processed from the intron spliced out of the *EFB1* pre-mRNA, and **(D)** *snR72-78*, a cluster of polycistronically encoded C/D box snoRNA species that are separated from each other by Rnt1 and then further 5' and 3' processed. Peaks covering the first fifty base pairs of *snR87*, *snR18*, and *snR72-78* are due to their 5' monophosphate ends becoming ligated to linkers due to library preparation, combined with a fifty-nucleotide sequencing read length. **(E)** *RPL11A*, a representative mRNA, is not affected by a disruption of the Mtr4-Trf5 interaction. **(F)** This analysis is highly reproducible from duplicate cultures of *TRF5* and *trf5* Δ *98-117* strains. The region showing *snR18* snoRNA and *EFB1* mRNA is provided as an example of this reproducibility.

Although twenty-three other snoRNA genes were not in the list of hits at 0.01 FDR, most of these were significantly up-regulated at reduced stringency (P -values 0.004 to 0.05; data not shown). Moreover, this group also was not enriched for a particular kind of snoRNA. This set included *snR33* ($P < 0.004$), which I had arbitrarily chosen to analyze via northern blotting (**Figure 4.4**).

The RNA-Seq hits included other ncRNA loci that have previously been shown to be substrates of the TRAMP complex and/or the RNA exosome. These include rRNA, *U1* snRNA, and *U6* snRNA, as well as the RNA subunits of the signal recognition particle, RNase P and RNase MRP (Allmang *et al.*, 1999b; van Hoof *et al.*, 2000a; San Paolo *et al.*, 2009; Wlotzka *et al.*, 2011). Additionally, the RNA-Seq hits include RNA transcribed by RNA polymerase I, II, and III. Overall, RNA analysis of *trf5 Δ 98-117* cells indicates that many polyadenylated TRAMP complex substrates accumulate if the Mtr4-Trf5 interaction is disrupted. Therefore, these poly(A)⁺ transcriptome sequencing data confirmed and extended my northern blotting analysis.

The Mtr4-Trf4/5 Interaction is Not Required for Viability

Published assays for this project included *trf4 Δ* , *trf5 Δ* strains complemented with a wild-type *TRF5* plasmid or a *trf5 Δ 98-117* plasmid, but do not include strains complemented with plasmids allowing for the expression of wild-type or mutant forms of Trf4 (Losh, King *et al.*, 2015; **Figure 4.4 A**). Since wild-type cells express both Trf4 and Trf5, and therefore multiple compositions of the TRAMP complex, I created a *trf4 Δ* , *trf5 Δ* strain that contains both *trf4 Δ 115-134* and *trf5 Δ 98-117* plasmids. Therefore, this strain expresses all components of the TRAMP complex, but the Mtr4-Trf4/5 interaction is disrupted.

When generating this strain, plasmids allowing for expression of *trf4 Δ 115-134* or *trf5 Δ 98-117* mutant protein also encoded selectable *URA3* or *LEU2* markers, respectively. I first tested the growth of this strain via serial dilutions on solid medium lacking both uracil

and leucine. Wild-type cells, as well as strains expressing only one of the Trf4/5 proteins, were used as controls. These strains were transformed with empty vector *URA3* or *LEU2* plasmids, as needed. This assay revealed that the strain expressing both *trf4* Δ 115-134 and *trf5* Δ 98-117 proteins grew similarly to a strain expressing just *trf4* Δ 115-134, but better than a strain expressing only *trf5* Δ 98-117 (**Figure 4.6**). The latter result could be due to the fact that the *trf4* Δ 115-134, *trf5* Δ 98-117 strain expresses both proteins and even though they are mutant variants, this improves growth in comparison to cells expressing only *trf5* Δ 98-117 protein. As previously mentioned, Trf4 and Trf5 appear to have different preferences for specific targets, so expression of both proteins likely promotes the efficient targeting of all TRAMP complex substrates (San Paolo *et al.*, 2009). Moreover, Trf5 is believed to be expressed at a lower level than Trf4 in wild-type yeast (Ghaemmaghami *et al.*, 2003; Kulak *et al.*, 2014). Therefore, the growth deficiency of *trf4* Δ , *trf5* Δ cells expressing only the *trf5* Δ 98-117 protein may be more related to the loss of Trf4 protein expression than to the loss of interaction with Mtr4. This possibility was previously introduced in the context of **Figure 4.4**.

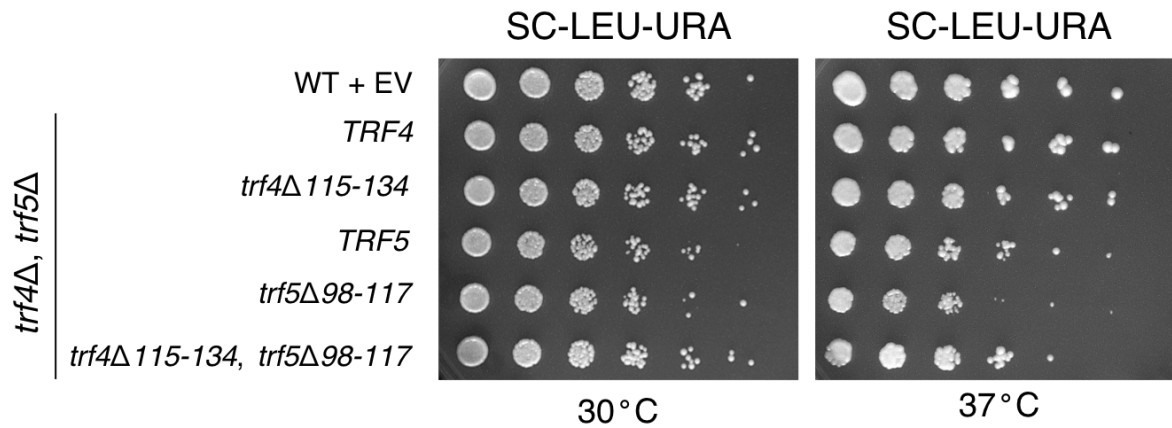


Figure 4.6 Disrupting stable TRAMP complex formation does not significantly impair yeast cell growth. The growth of *trf4Δ*, *trf5Δ* cells expressing only wild-type or mutant forms of one Trf4/5 protein was analyzed by performing serial dilutions, spotting onto solid complete yeast medium lacking uracil and leucine, and incubation at the indicated temperatures. A *trf4Δ*, *trf5Δ* strain complemented with plasmids that allow for the expression of both mutant forms of Trf4/5 that cannot interact with Mtr4 was included as a more complete representation of what results when the interaction between these TRAMP complex subunits is disrupted. A wild-type strain complemented with empty vectors for growth on this selective medium (EV) was included as a positive control for growth.

I performed western blotting to ensure that the Trf4/5 variants were expressed. When generating the [*trf4*Δ115-134, *URA3*] and [*trf5*Δ98-117, *LEU2*] plasmids, I included the endogenous *TRF4* or *TRF5* gene promoter, respectively. Additionally, I added TAP tags to these Trf4/5 mutants. In addition to wild-type cells, I included *trf4*Δ, *trf5*Δ strains expressing one or both wild-type or mutant variants of Trf4/5. Western blotting confirmed the expression of all TAP-tagged Trf4/5 constructs (**Figure 4.7**). Wild-type and mutant Trf5 bands were slightly higher than those of Trf4 constructs, which was expected due to the known lengths of the proteins. Levels of Trf5-TAP protein decreased significantly when both wild-type Trf4/5 constructs were expressed, supporting the earlier findings that Trf4 is more highly expressed (Ghaemmaghani *et al.*, 2003; Kulak *et al.*, 2014). Interestingly, expression levels of Trf4 and Trf5 were similar in *trf4*Δ, *trf5*Δ strains expressing only one of the proteins. This indicates that Trf5 is more highly expressed in *trf4*Δ, *trf5*Δ backgrounds in order to compensate for the loss of Trf4.

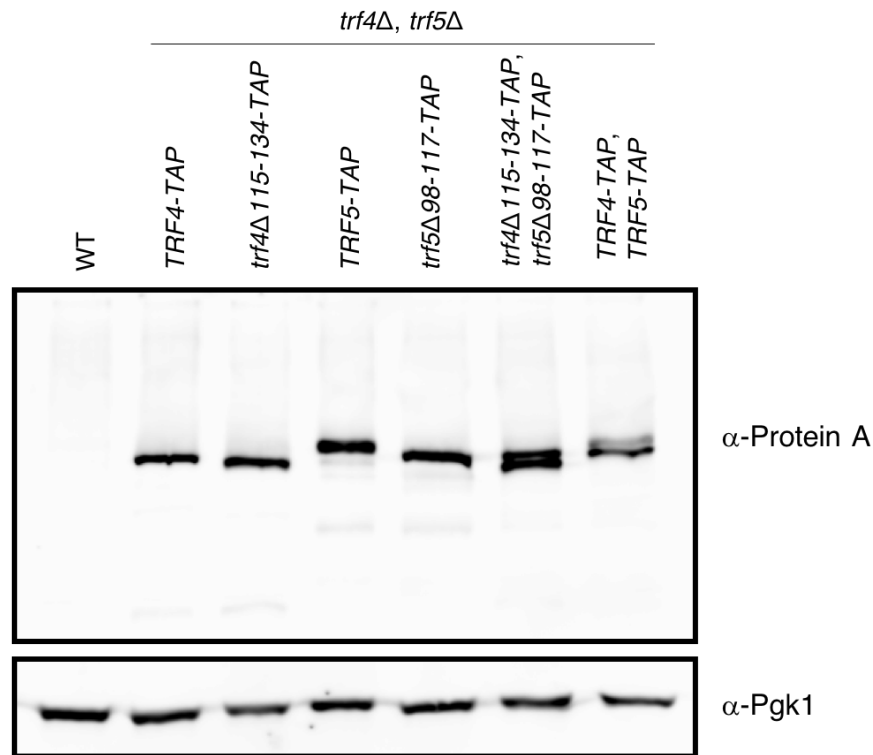


Figure 4.7 Trf4/5 protein variants that have lost the ability to interact with Mtr4 are expressed at wild-type levels. Lysates were obtained from *trf4Δ, trf5Δ* cells complemented with plasmids allowing for expression of TAP-tagged wild-type or mutant variants of one or both Trf4/5 proteins. Immunoblotting with α -Protein A antibody allowed for detection of these proteins. Two bands are clearly detected from the lysates of strains able to express both proteins. Bands migrated as expected based upon the known lengths of Trf4 and Trf5, which are 584 and 642 amino acids, respectively. Moreover, the mutant bands migrated slightly faster, which was expected since they are lacking the twenty residues required for interaction with Mtr4. α -Pgk1 antibody allowed for detection of the loading control, 3-phosphoglycerate kinase.

Additionally, I included RNA isolated from the *trf4* Δ , *trf5* Δ strain complemented with both *trf4* Δ 115-134 and *trf5* Δ 98-117 plasmids in my northern blotting analysis. In comparison to strains expressing only one of these variants, the expression of both proteins in this strain results in a more complete model for assessing the RNA accumulation that results from disrupting the Mtr4-Trf4/5 interaction. This strain accumulated just as much or more extended snoRNA than the strains expressing only one of the Trf4/5 mutants (**Figure 4.4 B**). Collectively, these northern blotting assays indicate that impairing the Mtr4-Trf4/5 interaction interferes with normal processing or degradation of 3' extended snoRNA transcripts, but not mature snoRNA.

Furthermore, I analyzed RNA from this *trf4* Δ 115-134, *trf5* Δ 98-117 strain for a more global analysis of the consequences that result from TRAMP complex instability. Duplicate RNA samples from this mutant strain and from *trf4* Δ , *trf5* Δ cells expressing both wild-type Trf4 and Trf5 were assessed via transcriptome sequencing. Preliminary bioinformatics analysis revealed that snRNA and snoRNA loci are abundantly present within the set of genes that are significantly affected upon disruption of the Mtr4-Trf4/5 interaction (**Figure 4.8**). Specifically, the abundance of all snRNA species and all but four snoRNA species was increased over twofold in the mutant strain when compared to the strain expressing wild-type Trf4/5. Gene Ontology analysis confirmed that the set of genes that were upregulated over twofold was strongly enriched for snoRNA genes but did not reveal additional enriched categories. As expected, many genes in this *trf4* Δ 115-134, *trf5* Δ 98-117 set were also upregulated in the previously described RNA-Seq analysis of *trf5* Δ 98-117 cells, even though the sequencing and bioinformatics analysis was performed slightly differently. These findings support the conclusion that disrupting the Mtr4-Trf4/5 interaction has a widespread effect on snoRNA biogenesis that is deleterious but not lethal.

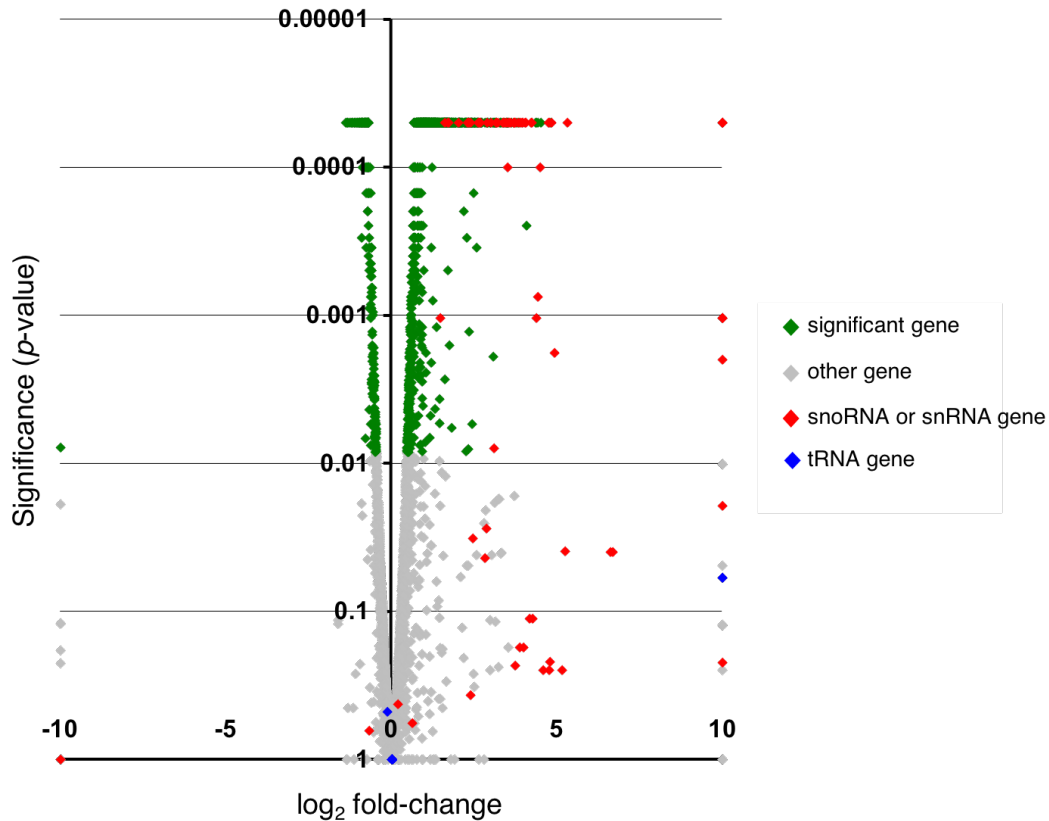


Figure 4.8 Disrupting stable TRAMP complex formation results in the overexpression of many snoRNA genes. RNA was isolated from biological replicates of *trf4* Δ , *trf5* Δ cells complemented with both *trf4* Δ 115-134 and *trf5* Δ 98-117 plasmids or with both *TRF4* and *TRF5* plasmids. Samples were enriched for poly(A)⁺ RNA, which was then converted into a sequencing library. Mapping reads to the yeast genome identified genes that are overexpressed in the *trf4* Δ 115-134, *trf5* Δ 98-117 strain. Hits were determined to be significant (green) or not (grey) based on a false discovery rate (FDR) of 0.05. A log₂ (fold-change) of infinity or negative infinity is plotted on the x-axis as either 10 or -10. Of the seventy-eight snoRNA and snRNA genes (red) in this data set, the majority are significantly overexpressed by at least fourfold. This data set also contains two tRNA genes, although their upregulation is not statistically significant (overlapping blue points on far right). All other two hundred fifty tRNA gene points are clustered at the origin (overlapping blue points at center).

Maintaining the Mtr4-Trf4/5 Interaction is Not Increasingly Important During Stress

The Mtr4-Trf4/5 interaction is likely conserved between metazoans and fungi, suggesting that it is more significant than currently appreciated. It is possible that maintaining this interaction is more important for growth and survival during exposure to certain stressors than under optimal conditions. Increased heat sensitivity has been described upon the repression of any RNA exosome subunit, so it is possible that a similar phenotype would result from mutations in RNA exosome cofactors (Allmang *et al.*, 1999b; Allmang *et al.*, 2000; van Hoof *et al.*, 2000a). I first assessed the effect of heat as a cellular stress by spotting serial dilutions of *trf4* Δ , *trf5* Δ cells expressing one or both mutants that cannot interact with Mtr4 onto complete medium. I included *trf4* Δ , *trf5* Δ strains expressing wild-type Trf4/5, as well as wild-type cells, as positive controls for maintenance of the Mtr4-Trf4/5 interaction. I additionally included *rrp44-exo* σ and *rrp6* Δ strains, which lack 3'-5' exonuclease activity, as positive controls for disruptions within the 3'-5' RNA degradation pathway and heat sensitivity. Incubation at 37°C did not affect the differences in growth that are already exhibited by these yeast strains at their optimal growth temperature of 30°C. Even after seven days, there was no growth of any strains at 42°C, which is known to induce heat shock in yeast (**Figure 4.9**). These results indicate that maintaining the Mtr4-Trf4/5 interaction is not increasingly important during heat stress.

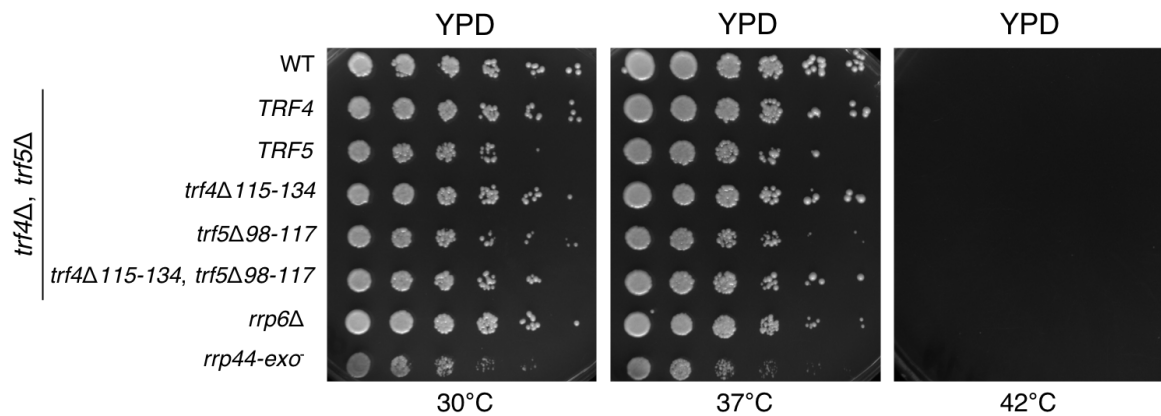


Figure 4.9 Maintaining the Mtr4-Trf4/5 interaction is not increasingly important during heat stress. While 30°C is the optimal growth temperature for yeast, 37°C and 42°C are considered stressful for growth, with the latter temperature high enough to induce heat shock. The growth of *trf4*Δ, *trf5*Δ cells expressing only wild-type or mutant forms of one Trf4/5 protein was analyzed by performing serial dilutions, spotting onto solid rich medium and incubation at the indicated temperatures. A *trf4*Δ, *trf5*Δ strain complemented with both *trf4*Δ115-134 and *trf5*Δ98-117 plasmids was included as a more complete representation of what results when the Mtr4-Trf4/5 interaction is disrupted. A wild-type strain was included as a positive control for growth, while *rrp44-exo* and *rrp6*Δ strains were included as negative controls for growth. No growth of any strains was detected after incubating at 42°C for one week.

I next tested for effects that various concentrations of 5-fluorouracil (5-FU) may have on strains with a disrupted Mtr4-Trf4/5 interaction. Yeast strains with mutations in the RNA exosome or certain RNA exosome cofactors are known to be hypersensitive to 5-FU and other DNA damaging agents (Walowsky *et al.*, 1999; Fang *et al.*, 2004; Lum *et al.*, 2004). 5-FU is a commonly used chemotherapeutic agent. When 5-FU is converted into multiple metabolites, it inhibits thymidylate synthase, resulting in decreased thymidine production during DNA replication. However, one metabolite of this drug can be incorporated into RNA, disrupting post-transcriptional modifications and transcript functions (Longley *et al.*, 2003). I spotted the strains that were included in the heat shock assay onto complete media supplemented with 5-FU at concentrations of 50 μ M, 100 μ M, or 200 μ M. The *trf4 Δ 115-134* and *trf5 Δ 98-117* strains did not exhibit hypersensitivity to 5-FU at 30°C, even after several days of growth (**Figure 4.10 A**). This finding indicates that loss of the Mtr4-Trf4/5 interaction does not cause increased susceptibility to 5-FU.

Interestingly, I saw a significant growth improvement in *trf4 Δ 115-134* cells when I repeated this experiment at 37°C. At this temperature, these cells grew better than wild-type, which was most noticeable after one day of growth (**Figure 4.10 B**). Based upon this result, I hypothesize that the Trf4 in this strain may be playing a significantly enhanced TRAMP complex-independent role in DNA damage repair, as described in earlier studies (Gellon *et al.*, 2008).

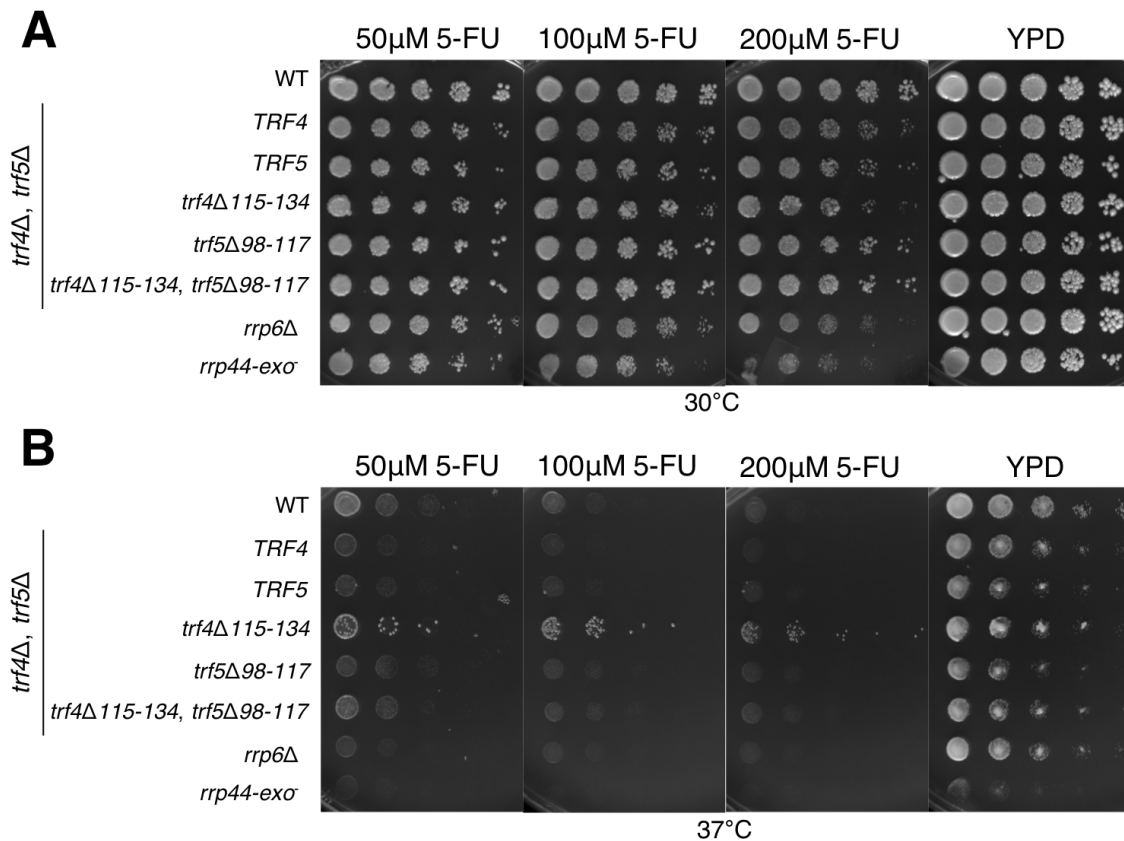


Figure 4.10 Maintaining the Mtr4-Trf4/5 interaction is not increasingly important during exposure to 5-fluorouracil. **(A)** The growth of *trf4Δ*, *trf5Δ* cells expressing only wild-type or mutant forms of one Trf4/5 protein was analyzed by performing serial dilutions and spotting onto solid rich media containing 50μM, 100μM, or 200μM 5-fluorouracil (5-FU), or lacking 5-FU completely. Plates were incubated at 30°C. A *trf4Δ*, *trf5Δ* strain complemented with both *trf4Δ115-134* and *trf5Δ98-117* plasmids was included as a more complete representation of what results when the Mtr4-Trf4/5 interaction is disrupted. *rrp44-exo* and *rrp6Δ* strains were included as positive controls for growth impairment during exposure to 5-FU. **(B)** This experimental set-up was repeated at 37°C to determine if maintaining the Mtr4-Trf4/5 interaction becomes increasingly important during combined drug and heat stress.

The Catalytic Core of Trf4/5 is Sufficient for Viability

In addition to the small N-terminal region that is required for Mtr4 interaction, the Trf4/5 C-termini contain several other short conserved regions, which may facilitate interaction with other proteins or form partially redundant sites for interaction with Mtr4. In fact, C-terminal residues of Trf4 interact with another nuclear cofactor of the RNA exosome, the NNS complex (Tudek *et al.*, 2014). This site of interaction with the NNS complex is not conserved in Trf5 and may be important for the functional diversification of Trf4 and Trf5.

To investigate the importance of these small conserved motifs within the large intrinsically disordered Trf4/5 termini, I created strains expressing only the catalytic core of either Trf4 or Trf5. Preliminary growth assays revealed that removing the termini results in significant growth deficiency. This phenotype was more severe than the growth deficiencies that result from deleting the N-terminal Trf4/5 sites that are necessary for interaction with Mtr4 (**Figure 4.11 A**). Yet, it is not clear if this phenotype is due to a negative effect on the TRAMP complex-dependent or –independent activities of Trf4/5. Western blot analysis showed that the terminally truncated Trf4/5 mutants are expressed at similar levels to wild-type Trf4/5, ruling out decreased expression as the cause of the growth deficiency (**Figure 4.12**). Despite the growth deficiencies, these assays revealed that the Trf4/5 termini are not essential and that the Trf4/5 catalytic core is sufficient for viability.

Additionally, I generated single terminal truncations to assess if the growth deficiency was dependent upon a specific terminus. Growth assays revealed that deleting the N-terminus, but not the C-terminus, causes a growth deficiency in Trf5. Yet while single terminal truncations of Trf4 were not significantly deleterious, loss of both regions resulted in growth deficiency (**Figure 4.11 B**). This phenotypic difference may indicate that the termini are important for TRAMP complex-independent functions, which are thought to be different for Trf4 and Trf5 due to their incomplete functional redundancy.

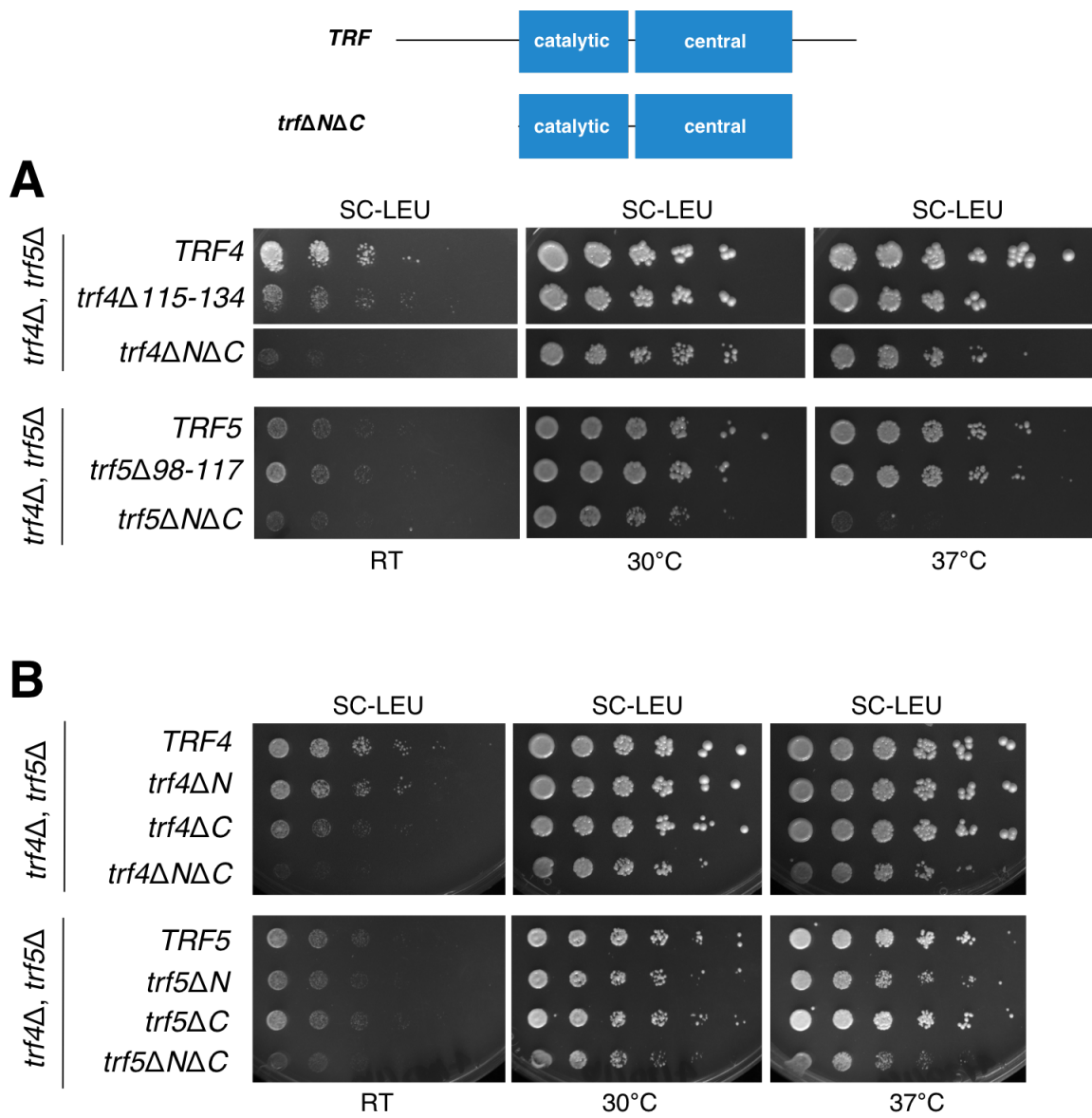


Figure 4.11 The N- and C-termini of Trf4/5 are not required for viability. The growth of *trf4Δ*, *trf5Δ* cells expressing only wild-type or mutant forms of one Trf4/5 protein was analyzed by performing serial dilutions, spotting onto solid selective medium lacking leucine, and incubation at the indicated temperatures. **(A)** The growth of *trf4Δ*, *trf5Δ* strains complemented with plasmids allowing for the expression of wild-type or mutant forms of Trf4/5 that cannot interact with Mtr4 was compared to those complemented with plasmids encoding Trf4/5 variants that lack both termini. Strains expressing Trf4 variants were assayed separately from those expressing Trf5 variants. While the *trf4ΔNΔC* strain

was assayed on the same plate as the *TRF4* and *trf4Δ115-134* strains, rows have been rearranged for this figure. **(B)** In order to determine which terminal truncations were responsible for growth impairment, this experimental set-up was repeated with strains complemented with plasmids that allow for the expression of Trf4/5 variants that lack just one terminus. Strains expressing Trf4 variants were assayed separately from those expressing Trf5 variants.

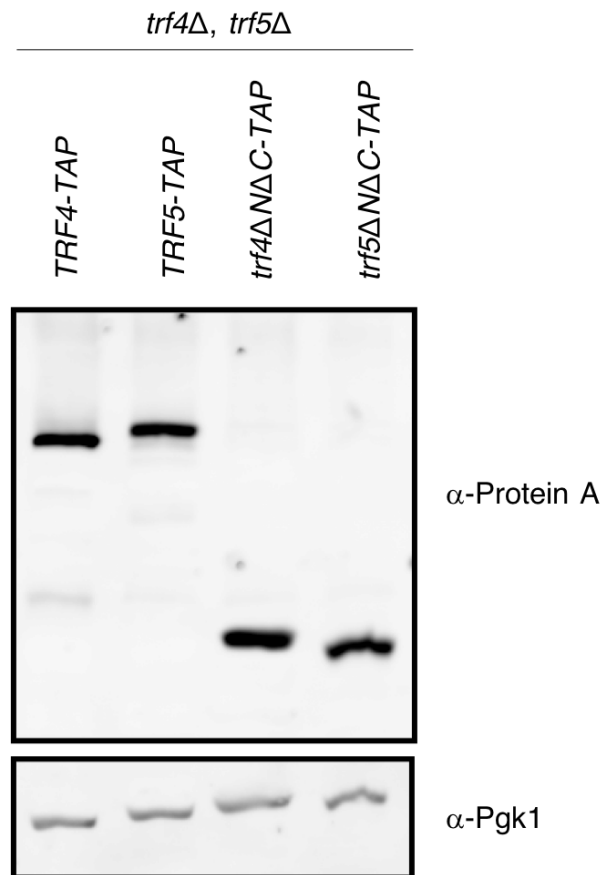


Figure 4.12 Trf4/5 protein variants that lack the N- and C-termini are expressed at wild-type levels. Lysates were obtained from *trf4* Δ , *trf5* Δ cells complemented with plasmids allowing for expression of TAP-tagged wild-type or mutant variants of one or both Trf4/5 proteins. Immunoblotting with α -Protein A antibody allowed for detection of these proteins. Bands migrated as expected based upon the known lengths of wild-type Trf4/5, which are 584 and 642 amino acids, respectively. Moreover, the mutant bands migrated significantly faster. This was expected since they are lacking the N- and C-termini, which each range from 95 to 160 amino acids in length. α -Pgk1 antibody allowed for detection of the loading control, 3-phosphoglycerate kinase.

For a more complete assessment of the effect of these terminal truncations, I generated a *trf4Δ, trf5Δ* strain expressing both *trf4ΔNΔC* and *trf5ΔNΔC* proteins. Transcriptome sequencing was performed on duplicate RNA samples isolated from these mutants, as well as from *trf4Δ, trf5Δ* cells expressing both wild-type Trf4 and Trf5 proteins. Preliminary analysis revealed that snRNA and snoRNA loci are abundantly present within the set of genes that are significantly affected by truncations of the Trf4/5 termini (**Figure 4.13**). Many genes in this set were also upregulated in the previously described RNA-Seq analyses of *trf4Δ, trf5Δ* cells expressing *trf4Δ115-134* and *trf5Δ98-117* proteins. Since the large terminal truncations result in the deletion of Trf4 residues 115-134 and Trf5 residues 98-117, it was expected that the genes affected by a disrupted Mtr4-Trf4/5 interaction would also be affected by a loss of the Trf4/5 termini. An additional similarity to these previous analyses is that no specific type of snoRNA appears to be affected more than others.

It is possible that the similar results of this sequencing indicate that TRAMP complex activity is also negatively impacted upon removal of the Trf4/5 termini. However, the TRAMP complex-independent activities of these proteins cannot be ruled out. Regardless, these findings indicate that loss of the Trf4/5 termini has a widespread deleterious effect on snoRNA biogenesis. Additional bioinformatics analysis will need to be performed in order to identify RNA species that are affected by the loss of the Trf4/5 termini but not by a disrupted Mtr4-Trf4/5 interaction. This analysis should attempt to identify any CUTs and SUTs among the hits, as these species were not detected in the primary gene analysis due to their derivation from inter- and intragenic regions.

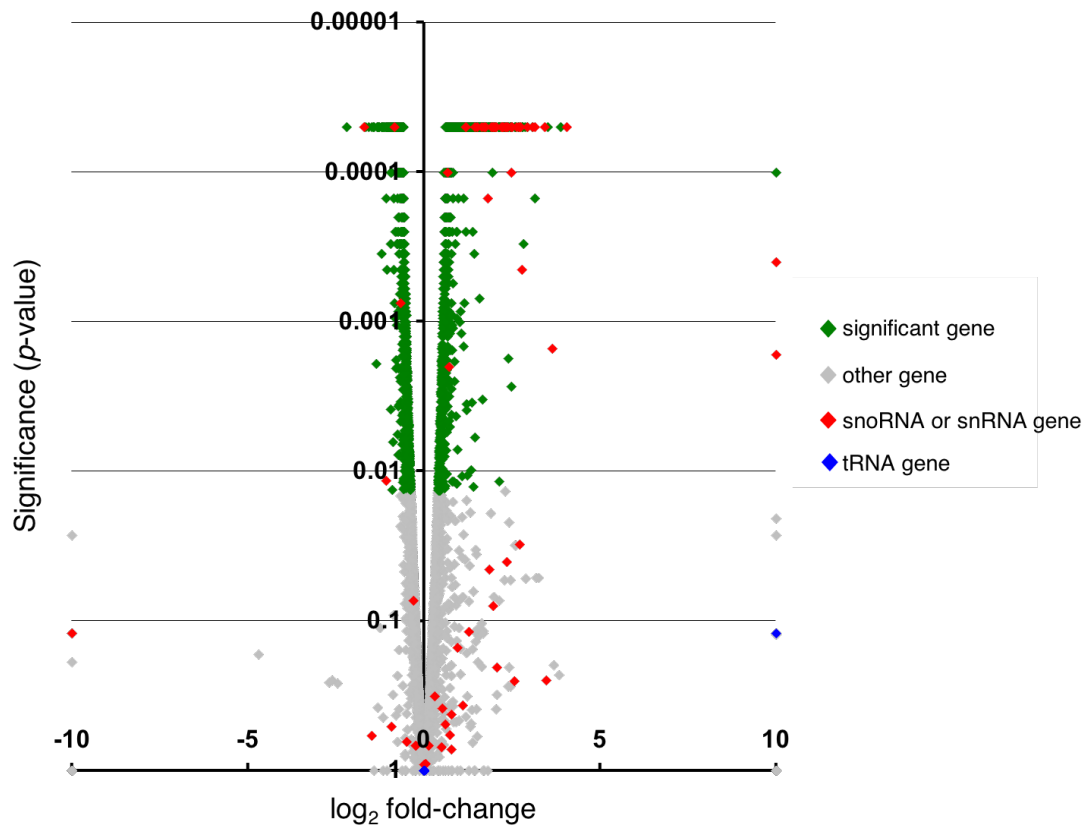


Figure 4.13 Loss of both Trf4/5 N- and C-termini results in the overexpression of many snoRNA genes. RNA was isolated from biological replicates of *trf4* Δ , *trf5* Δ cells complemented with both *trf4* Δ *N* Δ *C* and *trf5* Δ *N* Δ *C* plasmids or with both *TRF4* and *TRF5* plasmids. The results of this transcriptome sequencing were analyzed and plotted as described in **Figure 4.8**.

Trf4/5 Catalytic Activity is Required for Viability

Another possible explanation for the incomplete functional redundancy of Trf4/5 is that the catalytic activity of one of these poly(A) polymerases may be more important than that of the other. Two conserved aspartic acid residues are required for Trf4 and Trf5 to carry out polyadenylation of an RNA substrate. Specifically, these are Trf4 residues 236 and 238 and Trf5 residues 233 and 235. Catalytically inactive Trf4/5 proteins can be generated by substituting alanine residues at these positions, resulting in the “DADA” nickname given to these mutants (Wang *et al.*, 2000). The ability of Trf4 and Trf5 to polyadenylate substrates is not dependent upon each other, as both proteins exhibit catalytic activity when the other has been deleted (Houseley and Tollervey, 2006). It has been previously determined that expression of a catalytic inactive *trf4*-DADA mutant cannot complement the synthetic lethality of a *trf4* Δ , *trf5* Δ strain background (Wang *et al.*, 2000). However, the importance of maintaining Trf5 polyadenylation activity in *trf4* Δ , *trf5* Δ cells has not been previously published.

A visiting summer undergraduate student, Alex Morano, assisted me with modeling the inactivation of Trf4/5 polyadenylation. Overlap PCR was performed to change the two conserved aspartic acid residues of Trf4/5 to alanine residues. These products were cloned into plasmids with a *LEU2* marker. The plasmids were each used to transform *trf4* Δ , *trf5* Δ strains that already express wild-type Trf4 or Trf5 from a *URA3* plasmid. Transformed cells were grown on media lacking both leucine and uracil to ensure the expression of both wild-type and catalytically inactive mutant proteins. These strains were then serially diluted and spotted onto medium lacking leucine and uracil. They exhibited no significant growth deficiencies in comparison to wild-type controls or strains lacking the Mtr4-Trf4/5 interaction (**Figure 4.14**). A plasmid shuffle assay was additionally performed, by spotting these serial dilutions onto 5-FOA medium in order to abolish the expression of the wild-type Trf4 or Trf5 from the *URA3* plasmid (**Figure 4.14**). As expected, based on previous studies, the sole

expression of the *trf4*-DADA mutant is not enough to rescue *trf4* Δ , *trf5* Δ synthetic lethality.

This assay also reveals that cells expressing only *trf5*-DADA protein are inviable. Therefore, at minimum, cellular viability requires the catalytic activity of either Trf4 or Trf5 protein.

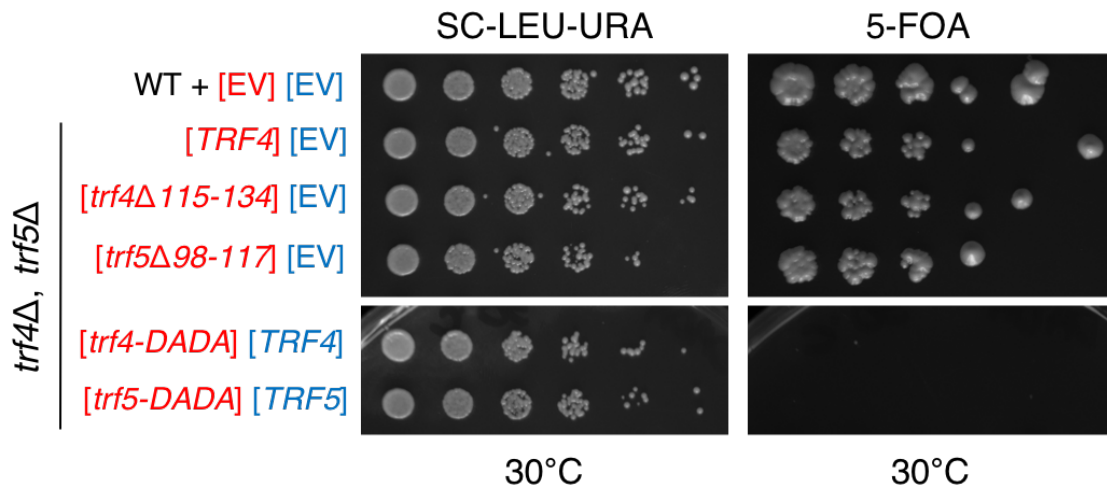


Figure 4.14 The catalytic activity of Trf4/5 is required for viability. The growth of *trf4Δ*, *trf5Δ* cells expressing only wild-type or mutant forms of one Trf4/5 protein was analyzed by performing serial dilutions, spotting onto solid selective medium lacking uracil and leucine, and incubation at 30°C. The plasmid shuffle assay was performed by additionally spotting these strains onto 5-FOA medium. The Trf4/5 variants expressed from *LEU2* and *URA3* marker plasmids are provided in red and blue, respectively. Marker plasmids that do not allow for expression of a Trf4/5 variant are designated as empty vectors (EV). While the strains expressing catalytically inactive *trf4-DADA* or *trf5-DADA* protein were assayed on the same plate as the other strains, rows have been rearranged for this figure. After loss of wild-type Trf4/5 protein expression, due to plating on 5-FOA medium, the expression of catalytically inactive *trf4-DADA* or *trf5-DADA* protein is not sufficient for cellular viability.

An Air1-Trf4 or Air1-Trf5 Interaction is Sufficient for the Essential Function of Trf4/5

Three studies, including our published work, support the hypothesis of additional direct subunit interactions that contribute to TRAMP complex integrity. Through different techniques, each study suggests that an N-terminal region of Air1/2 directly interacts with Mtr4 (Holub *et al.*, 2012; Falk *et al.*, 2014; Losh, King *et al.*, 2015). However, some results indicate that the Air1/2 N-terminus binds the Mtr4 core, while other data indicates that this interaction takes place with the Mtr4 arch.

The Mtr4 arch has been shown to directly interact with Nop53 and Utp18, two essential proteins involved in pre-rRNA processing. Specifically, this interaction occurs between the Mtr4 arch and an arch interaction motif (AIM), found in the N-termini of these proteins (Thoms *et al.*, 2015). The conserved AIM sequence is comprised of four hydrophobic residues, followed by an aspartate. I decided to examine if Air1/2 also possess an N-terminal AIM that may allow for interaction with Mtr4. I performed a multiple sequence alignment, which revealed the presence of this motif in the N-termini of both proteins (data not shown; Losh and van Hoof, 2015). Specifically, these AIMs are Air1 residues 15-19 and Air2 residues 7-11. As previously stated, the Mtr4 arch is not required for TRAMP complex-dependent activities. Therefore, I hypothesize that an Air1/2 AIM interaction with the Mtr4 arch may occur in a context that is independent of the TRAMP complex. Yet in terms of its TRAMP complex-dependent functions, I hypothesize that the Air1/2 subunit holds Mtr4 and Trf4/5 together, even when the Mtr4-Trf4/5 interaction has been disrupted (**Figure 4.15**).

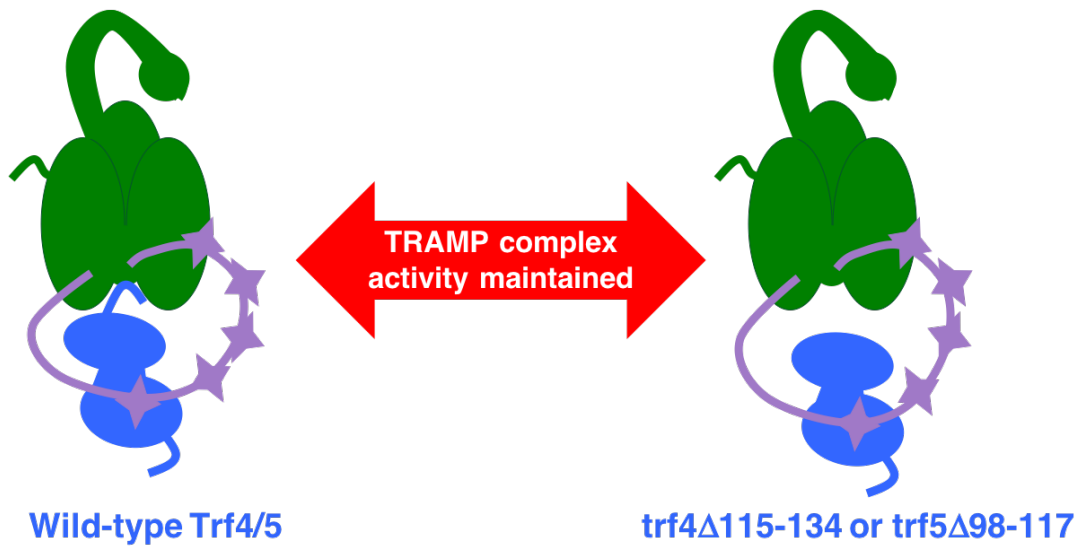


Figure 4.15 Model of TRAMP complex assembly in the presence or absence of the Mtr4-Trf4/5 interaction. Removing twenty residues within the N-terminus of Trf4/5 (top blue hook), abolishes direct interaction with Mtr4 (green). However, the Air1/2 subunit (purple), which is able to bind both Trf4/5 and Mtr4, may maintain TRAMP complex assembly regardless of the Mtr4-Trf4/5 interaction. Moreover, Air1/2 may hold the other two subunits together in close enough proximity so that the TRAMP complex retains a certain level of functionality even if the direct Mtr4-Trf4/5 interaction is lost.

If my hypothesis is correct, then the TRAMP complex is still assembled in strains that express *trf4* Δ ¹¹⁵⁻¹³⁴ and *trf5* Δ ⁹⁸⁻¹¹⁷ proteins. While a *trf4* Δ , *trf5* Δ double deletion is synthetic lethal, a double deletion of *air1* Δ , *air2* Δ is viable, although it does result in a significant accumulation of polyadenylated transcripts (Inoue *et al.*, 2000). Therefore, I aimed to delete both *AIR1* and *AIR2* in strains that already lack the Mtr4-Trf4/5 interaction. This would theoretically ensure that the TRAMP complex cannot assemble. Importantly, preventing the formation of the TRAMP complex would indicate how important the maintenance of the Mtr4-Trf4/5 interaction is for cellular viability.

I chose to knockout *AIR2* first, since the Air2 protein has been better characterized than Air1. Moreover, Air2 has not been shown to assemble into the TRAMP complex with Trf5 so I also chose to target *AIR2* first because I hypothesized that less severe phenotypes would arise from its deletion. Specifically, I did not want possible growth deficiencies arising from an *air1* Δ to then mask the effects of a subsequent *air2* Δ . For this gene deletion, I swapped *AIR2* with the *hphMX4* cassette via homologous recombination. This cassette includes the *Klebsiella pneumoniae hph* ORF which encodes a phosphotransferase that provides resistance to hygromycin B, a drug known to inhibit fungal protein synthesis.

After confirming that *AIR2* was replaced with the *hphMX4* cassette, I performed a growth assay to determine if the loss of *AIR2* was deleterious in strains only expressing Trf4 or Trf5 protein, but not both. Serial dilutions were spotted onto rich medium and incubated at 30°C. The only strains able to grow on medium containing hygromycin B were those lacking *AIR2*, which confirmed successful deletion of this gene. Importantly, introducing *air2* Δ in concert with *trf4* Δ and *trf5* Δ results in the presence of only one possible composition of the TRAMP complex in these strains. As previously shown, cells expressing *trf5* Δ ⁹⁸⁻¹¹⁷ protein had the most impaired growth when compared to strains expressing wild-type Trf4 or Trf5. While an additional deletion of *AIR2* appeared to slightly reduce growth, cells expressing

trf5 Δ 98-117 protein were most impaired (**Figure 4.16**). However, based on my model, I hypothesize that the TRAMP complex is maintained in these cells due to the presence of Air1.

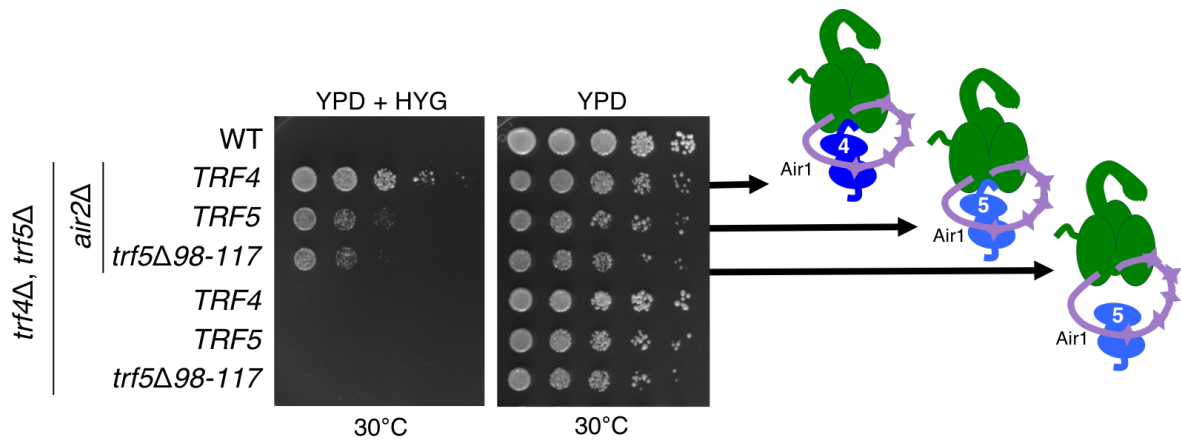


Figure 4.16 An additional deletion of *AIR2* in Trf4/5 mutant strains results in growth impairment but not loss of viability. The growth of *trf4Δ*, *trf5Δ* cells expressing only wild-type or mutant forms of one Trf4/5 protein was analyzed by performing serial dilutions, spotting onto solid rich medium with or without hygromycin B, and incubation at 30°C. An additional deletion of *AIR2*, which results in resistance to hygromycin B, allows for growth on medium containing this antibiotic. This confirmation of Air2 protein loss indicates that these strains each contain only one type of TRAMP complex composition (depicted to the right of arrows). Specifically, TRAMP complexes within these strains contain Mtr4 (green) and Air1 (purple). They additionally contain either wild-type Trf4 (dark blue), wild-type Trf5 (light blue), or a form of Trf5 that is unable to directly interact with Mtr4 (light blue, missing top hook).

I next attempted to similarly delete *AIR1* via homologous recombination or by genetic crosses. Although *air1* Δ and *air2* Δ are not reported to be synthetic lethal deletions, I included an *AIR2* plasmid in some of these experiments as a control. Despite extensive efforts, I was unable to generate *trf4* Δ , *trf5* Δ , *air1* Δ , *air2* Δ strains that were complemented with plasmids allowing for expression of various Trf4/5 and Air1/2 proteins. Troubleshooting indicated that the failure to obtain the desired strains could not be explained by synthetic lethality and various technical reasons were also eliminated. Therefore, it is not immediately evident as to why I could not generate *trf4* Δ , *trf5* Δ , *air1* Δ , *air2* Δ strain backgrounds. Regardless, these experiments indicate that although yeast cells normally contain multiple TRAMP complex compositions, a single composition containing an Air1 subunit and either a Trf4 or a Trf5 subunit is sufficient for viability.

CONCLUSIONS AND FUTURE DIRECTIONS

Based on new results and those previously published with our collaborators, I conclude that the TRAMP complex is composed of two well-folded catalytic cores that are brought together by short protein motifs. The majority of Mtr4 is structured and forms an RNA-dependent helicase core, while the catalytic core for polyadenylation is assembled from structured domains of the Trf4/5 and Air1/2 subunit (Hamill *et al.*, 2010; Jackson *et al.*, 2010; Weir *et al.*, 2010). In addition to these well-folded domains, each TRAMP complex subunit appears to have intrinsically disordered regions that function to mediate protein-protein interactions, either with the other two TRAMP complex subunits or with proteins that are not assembled in this complex. Interactions with other proteins may occur in the context of TRAMP complex-dependent or -independent activities.

In terms of TRAMP complex-dependent protein interactions, this project and previous work has identified the presence of small regions in the N-termini of Trf4/5 and Air1/2 that directly interact with Mtr4 (LaCava *et al.*, 2005; Falk *et al.*, 2014; Losh, King *et al.*, 2015). A deletion of either one of these regions impairs TRAMP complex formation, at least

to a level where Mtr4 is no longer immunoprecipitated with the Trf4/5 or Air1/2 subunit (Holub *et al.*, 2012; Falk *et al.*, 2014; Losh, King *et al.*, 2015). While each region establishes a relatively low affinity interaction, they combine for a high affinity *in vitro* interaction between the cores (Falk *et al.*, 2014). I hypothesize that deleting one of the interaction sites eliminates the *in vivo* formation of a stable TRAMP complex since no TRAMP complex formation has been detected under such conditions (Holub *et al.*, 2012; Falk *et al.*, 2014; Losh, King *et al.*, 2015). However, the possibility that a less stable or transient formation is mediated through the other TRAMP subunit interaction regions cannot be excluded.

The Site and Function of the Newly Characterized Mtr4-Trf4/5 Interaction May Be Conserved

Initial sequence analysis identified Tr4 residues 115-134 and Trf5 residues 98-117 to be conserved in orthologs from other ascomycetes. Although conservation in eukaryotes outside of this phylum was not readily detectable, it is notable that performing a multiple sequence alignment of Trf4/5 orthologs from vertebrates also identifies a small conserved region in an otherwise poorly conserved N-terminus. The sequence in vertebrates (EQxDFi/IP) is similar to the conserved sequence in ascomycetes (d/nNxDFIxf/I). Moreover, human orthologs of Mtr4 and Trf4 interact *in vitro* (Sudo *et al.*, 2016). Therefore, it is likely that this Mtr4-Trf4/5 interaction site is retained in animals, even though standard analysis tools fail to detect sequence conservation.

Both northern blotting and RNA-Seq analysis indicate that disrupting the Mtr4-Trf4/5 interaction leads to a defect in snoRNA processing and some other functions of the TRAMP complex. Most, if not all, snoRNA transcripts accumulate as 3' extended species in the poly(A)⁺ fraction. This suggests that these transcripts can still be polyadenylated by Trf4/5, but then fail to be degraded by the RNA exosome. The simplest interpretation is that stable TRAMP complex assembly is required for a substrate to be efficiently handed off from the Trf4/5 subunit to Mtr4 before it is subsequently delivered to the RNA exosome. However,

alternative explanations should be considered. For example, Mtr4 and Trf4/5 can affect each other's *in vitro* activity (Jia *et al.*, 2011; Jia *et al.*, 2012). Therefore, disrupting the Mtr4-Trf4/5 interaction may have effects beyond substrate handoff. One possibility is that abolishing this interaction would have a negative effect on the helicase activity of Mtr4. In this proposed scenario, even efficient handoff of substrates would not result in their eventual degradation by the RNA exosome because they would not be completely unwound.

While my collaborators and I have disrupted the Mtr4-Trf4/5 interaction via N-terminal deletions in *TRF4* and *TRF5*, mutations could be introduced into *MTR4* that would similarly disrupt this interaction. Assessing the helicase activity of mutant Mtr4 protein may help determine if it is negatively impacted when it is unable to interact with the Trf4/5 subunit. Specifically, its ability to unwind TRAMP complex substrates should be tested since Mtr4 also exhibits TRAMP complex-independent helicase activity. To additionally ensure that the TRAMP complex-dependent activity of this mutant Mtr4 is specifically assessed, the arch could also be removed, as this domain is known to only be required for its TRAMP complex-independent functions (Jackson *et al.*, 2010; Weir *et al.*, 2010).

The TRAMP Complex is Probably Unable to Significantly Relieve Widespread Cellular Stress

The significant growth improvement of the *trf4* Δ *115-134* strain on 5-FU medium at 37°C when compared to wild-type cells may be due to an enhancement of DNA damage repair. This Trf4 function is known to be important for survival during exposure to methyl methanesulfonate or hydrogen peroxide, which are alkylating or oxidizing agents, respectively (Gellon *et al.*, 2008). This may be a TRAMP complex-independent function of Trf4 since earlier work indicates that Trf5 has not retained the same activity (Edwards *et al.*, 2003). Interestingly, this provides a possible explanation as to why a similar growth improvement was not exhibited by the *trf5* Δ *98-117* strain in my assay. Regardless, my results did not indicate that maintenance of the Mtr4-Trf4/5 interaction is highly important for

survival during heat stress or exposure to 5-FU metabolites. This assay could be repeated with different stressors, such as 4-nitroquinolone, which causes DNA damage similar to UV treatment. However, it is important to consider that heat and drug stress affects a wide variety of cellular mechanisms, both directly and indirectly. Theoretically, the TRAMP complex would only be able to reduce the negative impacts of stress to a certain extent, especially as it is only present in the nucleus. Therefore, retaining or abolishing the Mtr4-Trf4/5 interaction may not make a significant difference in cellular survival during harsh growth conditions. However, optimal TRAMP complex formation is certainly important for alleviating the negative effects of RNA accumulation.

The Catalytic Core of the TRAMP Complex is Necessary and Sufficient for Trf4/5 Function

This work has shown that removing the termini of Trf4/5 does not affect protein expression or cellular viability, although removing each terminus results in varying levels of growth deficiency. Further assessment of this intriguing difference between the importance of Trf4/5 termini may provide more insight into the specific TRAMP complex-dependent and -independent roles of each protein. The termini may have varying structural importance or contain protein interaction sites that differ between Trf4 and Trf5. As explained in Chapter 1, Trf4/5 were first associated with topoisomerase activity. The studies that identified Trf4/5 found that 92 amino acids near the N-terminus of Trf4 are 21% identical and 43% similar to an N-terminal region of Top1. Moreover, 92 amino acids in the Trf5 C-terminus have 33% identity and 58% similarity to this N-terminal Top1 region (Sadoff *et al.*, 1995; Castaño *et al.*, 1996). Interestingly, this region of Top1 is not necessary for its catalytic activity, which may also be the case in Trf4/5 (Bjornsti and Wang, 1987).

It is unlikely that removal of the termini abolishes the catalytic activity of Trf4/5, since my results with cells expressing trf4-DADA and trf5-DADA proteins have indicated that this activity is indispensable. However, the termini could influence the conformation of Trf4/5,

which may indirectly affect polyadenylation activity if a substrate cannot be positioned correctly for this modification to be made. Assessment of polyadenylation activity, as previously described, could be performed on *trf4-DADA* and *trf5-DADA* mutant proteins and compared to that of wild-type *Trf4/5* (Vaňáčová *et al.*, 2005).

While my collaborators and I have shown that part of the *Trf4/5* N-terminus is required for interaction with *Mtr4*, neither the rest of the N-terminus nor the entire C-terminus have been shown to be involved in interactions with *Mtr4* or *Air1/2*. However, the *Trf4/5* termini may be important sites for interactions with other proteins in a context that is independent of the TRAMP complex. This could be elucidated by performing a binding assay that would compare wild-type *Trf4/5* with variants lacking one or both termini. Moreover, RNA-Seq analysis indicates that loss of the termini leads to a defect in snoRNA biogenesis, but it not clear if this reflects a disruption in TRAMP complex activity. While further characterization studies on the termini could help explain why both *Trf4/5* have been retained in yeast, I have shown that the termini are not essential for viability.

Additionally, this work has revealed that *trf5-DADA* protein expression cannot rescue *trf4Δ*, *trf5Δ* synthetic lethality, as has been previously shown for the expression of *trf4-DADA* (Wang *et al.*, 2000). Previous assays have also shown that expression of the *trf4-DADA* variant promotes the degradation of most of the transcripts that accumulate in a *trf4Δ* background, although wild-type *Trf5* protein was still expressed in both of these strains (Wyers *et al.*, 2005; San Paolo *et al.*, 2009). This suggests that *trf4-DADA*, and likely *trf5-DADA*, continues to promote RNA exosome activity even when it is unable to add poly(A) tails to its targets. One possible explanation is that these catalytically inactive proteins may retain the ability to interact with *Mtr4*. I hypothesize that these DADA mutants could still be incorporated within the TRAMP complex and therefore, positioned correctly to deliver a substrate into the helicase domain of *Mtr4*. In this scenario, *Mtr4* may still unwind the non-

polyadenylated substrate despite its known preference for poly(A) tails (Bernstein et al., 2008).

While expression of both *trf4* Δ 115-134 and *trf5* Δ 98-117 proteins is not synthetic lethal, expression of both *trf4*-DADA and *trf5*-DADA proteins is. Therefore, it is not possible to express variants of Trf4/5 that can neither interact with Mtr4 nor polyadenylate substrates. However, binding assays would reveal if *trf4*-DADA and *trf5*-DADA proteins can still interact with Mtr4, and additionally with Air1/2. Northern blotting could be performed to measure the accumulation of snoRNA substrates in cells expressing *trf4*-DADA or *trf5*-DADA proteins. This accumulation should be compared to that of wild-type cells, as well as strains lacking the Mtr4-Trf4/5 interaction. If expression of a catalytically defective Trf4/5 subunit results in similar or lower levels of accumulated substrates, it is likely that the TRAMP complexes in these cells are still able to efficiently prepare RNA for degradation by the RNA exosome.

Retaining Components of a Single TRAMP Complex Composition is Sufficient for Viability

While my multiple sequence alignment revealed an N-terminal AIM in Air1/2, the dynamics and stoichiometry of its interaction with the Mtr4 arch remain to be identified. However, it is possible that when Mtr4 is assembled into the TRAMP complex, the Air1/2 subunit binds the Mtr4 arch in order to block the access of other cofactors, such as Nop53 or Utp18. This would theoretically ensure that Mtr4 is only carrying out TRAMP complex-dependent activities when it is assembled within this complex. Interestingly, a recent structural study revealed that the Air2 and Nop53 AIMs interact with the Mtr4 arch in nearly identical conformations (Falk *et al.*, 2017b).

As previously stated, it is unclear as to why deleting *AIR1* was not successful, despite employing a variety of methods. However, the *air1* Δ strain from the Dharmacon™ Yeast Knockout Collection could be used as the starting point for generating cells that only express Mtr4 and one Trf4/5 subunit. Swapping out *AIR2* for the *hphMX4* cassette in this

*air1*Δ strain could be performed as previously. This homologous recombination method could also be employed for the deletion of *TRF4* and *TRF5*, although cells would need to be previously transformed with a plasmid encoding either Trf4 or Trf5 protein to prevent synthetic lethality. Alternatively, a newly created *air1*Δ, *air2*Δ strain could be mated with one of the various *trf4*Δ, *trf5*Δ background strains used in this study.

While I was not able to delete both *AIR1* and *AIR2* in concert with a loss of Trf4/5, I have shown that expressing subunits for only one TRAMP complex composition, as opposed to all three identified compositions, results in decreased growth. This growth deficiency was most markedly exhibited in a strain expressing only Mtr4, Air1, and *trf5*Δ98-117 subunits. Due to the disrupted Mtr4-Trf5 interaction, the Air1 subunit in these cells either holds the TRAMP complex together or these cells do not in fact contain assembled TRAMP complexes. In summary, while the essentiality of the TRAMP complex is still unknown, it is undoubtedly important for promoting the efficiency of RNA quality control.

CHAPTER 5
Final Conclusions and Perspectives

RNA Exosome Dysfunction Leads to Widespread Negative Cellular Effects

In summary, my collaborators and I have developed *S. cerevisiae* as a eukaryotic model system for performing introductory and straightforward analysis of PCH1b-associated mutations. This work has revealed that mutations linked to this disease are unlikely to result in a total loss of RNA exosome function, but they do significantly affect its stability and expression levels. Assessment of the yeast rrp40-W195R protein indicates that human EXOSC3-W238R ortholog is the most deleterious of the known PCH1b-associated mutations, due to its instability and negative impact on RNA exosome activity (Fasken, Losh *et al.*, 2017).

Optimal Assembly of the RNA Exosome is Promoted by Discriminating Mutant Subunits

Excitingly, this work has indicated that there is a mechanism for ensuring preferential incorporation of wild-type subunits into the RNA exosome. The PCH1b-associated mutations that my collaborators and I have modeled result in the expression of proteins that contain only a single point mutation. We have shown that these single mutations do not prevent subunits from assembling into the RNA exosome nor do they completely abolish RNA exosome function. However, these mutated subunits do not assemble as efficiently into the complex and they are increasingly unstable in the presence of their wild-type counterparts. This instability is likely due to the fact that RNA exosome subunits are rapidly degraded whenever they are not included within the complex. However, it is unclear how mutant subunits are excluded in favor of wild-type subunits. Further studies are needed to determine if this mechanism for preferential assembly is carried out by currently unidentified RNA exosome assembly factors or if mutant subunits simply detach from the complex at a higher rate than wild-type subunits.

Regardless of the mechanistic basis, this novel indication that the RNA exosome is assembled as properly as possible is understandable. Clearly, optimizing this essential complex results in increased levels of functional, processed RNA substrates and decreased

levels of harmful RNA accumulation. This would lead to more efficient nuclear and cytoplasmic processes within an individual cell. However, it would also provide a more widespread benefit in multicellular organisms since the RNA exosome is conserved within the cells of all eukaryotes, as well as within most types of tissues, that have been currently assessed.

Yeast is a Useful Model for Studying PCH1b-Associated Mutations

Yeast has long been employed as a model eukaryotic organism since it is genetically similar to human cells, but easier to manipulate. Previously published work on PCH1b consists mainly of clinical studies, which identified the mutations linked with this disease (Wan *et al.*, 2012; Biancheri *et al.*, 2013; Rudnik-Schöneborn *et al.*, 2013; Schwabova *et al.*, 2013; Zanni *et al.*, 2013; Eggens *et al.*, 2014; Halevy *et al.*, 2014). However, these studies have provided little insight into the molecular effects of PCH1b-associated mutations. Our yeast model system has revealed that these mutations likely affect interactions with other proteins and overall stability of the RNA exosome. A similar system and set of assays would likely be beneficial for the molecular characterization of other human disorders linked to mutations within the RNA exosome or its cofactors. While yeast is useful for initial characterization of PCH1b-associated mutations, multicellular models will be required for future studies, especially for determining the cause behind the tissue-specificity of patient phenotypes.

The Molecular Basis for Tissue-Specific Phenotypes of PCH1b Needs to be Elucidated

My collaborators and I have shown that *EXOSC3/rrp40* mutations associated with PCH1b disrupt the efficiency of the RNA exosome. The essentiality and ubiquitous nature of this complex, both in terms of cellular location and prevalence within many types of cells, provides some explanation as to why these subunit mutations might result in such serious phenotypes. Yet this does not necessarily explain why these symptoms are so tissue-specific. The levels of RNA exosome expression within all types of mammalian cells are not

known. However, RNA exosome subunit expression is comparable in cerebellar Purkinje cells, cerebellar cortex neurons, and hippocampal neurons, which indicates a similar prevalence of the RNA exosome between different regions of the brain (Uhlén *et al.*, 2015).

One explanation behind this phenotypic tissue-specificity of PCH1b-associated mutations is that changing these EXOSC3/Rrp40 residues affects both the expression levels and stability of the subunit, as well as the overall RNA exosome complex. Therefore, the characteristic brain and neural phenotypes of PCH1b, as well as other types of PCH, could be directly associated with a reduction in RNA exosome prevalence and efficiency within these tissues. However, the RNA exosome is present and significantly expressed within most, if not all, mammalian tissues (Uhlén *et al.*, 2015). Therefore, PCH1b-associated mutations would theoretically affect RNA exosome levels throughout the body. Why would a general reduction in RNA exosome levels specifically affect brain structure more than that of skin or bones?

While further studies are needed, I can propose several hypotheses for this question. First, it is possible that maintaining RNA exosome activity is most important in tissues with high rates of ATP usage and/or transcription in order to rapidly process premature transcripts and clear unnecessary transcripts. This would correlate with the significant brain, nervous system, and muscular defects of PCH1b patients, as neurons and myocytes utilize more ATP than many other types of cells (Rolfe and Brown, 1997). Moreover, while neurons are present throughout the body, they are most prevalent within brain tissue. Robust and tightly controlled transcription is critical for neuronal integrity (Greer and Greenberg, 2008).

Second, it is possible that maintaining RNA exosome activity is most important in the tissues that arise early in embryogenesis. The nervous system begins to form well before other organ systems (Spemann and Mangold, 1924). Interestingly, the development of the nervous system is preceded by a period of increased RNA transcription from embryonic genes, whereas only maternal RNA is used for the earliest stages of development

(Bachvarova *et al.*, 1966). This would result in the expression of PCH1b-associated EXOSC3 variants and therefore, faulty RNA exosome complexes, during brain and spinal cord formation, perhaps resulting in the significant brain abnormalities that characterize this disease.

Finally, it is possible that RNA exosome subunits interact with currently unknown, tissue-specific cofactors within certain cells. PCH1b-associated mutations may disrupt interactions with such cofactors, resulting in phenotypes that are most strongly associated with those tissues. Moreover, RNA exosome cofactors may undergo tissue-specific modifications that could further affect interactions with PCH1b-associated EXOSC3 mutants. For example, the nuclear RNA exosome cofactor, MPP6, co-immunoprecipitates with wild-type EXOSC3 but not with EXOSC3-W238R (Falk *et al.*, 2017a). Interestingly, MPP6 is known to be phosphorylated (Matsumoto-Taniura *et al.*, 1996). Perhaps this protein modification could influence the tissue-specific phenotypes that are associated with PCH1b if MPP6 is unable to interact with this mutant RNA exosome subunit. Further studies, including the use of multicellular models, will need to be performed in order to provide more insight into the tissue-specific consequences that result from the expression of mutant RNA exosome subunits.

TRAMP Complex Subunit Interactions are Important for Maintaining Its Function

In addition to my work on the RNA exosome, I have characterized a short region of Trf4/5 that is important for TRAMP complex assembly. This area of twenty nucleotides is essentially the only conserved sequence in the N-terminus of these TRAMP complex subunits and is required for their interaction with Mtr4. The deletion of this N-terminal 20-mer impairs complete assembly of the TRAMP complex and has a specific effect on the accumulation of 3' extended snoRNA (Losh, King *et al.*, 2015). I have also shown that the termini of Trf4/5 are not required for viability, although they appear to be functionally important.

The Direct Mtr4-Trf4/5 Interaction is Important but Not Essential

Cells expressing variants of Trf4/5 that lack the N-terminal Mtr4-interaction site remain viable, with only slight growth deficiencies. However, loss of this interaction negatively impacts snoRNA biogenesis. My results confirm that a TRAMP complex lacking the Mtr4-Trf4/5 interaction is not able to efficiently prepare precursor snoRNA substrates for the RNA exosome. Moreover, I have shown that no specific class of snoRNA is more affected by loss of this interaction than others. While other types of RNA accumulated as a result of a lack of interaction between Mtr4 and Trf4/5, snoRNA species were the most affected. It is currently unclear why snoRNA species are more affected than other known substrates of the TRAMP complex, although it is possible that this is simply due to their significant abundance in the nucleus.

Loss of interaction between the two catalytic subunits of this complex is not lethal and might seem to be an indication that the TRAMP complex is not essential. However, TRAMP complex assembly may be preserved by the Air1/2 subunit, which interacts with both Mtr4 and Trf4/5 (Wyers *et al.*, 2005; Houseley and Tollervey, 2006; Holub *et al.*, 2012; Falk *et al.*, 2014; Losh, King *et al.*, 2015). Specifically, Air1/2 may hold the other two subunits in close enough proximity that Mtr4 can still receive a polyadenylated substrate from Trf4/5 and prepare it for degradation by the RNA exosome. While I was not able to jointly delete *AIR1* and *AIR2* in a *trf4Δ*, *trf5Δ* background, I have shown that expression of just one possible TRAMP complex composition negatively affects cellular growth.

The TRAMP Complex May Not Be Essential for Life

This work has indicated that maintaining the Mtr4-Trf4/5 interaction is not essential for viability. Moreover, a double deletion of *AIR1* and *AIR2* is not synthetic lethal (Inuo *et al.*, 2000). As previously stated, these two findings could easily support the hypothesis that the TRAMP complex is not essential. However, it is possible that disrupting the Mtr4-Trf4/5 interaction in an *air1Δ*, *air2Δ* background is synthetic lethal (**Figure 5.1**). This would indicate

that only the interaction between the two catalytic subunits of the TRAMP complex is required for cellular viability. Therefore, Air1/2 may have been conserved as beneficial, but unnecessary, components of the TRAMP complex. One caveat to this hypothesis is that Air1/2 are believed to bring substrates to Trf4/5, which cannot bind RNA on their own (Wyers *et al.*, 2005; Fasken *et al.*, 2011). Interestingly, the mammalian ortholog of Trf4, PAPD5, can bind RNA directly but it may require the aid of other proteins to recognize its targets (Rammelt *et al.*, 2011). Furthermore, Mtr4 can bind RNA but this function is thought to be dispensable for TRAMP complex activity (Jackson *et al.*, 2010; Weir *et al.*, 2010). However, the intricacies of the interactions between TRAMP subunits, substrates, and other players of the RNA exosome pathway remain largely uncharacterized.

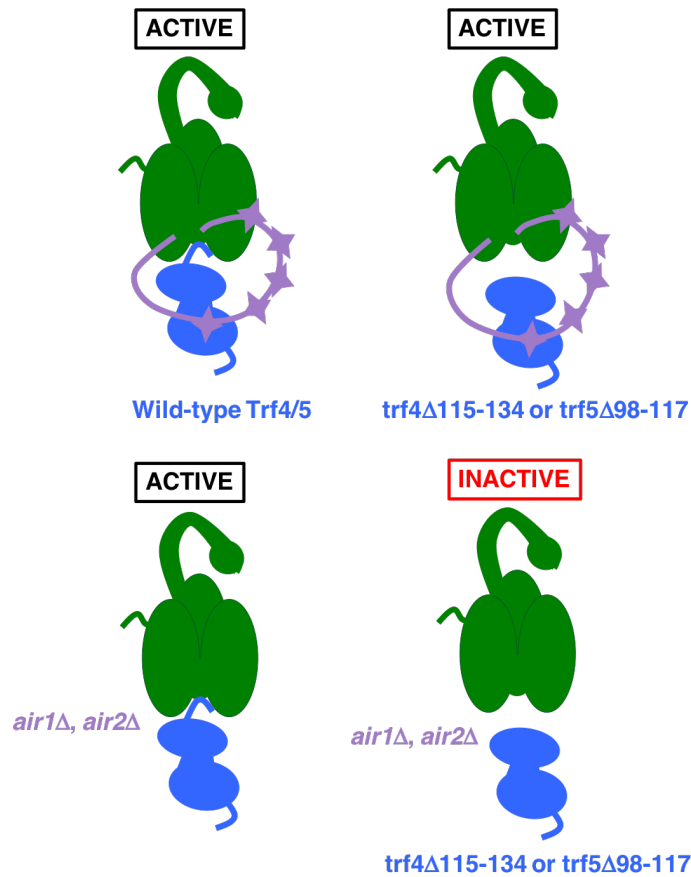


Figure 5.1 Model of TRAMP complex activity when specific subunit interactions are lost. While TRAMP complex activity is obviously maintained in the presence of all subunits and subunit interactions (top left), it may also be maintained as long as Mtr4 still directly interacts with Trf4/5 (bottom left) or Air1/2 is present to hold Mtr4 and Trf4/5 together if they can no longer directly interact (top right). However, if no Air1/2 subunit is present to hold the two catalytic subunits together when the Mtr4-Trf4/5 interaction has been lost, the TRAMP complex would no longer exist as a functional cofactor of the RNA exosome (bottom right). Further studies are needed to determine if this final scenario is synthetic lethal in cells. If not, this would indicate that TRAMP complex activity is not required for life.

My discovery of the N-terminal Air1/2 AIM, which allows for interaction with Mtr4, provides the possibility that Air1/2 can promote the TRAMP complex-dependent functions of Mtr4. Specifically, interaction between Mtr4 and the Air1/2 AIM may prevent additional interactions with Mtr4 cofactors that are involved in TRAMP complex-independent pathways. However, this is evidently not an essential activity due to the viability of *air1* Δ , *air2* Δ cells.

In addition to the two possible polymerase subunits and two possible RNA-binding subunits that have been conserved in yeast after the ancestral whole-genome duplication, characterizing the TRAMP complex is further convoluted by the fact that all of the subunits have TRAMP complex-independent functions. However, my work has clearly shown that maintaining complete TRAMP complex formation is beneficial for the RNA exosome-dependent pathway of 3' to 5' RNA processing and degradation. Specifically, efficient snoRNA biogenesis is dependent upon the interaction of Mtr4 and Trf4/5 within the TRAMP complex.

CONCLUDING REMARKS

The work presented in this dissertation has advanced our understanding of the assembly of the nuclear RNA exosome machinery. These findings have helped elucidate the molecular basis of the severe human disease, PCH1b, and identified specific subunit interaction sites within the TRAMP complex that are important for snoRNA biogenesis and the degradation of RNA substrates by the RNA exosome. The formation of these complexes has likely been conserved throughout eukaryotes, allowing for the use of *S. cerevisiae* as a model system for both genetic and biochemical studies. Further characterization of PCH1b-associated mutations, using both yeast and other model systems, will hopefully help further elucidate the basis of this serious neurodegenerative disorder. Additionally, continued characterization of the TRAMP complex will provide more mechanistic insight into its function and the reasons behind the conservation of its subunits throughout eukaryotic evolution, as well as after the yeast whole-genome duplication.

BIBLIOGRAPHY

- Agamy O, Ben Zeev B, Lev D, Marcus B, Fine D, Su D, Narkis G, Ofir R, Hoffmann C, Leshinsky-Silver E, Flusser H, Sivan S, Söll D, Lerman-Sagie T, Birk OS. **Mutations disrupting selenocysteine formation cause progressive cerebello-cerebral atrophy.** *Am J Hum Genet.* 2010; 87(4): 538-44.
- Ahmed MY, Chioza BA, Rajab A, Schmitz-Abe K, Al-Khayat A, Al-Turki S, Baple EL, Patton MA, Al-Memar AY, Hurles ME, Partlow JN, Hill RS, Evrony GD, Servattalab S, Markianos K, Walksh CA, Crosby AH, Mochida GH. **Loss of *PCLO* function underlies pontocerebellar hypoplasia type III.** *Neurology.* 2015; 84(17): 1745-50.
- Akizu N, Cantagrel V, Schroth J, Cai N, Vaux K, McCloskey D, Naviaux RK, Van Vleet J, Fenstermaker AG, Silhavy JL, Scheliga JS, Toyama K, Morisaki H, Sonmez FM, Celep F, Oraby A, Zaki MS, Al-Baradie R, Fageih EA, Saleh MA, Spencer E, Rosti RO, Scott E, Nickerson E, Gabriel S, Morisaki T, Holmes EW, Gleeson JG. ***AMPD2* regulates GTP synthesis and is mutated in a potentially treatable neurodegenerative brainstem disorder.** *Cell.* 2013; 154(3): 505-17.
- Allmang C, Petfalski E, Podtelejnikov A, Mann M, Tollervey D, Mitchell P. **The yeast exosome and human PM-Scl are related complexes of 3' → 5' exonucleases.** *Genes Dev.* 1999; 13(16): 2148-58.
- Allmang C, Kufel J, Chanfreau G, Mitchell P, Petfalski E, Tollervey D. **Functions of the exosome in rRNA, snoRNA and snRNA synthesis.** *EMBO J.* 1999; 18(19): 5399-410.
- Allmang C, Mitchell P, Petfalski E, Tollervey D. **Degradation of ribosomal RNA precursors by the exosome.** *Nucleic Acids Res.* 2000; 28(8): 1684-91.

- Araki Y, Takahashi S, Kobayashi T, Kajihō H, Hoshino S, Katada T. **Ski7p G protein interacts with the exosome and the Ski complex for 3'-to-5' mRNA decay in yeast.** *EMBO J.* 2001; 20(17): 4684-93.
- Astuti D, Morris MR, Cooper WN, Staals RH, Wake NC, Fews GA, Gill H, Gentle D, Shuib S, Ricketts CJ, Cole T, van Essen AJ, van Lingen RA, Neri G, Opitz JM, Rump P, Stolte-Dijkstra I, Müller F, Pruijn GJ, Latif F, Maher ER. **Germline mutations in *DIS3L2* cause Perlman syndrome of overgrowth and Wilms tumor susceptibility.** *Nat Genet.* 2012; 44(3): 277-84.
- Bachvarova R, Davidson EH, Allfrey VG, Mirsky AE. **Activation of RNA synthesis associated with gastrulation.** *Proc Natl Acad Sci USA.* 1996; 55(2): 358-65.
- Battini R, D'Arrigo S, Cassandrini D, Guzzetta A, Fiorillo C, Pantaleoni C, Romano A, Alfei E, Cioni G, Santorelli FM. **Novel mutations in *TSEN54* in pontocerebellar hypoplasia type 2.** *J Child Neurol.* 2014; 29(4): 520-5.
- Belle A, Tanay A, Bitincka L, Shamir R, O'Shea EK. **Quantification of protein half-lives in the budding yeast proteome.** *Proc Natl Acad Sci USA.* 2006; 103(35): 13004-9.
- Berndt H, Harnisch C, Rammelt C, Stöhr N, Zirkel A, Dohm JC, Himmelbauer H, Tavanez JP, Hüttelmaier S, Wahle E. **Maturation of mammalian H/ACA box snoRNAs: PAPD5-dependent adenylation and PARN-dependent trimming.** *RNA.* 2012; 18(5): 958-72.
- Bernstein J, Patterson DN, Wilson GM, Toth EA. **Characterization of the essential activities of *Saccharomyces cerevisiae* Mtr4p, a 3'→5' helicase partner of the nuclear exosome.** *J Biol Chem.* 2008; 283(8): 4930-42.

- Bernstein J, Ballin JD, Patterson DN, Wilson GM, Toth EA. **Unique properties of the Mtr4p-poly(A) complex suggest a role in substrate targeting.** *Biochemistry*. 2010; 49(49): 10357-70.
- Biancheri R, Cassandrini D, Pinto F, Trovato R, Di Rocco M, Mirabelli-Badenier M, Pedemonte M, Panicucci C, Trucks H, Sander T, Zara F, Rossi A, Striano P, Minetti C, Santorelli FM. **EXOSC3 mutations in isolated cerebellar hypoplasia and spinal anterior horn involvement.** *J Neurol*. 2013; 260(7): 1866-70.
- Bjornsti MA, Wang JC. **Expression of yeast DNA topoisomerase I can complement a conditional-lethal DNA topoisomerase I mutation in *Escherichia coli*.** *Proc Natl Acad Sci USA*. 1987; 84(24): 8971-5.
- Boczonadi V, Muller JS, Pyle A, Munkley J, Dor T, Quartararo J, Ferrero I, Karcagi V, Giunta M, Polvikoski T, Birchall D, Princzinger A, Cinnamon Y, Lützkendorf S, Piko H, Reza M, Florez L, Santibanez-Koref M, Griffin H, Schuelke M, Elpeleg O, Kalaydjieva L, Lochmüller H, Elliot DJ, Chinnery PF, Edvardson S, Horvath R. **EXOSC8 mutations alter mRNA metabolism and cause hypomyelination with spinal muscular atrophy and cerebellar hypoplasia.** *Nat Commun*. 2014; 5: 4287.
- Bonneau F, Basquin J, Ebert J, Lorentzen E, Conti E. **The yeast exosome functions as a macromolecular cage to channel RNA substrates for degradation.** *Cell*. 2009; 139(3): 547-59.
- Bousquet-Antonelli C, Presutti C, Tollervey D. **Identification of a regulated pathway for nuclear pre-mRNA turnover.** *Cell*. 2000; 102(6): 765-75.
- Brachmann CB, Davies A, Cost GJ, Caputo E, Li J, Hieter P, Boeke JD. **Designer deletion strains derived from *Saccharomyces cerevisiae* S288C: a useful set of strains and plasmids for PCR-mediated gene disruption and other applications.** *Yeast*. 1998; 14: 115-32.

Breuss MW, Sultan T, James KN, Rosti RO, Scott E, Musaev D, Furia B, Reis A, Sticht H, Al-Owain M, Alkuraya FS, Reuter MS, Abou Jamra R, Trotta CR, Gleeson JG.

Autosomal-recessive mutations in the tRNA splicing endonuclease subunit

TSEN15 cause pontocerebellar hypoplasia and progressive microcephaly. *Am*

J Hum Genet. 2016; 99(1): 228-35. Erratum in: *Am J Hum Genet.* 2016; 99(3): 785.

Briggs MW, Burkard KT, Butler JS. **Rrp6p, the yeast homologue of the human PM-Scl**

100-kDa autoantigen, is essential for efficient 5.8S rRNA 3' end formation. *J*

Biol Chem. 1998; 273(21): 13255-63.

Brill SJ, DiNardo S, Voelkel-Meiman K, Sternglanz R. **Need for DNA topoisomerase**

activity as a swivel for DNA replication for transcription of ribosomal RNA.

Nature. 1987; 326(6111): 414-6.

Brouwer R, Allmang C, Raijmakers R, van Aarssen Y, Egberts WV, Petfalski E, van Venrooij

WJ, Tollervey D, Pruijn GJ. **Three novel components of the human exosome. *J***

Biol Chem. 2001; 276(9): 6177-84.

Brown JT, Bai X, Johnson AW. **The yeast antiviral proteins Ski2p, Ski3p, and Ski8p exist**

as a complex *in vivo*. *RNA.* 2000; 6(3): 449-57.

Budde BS, Namavar Y, Barth PG, Poll-Thé BT, Nürnberg G, Becker C, van Ruissen F,

Weterman MA, Fluiters K, te Beek ET, Aronica E, van der Knaap MS, Höhne W, Toliai

MR, Crow YJ, Steinling M, Voit T, Roelenso F, Brussel W, Brockmann K, Kyllerman

M, Boltshauser E, Hammersen G, Willemsen M, Basel-Vanagaite L, Krägeloh-Mann

I, de Vries LS, Sztriha L, Muntoni F, Ferrie CD, Battini R, Hennekam RC, Grillo E,

Beemer FA, Stoets LM, Wollnik B, Nürnberg P, Baas F. **tRNA splicing**

endonuclease mutations cause pontocerebellar hypoplasia. *Nat Genet.* 2008;

40(9): 1113-8.

- Bühler M, Haas W, Gygi SP, Moazed D. **RNAi-dependent and -independent RNA turnover mechanisms contribute to heterochromatic gene silencing.** *Cell.* 2007; 129(4): 707-21.
- Büttner K, Wenig K, Hopfner KP. **Structural framework for the mechanism of archaeal exosomes in RNA processing.** *Mol Cell.* 2005; 20(3): 461-71.
- Byrne KP, Wolfe KH. **The Yeast Gene Order Browser: combining curated homology and syntenic context reveals gene fate in polyploid species.** *Genome Res.* 2005; 15(10): 1456-61.
- Cambridge SB, Gnad F, Nguyen C, Bermejo JL, Krüger M, Mann M. **Systems-wide proteomic analysis in mammalian cells reveals conserved, functional protein turnover.** *J Proteome Res.* 2011; 10(12): 5275-84.
- Caponigro G, Muhlrud D, Parker R. **A small segment of the MAT alpha 1 transcript promotes mRNA decay in *Saccharomyces cerevisiae*: a stimulatory role for rare codons.** *Mol Cell Biol.* 1993; 13(9): 5141-8.
- Carroll KL, Pradhan DA, Granek JA, Clarke ND, Corden JL. **Identification of *cis* elements directing termination of yeast nonpolyadenylated snoRNA transcripts.** *Mol Cell Biol.* 2004; 24(14): 6241-52.
- Castaño IB, Heath-Pagliuso S, Sadoff BU, Fitzhugh DJ, Christman MF. **A novel family of TRF (DNA topoisomerase I-related function) genes required for proper nuclear segregation.** *Nucleic Acids Res.* 1996; 24(12): 2404-10.
- Chen CY, Gherzi R, Ong SE, Chan EL, Raijmakers R, Pruijn GJ, Stoecklin G, Moroni C, Mann M, Karin M. **AU binding proteins recruit the exosome to degrade ARE-containing mRNAs.** *Cell.* 2001; 107(4): 451-64.

- Cheng ZF, Deutscher MP. **An important role for RNase R in mRNA decay.** *Mol Cell.* 2005; 17(2): 313-8.
- Chlebowski A, Tomecki R, López ME, Séraphin B, Dziembowski A. **Catalytic properties of the eukaryotic exosome.** *Adv Exp Med Biol.* 2010; 702: 63-78.
- Chu S, Archer RH, Zengel JM, Lindahl L. **The RNA of RNase MRP is required for normal processing of ribosomal RNA.** *Proc Natl Acad Sci USA.* 1994; 91(2): 659-63.
- Ciais D, Bohnsack MT, Tollervey D. **The mRNA encoding the yeast ARE-binding protein Cth2 is generated by a novel 3' processing pathway.** *Nucleic Acids Res.* 2008; 36(9): 3075-84.
- Cristodero M, Clayton CE. **Trypanosome MTR4 is involved in RNA processing.** *Nucleic Acids Res.* 2007; 35(20): 7023-30.
- de la Cruz J, Kressler D, Tollervey D, Linder P. **Dob1p (Mtr4p) is a putative ATP-dependent RNA helicase required for the 3' end formation of 5.8S rRNA in *Saccharomyces cerevisiae*.** *EMBO J.* 1998; 17(4): 1128-40.
- Delan-Forino C, Schneider C, Tollervey D. **Transcriptome-wide analysis of alternative routes for RNA substrates into the exosome complex.** *PLoS Genet.* 2017; 13(3): e1006699.
- Dhungel N. **tRNA splicing endonuclease: novel and essential function beyond tRNA splicing and subunit interactions.** Electronic Thesis or Dissertation. Ohio State University, 2012. *OhioLINK Electronic Theses and Dissertations Center.*
- Di Donato N, Neuhann T, Kahlert AK, Klink B, Hackmann K, Neuhann I, Novotna B, Schallner J, Krause C, Glass IA, Parnell SE, Benet-Pages A, Nissen AM, Berger W, Altmüller J, Thiele H, Weber BHF, Schrock E, Dobyns WB, Bier A, Rump A. **Mutations in *EXOSC2* are associated with a novel syndrome characterized by**

- retinitis pigmentosa, progressive hearing loss, premature aging, short stature, mild intellectual disability and distinctive gestalt.** *J Med Gen.* 2016; 53(6): 419-25.
- Ding L, Ley TJ, Larson DE, Miller CA, Koboldt DC, Welch JS, Ritchey JK, Young MA, Lamprecht T, McLellan MD, McMichael JF, Wallis JW, Lu C, Shen D, Harris CC, Dooling DJ, Fulton RS, Fulton LL, Chen K, Schmidt H, Kalicki-Veizer J, Magrini VJ, Cook L, McGrath SD, Vickery TL, Wendl MC, Heath S, Watson MA, Link DC, Tomasson MH, Shannon WD, Payton JE, Kulkarni S, Westervelt P, Walter MJ, Graubert TA, Mardis ER, Wilson RK, DiPersio JF. **Clonal evolution in relapsed acute myeloid leukemia revealed by whole-genome sequencing.** *Nature.* 2012; 481(7382): 506-10.
- Doma MK, Parker R. **Endonucleolytic cleavage of eukaryotic mRNAs with stalls in translation elongation.** *Nature.* 2006; 440(7083): 561-4.
- Donkervoort S, Müller J, Knierim E, Bharucha-Goebel D, Dyack S, Burns D, Hu Y, Baker L, Ezzo D, Scavina M, Foley A, Schülke M, Schülke M, Bönnemann C. **Recessive mutation in *EXOSC9* disrupts the exosome complex resulting in a novel form of cerebellar hypoplasia/atrophy with early motor neuronopathy.** *Neuromuscul Disord.* 2017; 27(S2): S176-7.
- D'Souza V, Summers MF. **How retroviruses select their genomes.** *Nat Rev Microbiol.* 2005; 3(8): 643-55.
- Dziembowski A, Lorentzen E, Conti E, Séraphin B. **A single subunit, Dis3, is essentially responsible for yeast exosome core activity.** *Nat Struct Mol Biol.* 2007; 14: 15-22.
- Edvardson S, Shaag A, Kolesnikova O, Gomori JM, Tarassov I, Einbinder T, Saada A, Elpeleg O. **Deleterious mutation in the mitochondrial arginyl-transfer RNA**

- synthetase gene is associated with pontocerebellar hypoplasia.** *Am J Hum Genet.* 2007; 81(4): 857-62.
- Edwards S, Li CM, Levy DL, Brown J, Snow PM, Campbell JL. **Saccharomyces cerevisiae DNA polymerase ϵ and polymerase σ interact physically and functionally, suggesting a role for polymerase ϵ in sister chromatid cohesion.** *Mol Cell Biol.* 2003; 23(8): 2733-48.
- Eggens VR, Barth PG, Niermeijer JM, Berg JN, Darin N, Dixit A, Fluss J, Foulds N, Fowler D, Hortobágyi T, Jacques T, King MD, Makrythanasis P, Máté A, Nicoll JA, O'Rourke D, Price S, Williams AN, Wilson L, Suri M, Sztriha L, Dijns-de Wissel MB, van Meegen MT, van Ruissen F, Aronica E, Troost D, Majoie CB, Marquering HA, Poll-Thé BT, Baas F. **EXOSC3 mutations in pontocerebellar hypoplasia type 1: novel mutations and genotype-phenotype correlations.** *Orphanet J Rare Dis.* 2014; 9: 23.
- Estévez AM, Kempf T, Clayton C. **The exosome of Trypanosoma brucei.** *EMBO J.* 2001; 20(14): 3831-9.
- Estévez AM, Lehner B, Sanderson CM, Ruppert T, Clayton C. **The roles of intersubunit interactions in exosome stability.** *J Biol Chem.* 2003; 278(37): 34943-51.
- Evguenieva-Hackenberg E, Walter P, Hochleitner E, Lottspeich F, Klug G. **An exosome-like complex in Sulfolobus solfataricus.** *EMBO Rep.* 2003; 4(9): 889-93.
- Fabre A, Charroux B, Martinez-Vinson C, Roquelaure B, Odul E, Sayar E, Smith H, Colomb V, Andre N, Hugot JP, Goulet O, Lacoste C, Sarles J, Royet J, Levy N, Badens C. **SKIV2L mutations cause syndromic diarrhea, or trichohepatoenteric syndrome.** *Am J Hum Genet.* 2012; 90: 689-92.
- Falk S, Weir JR, Hentschel J, Reichelt P, Bonneau F, Conti E. **The molecular architecture**

- of the TRAMP complex reveals the organization and interplay of its two catalytic activities.** *Mol Cell.* 2014; 55: 1-12.
- Falk S, Bonneau F, Ebert J, Kögel A, Conti E. **Mpp6 incorporation into the nuclear exosome contributes to RNA channeling through the Mtr4 helicase.** *Cell Rep.* 2017; 20(10): 2279-86.
- Falk S, Tants JN, Basquin J, Thoms M, Hurt E, Sattler M, Conti E. **Structural insights into the interaction of the nuclear exosome helicase Mtr4 with the preribosomal protein Nop53.** *RNA.* 2017; 23(12): 1780-7.
- Fang F, Hoskins J, Butler JS. **5-fluorouracil enhances exosome-dependent accumulation of polyadenylated rRNAs.** *Mol Cell Biol.* 2004; 24(24): 10766-76.
- Fasken MB, Leung SW, Banerjee A, Kodani MO, Chavez R, Bowman EA, Purohit MK, Rubinson ME, Rubinson EH, Corbett AH. **Air1 zinc knuckles 4 and 5 and a conserved IWRXY motif are critical for the function and integrity of the Trf4/5-Air1/2-Mtr4 polyadenylation (TRAMP) RNA quality control complex.** *J Biol Chem.* 2011; 286(43): 37429-45.
- Fasken MB, Larabee RN, Corbett AH. **Nab3 facilitates the function of the TRAMP complex in RNA processing via recruitment of Rrp6 independent of Nrd1.** *PLoS Genet.* 2015; 11(3): e1005044.
- Fasken MB, Losh JS, Leung SW, Brutus S, Avin B, Vaught JC, Potter-Birrel J, Craig T, Tsanova B, Conn GL, Millis-Lujan K, Corbett A, van Hoof A. **Insight into the RNA exosome complex through modeling pontocerebellar hypoplasia type 1b disease mutations in yeast.** *Genetics.* 2017; 205(1): 221-37.
- Feinstein M, Flusser H, Lerman-Sagie T, Ben-Zeev B, Lev D, Agamy O, Cohen I, Kadir R, Sivan S, Leshinsky-Silver E, Markus B, Birk OS. **VPS53 mutations cause**

- progressive cerebello-cerebral atrophy type 2 (PCCA2).** *J Med Genet.* 2014; 51(5): 303-8.
- Fox MJ, Gao H, Smith-Kinnaman WR, Liu Y, Mosley AL. **The exosome component Rrp6 is required for RNA polymerase II termination at specific targets of the Nrd1-Nab3 pathway.** *PLoS Genet.* 2015; 11(2): e1004999.
- Flynn RA, Almada AE, Zamudio JR, Sharp PA. **Antisense RNA polymerase II divergent transcripts are P-TEFb dependent and substrates for the RNA exosome.** *Proc Natl Acad Sci USA.* 2011; 108(26): 10460-5.
- Gatfield D, Izaurralde E. **Nonsense-mediated messenger RNA decay is initiated by endonucleolytic cleavage in *Drosophila*.** *Nature.* 2004; 429(6991): 575-8.
- Gellon L, Carson DR, Carson JP, Demple B. **Intrinsic 5'-deoxyribose-5-phosphate lyase activity in *Saccharomyces cerevisiae* Trf4 protein with a possible role in base excision DNA repair.** *DNA Repair (Amst).* 2008; 7(2): 187-98.
- Ghaemmaghami S, Huh WK, Bower K, Howson RW, Belle A, Dephoure N, O'Shea EK, Weissman JS. **Global analysis of protein expression in yeast.** *Nature.* 2003; 425(6959): 737-41.
- Giaever G, Chu AM, Ni L, Connelly C, Riles L, Véronneau S, Dow S, Lucau-Danila A, Anderson K, André B, Arkin AP, Astromoff A, El-Bakkoury M, Bangham R, Benito R, Brachat S, Campanaro S, Curtiss M, Davis K, Deutschbauer A, Entian KD, Flaherty P, Foury F, Garfinkel DJ, Gerstein M, Gotte D, Güldener U, Hegemann JH, Hempel S, Herman Z, Jaramillo DF, Kelly DE, Kelly SL, Kötter P, LaBonte D, Lamb DC, Lan N, Liang H, Liao H, Liu L, Luo C, Lussier M, Mao R, Menard P, Ooi SL, Revuelta JL, Roberts CJ, Rose M, Ross-Macdonald P, Scherens B, Schimmack G, Shafer B, Shoemaker DD, Sookhai-Mahadeo S, Storms RK, Strathern JN, Valle G, Voet M, Volckaert G, Wang CY, Ward TR, Wilhelmy J, Winzeler EA, Yang Y, Yen G,

- Youngman E, Yu K, Bussey H, Boeke JD, Snyder M, Philippsen P, Davis RW, Johnston M. **Functional profiling of the *Saccharomyces cerevisiae* genome.** *Nature*. 2002; 418(6896): 387-91.
- Gietz D and Schiestl RH. **Transforming yeast with DNA.** *Methods Mol Cell Biol*. 1995; 5: 255-69.
- Gillespie A, Gabunilas J, Jen JC, Chanfreau GF. **Mutations of EXOSC3/Rrp40p associated with neurological diseases impact ribosomal RNA processing functions of the exosome in *S. cerevisiae*.** *RNA*. 2017; 23(4): 466-72.
- Giunta M, Edvardson S, Xu Y, Schuelke M, Gomez-Duran A, Boczonadi V, Elpeleg O, Müller JS, Horvath R. **Altered RNA metabolism due to a homozygous *RBM7* mutation in a patient with spinal motor neuropathy.** *Hum Mol Genet*. 2016; 25(14): 2985-996.
- Goldstein AL, McCusker JH. **Three new dominant drug resistance cassettes for gene disruption in *Saccharomyces cerevisiae*.** *Yeast*. 1999; 15(14): 1541-53.
- Greer PL, Greenberg ME. **From synapse to nucleus: calcium-dependent gene transcription in the control of synapse development and function.** *Neuron*. 2008; 59(6): 846-60.
- Grzechnik P, Kufel J. **Polyadenylation linked to transcription termination directs the processing of snoRNA precursors in yeast.** *Mol Cell*. 2008; 32: 247-58.
- Halevy A, Lerer I, Cohen R, Kornreich L, Shuper A, Gamliel M, Zimerman BE, Korabi I, Meiner V, Straussberg R, Lossos A. **Novel *EXOSC3* mutation causes complicated hereditary spastic paraplegia.** *J Neurol*. 2014; 261(11): 2165-9.

- Hamill S, Wolin SL, Reinisch KM. **Structure and function of the polymerase core of TRAMP, a RNA surveillance complex.** *Proc Natl Acad Sci USA.* 2010; 107(34): 15045-50.
- Han J, van Hoof A. **The RNA exosome channeling and direct access conformations have distinct *in vivo* functions.** *Cell Rep.* 2016; 16(12): 3348-58.
- Hanada T, Weitzer S, Mair B, Bernreuther C, Wainger BJ, Ichida J, Hanada R, Orthofer M, Cronin SJ, Komnenovic V, Minis A, Sato F, Mimata H, Yoshimura A, Tamir I, Rainer J, Kofler R, Yaron A, Eggan KC, Woolf CJ, Glatzel M, Herbst R, Martinez J, Penninger JM. **CLP1 links tRNA metabolism to progressive motor-neuron loss.** *Nature.* 2013; 495(7442): 474-80.
- Haracska L, Johnson RE, Prakash L, Prakash S. **Trf4 and Trf5 proteins of *Saccharomyces cerevisiae* exhibit poly(A) RNA polymerase activity but no DNA polymerase activity.** *Mol Cell Biol.* 2005; 25(22): 10183-9.
- Harnisch C, Cuzic-Feltens S, Dohm JC, Götze M, Himmelbauer H, Wahle E. **Oligoadenylation of 3' decay intermediates promotes cytoplasmic mRNA degradation in *Drosophila* cells.** *RNA.* 2016; 22(3): 428-42.
- Hartley JL, Zachos NC, Dawood B, Donowitz M, Forman J, Pollitt RJ, Morgan NV, Tee L, Gissen P, Kahr WH, Knisely AS, Watson S, Chitayat D, Booth IW, Protheroe S, Murphy S, de Vries E, Kelly DA, Maher ER. **Mutations in *TTC37* cause trichohepatoenteric syndrome (phenotypic diarrhea of infancy).** *Gastroenterology.* 2010; 138: 2388-98.
- He F, Amrani N, Johansson MJ, Jacobson A. **Qualitative and quantitative assessment of the activity of the yeast nonsense-mediated mRNA decay pathway.** *Methods Enzymol.* 2008; 449: 127-47.

- Holub P, Lalakova J, Cerna H, Pasulka J, Sarazova M, Hrazdilova K, Arce MS, Hobor F, Stefl R, Vaňáčková S. **Air2p is critical for the assembly and RNA-binding of the TRAMP complex and the KOW domain of Mtr4p is crucial for exosome activation.** *Nuc Acids Res.* 2012; 40(12): 5679-93.
- Hoskins JW, Ibrahim A, Emmanuel MA, Manmiller SM, Wu Y, O'Neill M, Jia J, Collins I, Zhang M, Thomas JV, Rost LM, Das S, Parikh H, Haake JM, Matters GL, Kurtz RC, Bamlet WR, Klein A, Stolzenberg-Solomon R, Wolpin BM, Yarden R, Wang Z, Smith J, Olson SH, Andresson T, Petersen GM, Amundadottir LT. **Functional characterization of a chr13q22.1 pancreatic cancer risk locus reveals long-range interaction and allele-specific effects on *DIS3* expression.** *Hum Mol Genet.* 2016; 25(21): 4726-38.
- Houseley J, Tollervey D. **Yeast Trf5p is a nuclear poly(A)polymerase.** *EMBO Rep.* 2006; 7(2) 205-11.
- Houseley J, Kotovic K, El Hage A, Tollervey D. **Trf4 targets ncRNAs from telomeric and rDNA spacer regions and functions in rDNA copy number control.** *EMBO J.* 2007; 26(24): 4996-5006.
- Houseley J, Tollervey D. **Repeat expansion in the budding yeast ribosomal DNA can occur independently of the canonical homologous recombination machinery.** *Nucleic Acids Res.* 2011; 39(20): 8778-91.
- Hrossova D, Sikorsky T, Potesil D, Bartosovic M, Pasulka J, Zdrahal Z, Stefl R, Vaňáčková S. **RBM7 subunit of the NEXT complex binds U-rich sequences and targets 3'-end extended forms of snRNAs.** *Nucleic Acids Res.* 2015; 43(8): 4236-48.
- Inoue K, Mizuno T, Wada K, Hagiwara M. **Novel RING finger proteins, Air1p and Air2p, interact with Hmt1p and inhibit the arginine methylation of Npl3p.** *J Biol Chem.* 2000; 275(42): 32793-9.

- Jackson RN, Klauer AA, Hintze BJ, Robinson H, van Hoof A, Johnson SJ. **The crystal structure of Mtr4 reveals a novel arch domain required for rRNA processing.** *EMBO J.* 2010; 29(13): 2205-16.
- Jacobs Anderson JS, Parker R. **The 3' to 5' degradation of yeast mRNAs is a general mechanism for mRNA turnover that requires the SKI2 DEVH box protein and 3' to 5' exonucleases of the exosome complex.** *EMBO J.* 1998; 17(5): 1497-506.
- Jia H, Wang X, Liu F, Guenther UP, Srinivasan S, Anderson JT, Jankowsky E. **The RNA helicase Mtr4p modulates polyadenylation in the TRAMP complex.** *Cell.* 2011; 145(6): 890-901.
- Jia H, Wang X, Anderson JT, Jankowsky E. **RNA unwinding by the Trf4/Air2/Mtr4 polyadenylation (TRAMP) complex.** *Proc Natl Acad Sci USA.* 2012; 109(19): 7292-7.
- Kadowaki T, Chen S, Hitomi M, Jacobs E, Kumagai C, Liang S, Schneider R, Singleton D, Wisniewska J, Tartakoff AM. **Isolation and characterization of *Saccharomyces cerevisiae* mRNA transport-defective (*mtr*) mutants.** *J Cell Biol.* 1994; 126(3): 649-59.
- Kadowaki T, Schneider R, Hitomi M, Tartakoff AM. **Mutations in nucleolar proteins lead to nucleolar accumulation of polyA+ RNA in *Saccharomyces cerevisiae*.** *Mol Biol Cell.* 1995; 6(9): 1103-10.
- Keller C, Woolcock K, Hess D, Bühler M. **Proteomic and functional analysis of the noncanonical poly(A) polymerase Cid14.** *RNA.* 2010; 16(6): 1124-9.
- Kellis M, Birren BW, Lander ES. **Proof and evolutionary analysis of ancient genome duplication in the yeast *Saccharomyces cerevisiae*.** *Nature.* 2004; 428(6983): 617-24.

- Klauer AA, van Hoof A. **Genetic interactions suggest multiple distinct roles of the arch and core helicase domains of Mtr4 in Rrp6 and exosome function.** *Nucleic Acids Res.* 2013; 41(1): 533-41.
- Klebe RJ, Ruddle FH. **Neuroblastoma: cell culture analysis of a differentiating stem cell system.** *J Cell Biol.* 1969; 43: 69a.
- Kress TL, Krogan NJ, Guthrie C. **A single SR-like protein, Npl3, promotes pre-mRNA splicing in budding yeast.** *Mol Cell.* 2008; 32(5): 727-34.
- Kulak NA, Pichler G, Paron I, Nagaraj N, Mann M. **Minimal, encapsulated proteomic-sample processing applied to copy-number estimation in eukaryotic cells.** *Nat Methods.* 2014; 11(3): 319-24.
- Kyrpides NC, Woese CR, Ouzounis CA. **KOW: a novel motif linking a bacterial transcription factor with ribosomal proteins.** *Trends Biochem Sci.* 1996; 21(11): 425-6.
- LaCava J, Houseley J, Saveanu C, Petfalski E, Thompson E, Jacquier A, Tollervey D. **RNA degradation by the exosome is promoted by a nuclear polyadenylation complex.** *Cell.* 2005; 121: 713-24.
- Lardelli RM, Schaffer AE, Eggens VR, Zaki MS, Grainger S, Sathe S, Van Nostrand EL, Schlachetzki Z, Rosti B, Akizu N, Scott E, Silhavy JL, Heckman LD, Rosti RO, Dikoglu E, Gregor A, Guemez-Gamboa A, Musaev D, Mande R, Widjaja A, Shaw TL, Markmiller S, Marin-Valencia I, Davies JH, de Meirleir L, Kayserili H, Altunoglu U, Freckmann ML, Warwick L, Chitayat D, Blaser S, Çağlayan AO, Bilguvar K, Per H, Fagerberg C, Christesen HT, Kibaek M, Aldinger KA, Manchester D, Matsumoto N, Muramatsu K, Saitsu H, Shiina M, Ogata K, Foulds N, Dobyns WB, Chi NC, Traver D, Spaccini L, Bova SM, Gabriel SB, Gunel M, Valente EM, Nassogne MC, Bennett EJ, Yeo GW, Baas F, Lykke-Andersen J, Gleeson JG. **Biallelic mutations in the 3'**

- exonuclease *TOE1* cause pontocerebellar hypoplasia and uncover a role in snRNA processing.** *Nat Genet.* 2017; 49(3): 457-64.
- Lauinger L, Diernfellner A, Falk S, Brunner M. **The RNA helicase FRH is an ATP-dependent regulator of CK1a in the circadian clock of *Neurospora crassa*.** *Nat Commun.* 2014; 5: 3598.
- Lebreton A, Tomecki R, Dziembowski A, Séraphin B. **Endonucleolytic RNA cleavage by a eukaryotic exosome.** *Nature.* 2008; 456(7224): 993-6.
- Lee NN, Chalamcharla VR, Reyes-Turcu F, Mehta S, Zofall M, Balachandran V, Dhakshnamoorthy J, Taneja N, Yamanaka S, Zhou M, Grewel SI. **Mtr4-like protein coordinates nuclear RNA processing for heterochromatin assembly and for telomere maintenance.** *Cell.* 2013; 155(5): 1061-74.
- Lejeune F, Li X, Maquat LE. **Nonsense-mediated mRNA decay in mammalian cells involves decapping, deadenylation, and exonucleolytic activities.** *Mol Cell.* 2003; 12(3): 675-87.
- Liang S, Hitomi M, Hu YH, Liu Y, Tartakoff AM. **A DEAD-box-family protein is required for nucleocytoplasmic transport of yeast mRNA.** *Mol Cell Biol.* 1996; 16(9): 5139-46.
- Liu JJ, Bratkowski MA, Liu X, Niu CY, Ke A, Wang HW. **Visualization of distinct substrate-recruitment pathways in the yeast exosome by EM.** *Nat Struct Mol Biol.* 2014; 21(1): 95-102.
- Liu Q, Greimann JC, Lima CD. **Reconstitution, activities, and structure of the eukaryotic RNA exosome.** *Cell.* 2006; 127: 1223-7.
- Longley DB, Harkin DP, Johnston PG. **5-fluorouracil: mechanisms of action and clinical strategies.** *Nat Rev Cancer.* 2003; 3(5): 330-8.

- Lorentzen E, Walter P, Fribourg S, Evguenieva-Hackenberg E, Klug G, Conti E. **The archaeal exosome core is a hexameric ring structure with three catalytic subunits.** *Nat Struct Mol Biol.* 2005; 12(7): 575-81.
- Lorentzen E, Dziembowski A, Lindner D, Séraphin B, Conti E. **RNA channeling by the archaeal exosome.** *EMBO Rep.* 2007; 8(5): 470-6.
- Losh JS, King AK, Bakelar J, Taylor L, Loomis J, Rosenzweig JA, Johnson SJ, van Hoof A. **Interaction between the RNA-dependent ATPase and poly(A) polymerase subunits of the TRAMP complex is mediated by short peptides and important for snoRNA processing.** *Nuc Acids Res.* 2015; 43(3): 1848-58.
- Losh JS, van Hoof A. **Gateway arch to the RNA exosome.** *Cell.* 2015; 162(5): 940-1.
- Lubas M, Christensen MS, Kristiansen MS, Domanski M, Falkenby LG, Lykke-Andersen S, Andersen JS, Dziembowski A, Jensen TH. **Interaction profiling identifies the human nuclear exosome targeting complex.** *Mol Cell.* 2011; 43: 624-37.
- Lubas M, Damgaard CK, Tomecki R, Cysewski D, Jensen TH, Dziembowski A. **Exonuclease hDIS3L2 specifies an exosome-independent 3'-5' degradation pathway of human cytoplasmic mRNA.** *EMBO J.* 2013; 32(13): 1855-68.
- Lum PY, Armour CD, Stepaniants SB, Cavet G, Wolf MK, Butler JS, Hinshaw JC, Garnier P, Prestwich GD, Leonardson A, Garrett-Engele P, Rush CM, Bard M, Schimmack G, Phillips JW, Roberts CJ, Shoemaker DD. **Discovering modes of action for therapeutic compounds using a genome-wide screen of yeast heterozygotes.** *Cell.* 2004; 116(1): 121-37.
- Makino DL, Baumgartner M, Conti E. **Crystal structure of an RNA-bound 11-subunit eukaryotic exosome complex.** *Nature.* 2013; 495: 70-5.

- Malecki M, Viegas SC, Carneiro T, Golik P, Dressaire C, Ferreira MG, Arraiano CM. **The exoribonuclease Dis3L2 defines a novel eukaryotic RNA degradation pathway.** *EMBO J.* 2013; 32(13): 1842-54.
- Malet H, Topf M, Clare DK, Ebert J, Bonneau F, Basquin J, Drazkowska K, Tomecki R, Dziembowski A, Conti E, Sibil HR, Lorentzen E. **RNA channeling by the eukaryotic exosome.** *EMBO Rep.* 2010; 11(12): 936-42.
- Marquardt S, Hazelbaker DZ, Buratowski S. **Distinct RNA degradation pathways and 3' extensions of yeast non-coding RNA species.** *Transcription.* 2011; 2(3): 145-54.
- Matsumoto-Taniura N, Pirolet F, Monroe R, Gerace L, Westendorf JM. **Identification of novel M phase phosphoproteins by expression cloning.** *Mol Biol Cell.* 1996; 7(9): 1455-69.
- Mayer SA, Dieckmann CL. **The yeast *CBP1* gene produces two differentially regulated transcripts by alternative 3'-end formation.** *Mol Cell Biol.* 1989; 9(10): 4161-9.
- Meaux S, van Hoof A. **Yeast transcripts cleaved by an internal ribozyme provide new insight into the role of the cap and poly(A) tail in translation and mRNA decay.** *RNA.* 2006; 12(7): 1323-37.
- Meola N, Domanski M, Karadoulama E, Chen Y, Gentil C, Pultz D, Vitting-Seerup K, Lykke-Andersen S, Andersen JS, Sandelin A, Jensen TH. **Identification of a nuclear exosome decay pathway for processed transcripts.** *Mol Cell.* 2016; 64(3): 520-33.
- Milligan L, Decourty L, Saveanu C, Rappsilber J, Ceulemans H, Jacquier A, Tollervey D. **A yeast exosome cofactor, Mpp6, functions in RNA surveillance and in the degradation of noncoding RNA transcripts.** *Mol Cell Biol.* 2008; 28(17): 5446-57.

- Millonigg S, Minasaki R, Nousch M, Eckmann CR. **GLD-4 mediated translational activation regulates the size of the proliferative germ cell pool in the adult *C. elegans* germ line.** *PLoS Genet.* 2014; 10(9): e1004647. Erratum in: *PLoS Genet.* 2016; 12(2): e1005862. Novak J [added].
- Mitchell P, Petfalski E, Tollervey D. **The 3' end of yeast 5.8S rRNA is generated by an exonuclease processing mechanism.** *Genes Dev.* 1996; 10(4): 502-13.
- Mitchell P, Petfalski E, Schevchenko A, Mann M, Tollervey D. **The exosome: a conserved eukaryotic RNA processing complex containing multiple 3' → 5' exoribonucleases.** *Cell.* 1997; 91(4): 457-66.
- Mitchell P, Petfalski E, Houalla R, Podtelejnikov A, Mann M, Tollervey D. **Rrp47p is an exosome-associated protein required for the 3' processing of stable RNAs.** *Mol Cell Biol.* 2003; 23(19): 6982-92.
- Mitchell P, Tollervey D. **An NMD pathway in yeast involving accelerated deadenylation and exosome-mediated 3' → 5' degradation.** *Mol Cell.* 2003; 11(5): 1405-13.
- Mochida GH, Ganesh VS, de Michelena MI, Dias H, Atabay KD, Kathrein KL, Huang HT, Hill RS, Felie JM, Rakiec D, Gleason D, Hill AD, Malik AN, Barry BJ, Partlow JN, Tan WH, Glader LJ, Barkovich AJ, Dobyns WB, Zon LI, Walsh CA. **CHMP1A encodes an essential regulator of BMI1-INK4A in cerebellar development.** *Nat Genet.* 2012; 44(11): 1260-4.
- Molleston JM, Sabin LR, Moy RH, Menghani SV, Rausch K, Gordesky-Gold B, Hopkins KC, Zhou R, Jensen TH, Wilusz JE, Cherry S. **A conserved virus-induced cytoplasmic TRAMP-like complex recruits the exosome to target viral RNA for degradation.** *Genes Dev.* 2016; 30(14): 1658-70.

- Moreira MC, Klur S, Watanabe M, Németh AH, Le Ber I, Moniz JC, Tranchant C, Aubourg P, Tazir M, Schöls L, Pandolfo M, Schulz JB, Pouget J, Calvas P, Shizuka-Ikeda M, Shoji M, Tanaka M, Izatt L, Shaw CE, M'Zahem A, Dunne E, Bomont P, Benhassine T, Bouslam N, Stevanin G, Brice A, Guimarães J, Mendonça P, Barbot C, Coutinho P, Sequeiros J, Dürr A, Warter JM, Koenig M. **Senataxin, the ortholog of a yeast RNA helicase, is mutant in ataxia-ocular apraxia 2.** *Nat Genet.* 2004; 36(3): 225-7.
- Nakamura R, Takeuchi R, Takata K, Shimanouchi K, Abe Y, Kanai Y, Ruike T, Ihara A, Sakaguchi K. **TRF4 is involved in polyadenylation of snRNAs in *Drosophila melanogaster*.** *Mol Cell Biol.* 2008; 28(21): 6620-31.
- Namavar Y, Chitayat D, Barth PG, van Ruissen F, de Wissel MB, Poll-Thé BT, Silver R, Baas F. **TSEN54 mutations cause pontocerebellar hypoplasia type 5.** *Eur J Hum Genet.* 2011; 19(6): 724-6.
- Oddone A, Lorentzen E, Basquin J, Gasch A, Rybin V, Conti E, Sattler M. **Structural and biochemical characterization of the yeast exosome component Rrp40.** *EMBO Rep.* 2007; 8(1): 63-9.
- O'Hara EB, Chekanova JA, Ingle CA, Kushner ZR, Peters E, Kushner SR. **Polyadenylation helps regulate mRNA decay in *Escherichia coli*.** *Proc Natl Acad Sci USA.* 1995; 92(6): 1807-11.
- Orban TI, Izaurralde E. **Decay of mRNAs targeted by RISC requires XRN1, the Ski complex, and the exosome.** *RNA.* 2005; 11(4): 459-69.
- Pefanis E, Wang J, Rothschild G, Lim J, Chao J, Rabadan R, Economides AN, Basu U. **Noncoding RNA transcription targets AID to divergently transcribed loci in B cells.** *Nature.* 2014; 514(7522): 389-93.

- Porrúa O, Libri D. **A bacterial-like mechanism for transcription termination by the Sen1p helicase in budding yeast.** *Nat Struct Mol Biol.* 2013; 20(7): 884-91.
- Preker P, Nielsen J, Kammler S, Lykke-Andersen S, Christensen MS, Mapendano CK, Schierup MH, Jensen TH. **RNA exosome depletion reveals transcription upstream of active human promoters.** *Science.* 2008; 322(5909): 1851-4.
- Rammelt C, Bilen B, Zavolan M, Keller W. **PAPD5, a noncanonical poly(A) polymerase with an unusual RNA-binding motif.** *RNA.* 2011; 17(9): 1737-46.
- Reimer G, Scheer U, Peters JM, Tan EM. **Immunolocalization and partial characterization of a nucleolar autoantigen (PM-Scl) associated with polymyositis/scleroderma overlap syndromes.** *J Immunol.* 1986; 137(12): 3802-8.
- Renbaum P, Kellerman E, Jaron R, Geiger D, Segel R, Lee M, King MC, Levy-Lahad E. **Spinal muscular atrophy with pontocerebellar hypoplasia is caused by a mutation in the *VRK1* gene.** *Am J Hum Genet.* 2009; 85(2): 281-9.
- Ridley SP, Sommer SS, Wickner RB. **Superkiller mutations in *Saccharomyces cerevisiae* suppress exclusion of M2 double-stranded RNA by L-A-HN and confer cold sensitivity in the presence of M and L-A-HN.** *Mol Cell Biol.* 1984; 4(4): 761-70.
- Robinson MD, McCarthy DJ, Smyth GK. **edgeR: a Bioconductor package for differential expression analysis of digital gene expression data.** *Bioinformatics.* 2010; 26(1): 139-40.
- Rolfe DF, Brown GC. **Cellular energy utilization and molecular origin of standard metabolic rate in mammals.** *Physiol Rev.* 1997; 77(3): 731-58.

- Roth KM, Byam J, Fang F, Butler JS. **Regulation of *NAB2* mRNA 3'-end formation requires the core exosome and the Trf4p component of the TRAMP complex.** *RNA*. 2009; 15(6): 1045-58.
- Rougemaille M, Gudipati RK, Olesen JR, Thomsen R, Séraphin B, Libri D, Jensen TH. **Dissecting mechanisms of nuclear mRNA surveillance in THO/sub2 complex mutants.** *EMBO J*. 2007; 26: 2317-26.
- Rudnik-Schöneborn S, Senderek J, Jen JC, Houge G, Seeman P, Puchmajerová A, Graul-Neumann L, Seidel U, Korinthenberg R, Kirschner J, Seeger J, Ryan MM, Muntoni F, Steinlin M, Sztriha L, Colomer J, Hübner C, Brockmann K, Van Maldergem L, Schiff M, Holzinger A, Barth P, Reardon W, Yourshaw M, Nelson SF, Eggermann T, Zerres K. **Pontocerebellar hypoplasia type 1: clinical spectrum and relevance of *EXOSC3* mutations.** *Neurology*. 2013; 80: 438-46.
- Sadoff BU, Heath-Pagliuso S, Castaño IB, Zhu Y, Kieff FS, Christman MF. **Isolation of mutants of *Saccharomyces cerevisiae* requiring DNA topoisomerase I.** *Genetics*. 1995; 141(2): 465-79.
- San Paolo S, Vaňáčová S, Schenk L, Scherrer T, Blank D, Keller W, Gerber AP. **Distinct roles of non-canonical poly(A) polymerases in RNA metabolism.** *PLoS Gen*. 2009; 5(7): e1000555.
- Schaeffer D, Meaux S, Clark A, van Hoof A. **Determining *in vivo* activity of the yeast cytoplasmic exosome.** *Methods Enzymol*. 2008; 448: 227-39.
- Schaeffer D, Tsanova B, Barbas A, Reis FP, Dastidar EG, Sanchez-Rotunno M, Arraiano CM, van Hoof A. **The exosome contains domains with specific endoribonuclease, exoribonuclease, and cytoplasmic mRNA decay activities.** *Nat Struct Mol Biol*. 2009; 16(1): 56-62.

Schaffer AE, Eggens VR, Çağlayan AO, Reuter MS, Scott E, Coufal NG, Silhavy JL, Xue Y, Kayserili H, Yasuno K, Rosti RO, Abdellateef M, Caglar C, Kasher PR, Cazemier JL, Weterman MA, Cantagrel V, Cai N, Zweier C, Altunoglu U, Satkin NB, Aktar F, Tuysuz B, Yalcinkaya C, Caksen H, Bilguvar K, Fu XD, Trotta CR, Gabriel S, Reis A, Gunel M, Baas F, Gleeson JG. **CLP1 founder mutation links tRNA splicing and maturation to cerebellar development and neurodegeneration.** *Cell*. 2014; 157(3): 651-63.

Schilders G, Raijmakers R, Raats JM, Pruijn GJ. **MPP6 is an exosome-associated RNA-binding protein involved in 5.8S rRNA maturation.** *Nucleic Acids Res*. 2005; 33(21): 6795-804.

Schilders G, van Dijk E, Pruijn GJ. **C1D and hMtr4p associate with the human exosome subunit PM/Sci-100 and are involved in pre-rRNA processing.** *Nucleic Acids Res*. 2007; 35(8): 2564-72.

Schmidt K, Xu Z, Mathews DH, Butler JS. **Air proteins control differential TRAMP substrate specificity for nuclear RNA surveillance.** *RNA*. 2012; 18(10): 1934-45.

Schneider C, Leung E, Brown J, Tollervey D. **The N-terminal PIN domain of the exosome subunit Rrp44 harbors endonuclease activity and tethers Rrp44 to the yeast core exosome.** *Nucleic Acids Res*. 2009; 37(4): 1127-40.

Schneider C, Kudla G, Wlotzka W, Tuck A, Tollervey D. **Transcriptome-wide analysis of exosome targets.** *Mol Cell*. 2012; 48(3): 422-33.

Schottmann G, Picker-Minh S, Schwarz JM, Gill E, Rodenburg RJT, Stenzel W, Kaindl AM, Schuelke M. **Recessive mutation in EXOSC3 associates with mitochondrial dysfunction and pontocerebellar hypoplasia.** *Mitochondrion*. 2017; 37: 46-54.

- Schuch B, Feigenbutz M, Makino DL, Falk S, Basquin C, Mitchell P, Conti E. **The exosome-binding factors Rrp6 and Rrp47 form a composite surface for recruiting the Mtr4 helicase.** *EMBO J.* 2014; 33(23): 2829-46.
- Schuller JM, Falk S, Fromm L, Hurt E, Conti E. **Structure of the nuclear exosome captured on a maturing preribosome.** *Science.* 2018; pii: eaar5428.
- Schulz D, Schwalb B, Kiesel A, Baejen C, Torkler P, Gagneur J, Soeding J, Cramer P. **Transcriptome surveillance by selective termination of noncoding RNA synthesis.** *Cell.* 2013; 155(5): 1075-87.
- Schwabova J, Brozkova DS, Petrak B, Mojzisova M, Pavlickova K, Haberlova J, Mrazkova L, Hedvicakova P, Hornofova L, Kaluzova M, Fencel F, Krutova M, Zamecnik J, Seeman P. **Homozygous EXOSC3 mutation c.92G→C, p.G31A is a founder mutation causing severe pontocerebellar hypoplasia type 1 among the Czech Roma.** *J Neurogenet.* 2013; 27(4): 163-9.
- Schwanhäusser B, Busse D, Li N, Dittmar G, Schuchhardt J, Wolf J, Chen W, Selbach M. **Corrigendum: Global quantification of mammalian gene expression control.** *Nature.* 2013; 485(7439): 126-7.
- Shcherbik N, Wang M, Lapik YR, Srivastava L, Pestov DG. **Polyadenylation and degradation of incomplete RNA polymerase I transcripts in mammalian cells.** *EMBO Rep.* 2010; 11(2): 106-11.
- Shin J, Paek KY, Ivshina M, Stackpole EE, Richter JD. **Essential role for non-canonical poly(A) polymerase GLD4 in cytoplasmic polyadenylation and carbohydrate metabolism.** *Nucleic Acids Res.* 2017; 45(11): 6793-804.

- Shin JH, Wang HL, Lee J, Dinwiddie BL, Belostotsky DA, Chekanova JA. **The role of the *Arabidopsis* exosome in siRNA-independent silencing of heterochromatic loci.** *PLoS Genet.* 2013; 9(3): e1003411.
- Siebel CW, Guthrie C. **The essential yeast RNA binding protein Npl3p is methylated.** *Proc Natl Acad Sci USA.* 1996; 93(24): 13641-6.
- Sikorska N, Zuber H, Gobert A, Lange H, Gagliardi D. **RNA degradation by the plant RNA exosome involves both phosphorolytic and hydrolytic activities.** *Nat Commun.* 2017; 8(1): 2162.
- Sikorski RS, Hieter P. **A system of shuttle vectors in yeast host strains designed for efficient manipulation of DNA in *Saccharomyces cerevisiae*.** *Genetics.* 1989; 122(1): 19-27.
- Spemann H, Mangold H. **Über Induktion von Embryonalanlagen durch Implantation artfremder Organisatoren [On induction of embryo Anlagen by implantation of organizers of other species].** *Archiv Mikroskop Anat Entwicklungsmech.* 1924; 100: 599-638.
- Stead JA, Costello JL, Livingstone MJ, Mitchell P. **The PMC2NT domain of the catalytic exosome subunit Rrp6p provides the interface for binding with its cofactor Rrp47p, a nucleic acid-binding protein.** *Nucleic Acids Res.* 2007; 35(16): 5556-67.
- Subtelny AO, Eichhorn SW, Chen GR, Sive H, Bartel DP. **Poly(A)-tail profiling reveals an embryonic switch in translational control.** *Nature.* 2014; 508(7494): 66-71.
- Sudo H, Nozaki A, Uno H, Ishida Y, Nagahama M. **Interaction properties of human TRAMP-like proteins and their role in pre-rRNA 5'ETS turnover.** *FEBS Lett.* 2016; 590(17): 2963-72.

- Synowsky SA, Heck AJ. **The yeast Ski complex is a hetero-tetramer.** *Protein Sci.* 2008; 17(1): 119-25.
- Taylor LL, Jackson RN, Rexhepaj M, King AK, Lott LK, van Hoof A, Johnson SJ. **The Mtr4 ratchet helix and arch domain both function to promote RNA unwinding.** *Nucleic Acids Res.* 2014; 42(22): 13861-72.
- Thiebaut M, Kisseleva-Romanova E, Rougemaille M, Boulay J, Libri D. **Transcription termination and nuclear degradation of cryptic unstable transcripts: a role for the Nrd1-Nab3 pathways in genome surveillance.** *Mol Cell.* 2006; 23(6): 854-64.
- Thoms M, Thomson E, Baßler J, Gnädig M, Griesel S, Hurt E. **The exosome is recruited to RNA substrates through specific adaptor proteins.** *Cell.* 2015; 162(5): 1029-38.
- Thomson E, Tollervey D. **The final step in 5.8S rRNA processing is cytoplasmic in *Saccharomyces cerevisiae*.** *Mol Cell Biol.* 2010; 30(4): 976-84.
- Tomecki R, Drazkowska K, Kucinski I, Stodus K, Szczesny RJ, Gruchota J, Owczarek EP, Kalisiak K, Dziembowski A. **Multiple myeloma-associated *hDIS3* mutations cause perturbations in cellular RNA metabolism and suggest hDIS3 PIN domain as a potential drug target.** *Nucleic Acids Res.* 2014; 42: 1270-90.
- Tsuboi T, Yamazaki R, Nobuta R, Ikeuchi K, Makino S, Ohtaki A, Suzuki Y, Yoshihisa T, Trotta C, Inada T. **The tRNA splicing endonuclease complex cleaves mitochondria-localized *CBP1* mRNA.** *J Biol Chem.* 2015; 290(26): 16021-30.
- Tudek A, Porrua O, Kabzinski T, Lidschreiber M, Kubicek K, Fortova A, Lacroute F, Vaňáčová S, Cramer P, Stefl R, Libri D. **Molecular basis for coordinating transcription termination with noncoding RNA degradation.** *Mol Cell.* 2014; 55(3): 467-81.

Uhlén M, Fagerberg L, Hallström BM, Lindskog C, Oksvold P, Mardinoglu A, Sivertsson Å, Kampf C, Sjöstedt E, Asplund A, Olsson I, Edlund K, Lundberg E, Navani S, Szigyrto CA, Odeberg J, Djureinovic D, Takanen JO, Hober S, Alm T, Edqvist PH, Berling H, Tegel H, Mulder J, Rockberg J, Nilsson P, Schwenk JM, Hamsten M, von Feilitzen K, Forsberg M, Persson L, Johansson F, Zwahlen M, von Heijne G, Nielsen J, Pontén F. **Tissue-based map of the human proteome.** *Science*. 2015; 347(6220): 1260419.

Vaňáčová S, Wolf J, Martin G, Blank D, Dettwiler S, Friedlein A, Langen H, Keith G, Keller W. **A new yeast poly(A) polymerase complex involved in RNA quality control.** *PLoS Biol*. 2005; 3(6): 986-97.

van Dijk EL, Schilders G, Pruijn GJ. **Human cell growth requires a functional cytoplasmic exosome, which is involved in various mRNA decay pathways.** *RNA*. 2007; 13(7): 1027-35.

van Hoof A, Lennertz P, Parker R. **Yeast exosome mutants accumulate 3'-extended polyadenylated forms of U4 small nuclear RNA and small nucleolar RNAs.** *Mol Cell Biol*. 2000; 20(2): 441-52.

van Hoof A, Staples RR, Baker RE, Parker R. **Function of the Ski4p (Csl4p) and Ski7p proteins in 3'-to-5' degradation of mRNA.** *Mol Cell Biol*. 2000; 20(21): 8230-43.

van Hoof A, Frischmeyer PA, Dietz HC, Parker R. **Exosome-mediated recognition and degradation of mRNAs lacking a termination codon.** *Science*. 2002; 295: 2262-4.

Vasiljeva L, Buratowski S. **Nrd1 interacts with the nuclear exosome for 3' processing of RNA polymerase II transcripts.** *Mol Cell*. 2006; 21(2): 239-48.

Wahba L, Gore SK, Koshland D. **The homologous recombination machinery modulates the formation of RNA-DNA hybrids and associated chromosome instability.**

Elife. 2013; 2: e00505.

Walowsky C, Fitzhugh DJ, Castaño IB, Ju JY, Levin NA, Christman MF. **The topoisomerase-related function gene *TRF4* affects cellular sensitivity to the antitumor agent camptothecin.** *J Biol Chem*. 1999; 274(11): 7302-8.

Wan J, Yourshaw M, Mamsa H, Rudnik-Schöneborn S, Menezes MP, Hong JE, Leong DW, Senderek J, Salman MS, Chitayat D, Seeman P, von Moers A, Graul-Neumann L, Kornberg AJ, Castro-Gago M, Sobrido MJ, Sanefuji M, Shieh PB, Salamon N, Kim RC, Vinters HV, Chen Z, Zerres K, Ryan MM, Nelson SF, Jen JC. **Mutations in the RNA exosome component gene *EXOSC3* cause pontocerebellar hypoplasia and spinal motor neuron degeneration.** *Nat Gen*. 2012; 44(6): 704-708.

Wang L, Lewis MS, Johnson AW. **Domain interactions within the Ski2/3/8 complex and between the Ski complex and Ski7p.** *RNA*. 2005; 11(8): 1291-302.

Wang Y, Liu CL, Storey JD, Tibshirani RJ, Herschlag D, Brown PO. **Precision and functional specificity in mRNA decay.** *Proc Natl Acad Sci USA*. 2002; 99(9): 5860-5.

Wang Z, Castaño IB, De Las Peñas A, Adams C, Christman MF. **Pol κ : a DNA polymerase required for sister chromatid cohesion.** *Science*. 2000; 289(5480): 774-9.

Wasmuth EV, Januszyk K, Lima CD. **Structure of an Rrp6-RNA exosome complex bound to poly(A) RNA.** *Nature*. 2014; 511: 435-9.

Wasmuth EV, Zinder JC, Zattas D, Das M, Lima CD. **Structure and reconstitution of yeast Mpp6-nuclear exosome complexes reveals that Mpp6 stimulates RNA decay and recruits the Mtr4 helicase.** *Elife*. 2017; 6: e29062.

- Weir JR, Bonneau F, Hentschel J, Conti E. **Structural analysis reveals the characteristic features of Mtr4, a DExH helicase involved in nuclear RNA processing and surveillance.** *Proc Natl Acad Sci USA.* 2010; 107(27): 12139-44.
- Wen T, Oussenko IA, Pellegrini O, Bechhofer DH, Condon C. **Ribonuclease PH plays a major role in the exonucleolytic maturation of CCA-containing tRNA precursors in *Bacillus subtilis*.** *Nucleic Acids Res.* 2005; 33(11): 3636-43.
- Win TZ, Draper S, Read RL, Pearce J, Norbury CJ, Wang SW. **Requirement of fission yeast Cid14 in polyadenylation of rRNAs.** *Mol Cell Biol.* 2006; 26(5): 1710-21.
- Wlotzka W, Kudla G, Granneman S, Tollervey D. **The nuclear RNA polymerase II surveillance system targets polymerase III transcripts.** *EMBO J.* 2011; 30(9): 1790-803.
- Wu J, Hopper AK. **Healing for destruction: tRNA intron degradation in yeast is a two-step cytoplasmic process catalyzed by tRNA ligase Rlg1 and 5'-to-3' exonuclease Xrn1.** *Genes Dev.* 2014; 28(14): 1556-61.
- Wyers F, Rougemaille M, Badis G, Rouselle JC, Dufour ME, Boulay J, Régnault B, Devaux F, Namane A, Séraphin B, Libri D, Jacquier A. **Cryptic pol II transcripts are degraded by a nuclear quality control pathway involving a new poly(A) polymerase.** *Cell.* 2005; 121: 725-37.
- Xu Z, Wei W, Gagneur J, Perocchi F, Clauder-Munster S, Camblong J, Guffanti E, Stutz F, Huber W, Steinmetz LM. **Bidirectional promoters generate pervasive transcription in yeast.** *Nature.* 2009; 457: 1033-7.
- Zanchin NI, Goldfarb DS. **The exosome subunit Rrp43p is required for the efficient maturation of 5.8S, 18S, and 25S rRNA.** *Nucleic Acids Res.* 1999; 27(5): 1283-8.

Zanni G, Scotton C, Passarelli C, Fang M, Barresi S, Dallapiccola B, Wu B, Gualandi F, Ferlini A, Bertini E, Wei W. **Exome sequencing in a family with intellectual disability, early onset spasticity, and cerebellar atrophy detects a novel mutation in *EXOSC3***. *Neurogenetics*. 2013; 14(3-4): 247-50.

Zhou Y, Zhu J, Schermann G, Ohle C, Bendrin K, Sugioka-Sugiyama R, Sugiyama T, Fischer T. **The fission yeast MTREC complex targets CUTs and unspliced pre-mRNAs to the nuclear exosome**. *Nat Commun*. 2015; 6: 7050.

VITA

Jillian Strother Losh was born in San Antonio, Texas on May 20, 1988. She graduated from Edmond Memorial High School, Edmond, Oklahoma in 2006. In January of 2009, she entered Lone Star College in Houston, Texas where she received the degree of Associate of Science after two semesters. In August of 2009, she entered The University of Houston-Downtown. She received the degree of Bachelor of Science with a major in Microbiology and double minors in Biology and Chemistry in August of 2012. In that same month, she entered The University of Texas MD Anderson Cancer Center UTHealth Graduate School of Biomedical Sciences. She joined the laboratory of Ambro van Hoof, Ph.D. in May of 2013.

Permanent address:

7575 Cambridge Street
Unit #3307
Houston, Texas 77054